ELECTRIC SPRING CONTROL FOR SMART GRID PERFORMANCE IMPROVEMENT

BY

MUHAMMAD SHARJEEL JAVAID

A Thesis Presented to the
DEANSHIP OF GRADUATE STUDIES

KING FAHD UNIVERSITY OF PETROLEUM & MINERALS
DHAHRAN, SAUDI ARABIA

In Partial Fulfillment of the
Requirements for the Degree of

MASTER OF SCIENCE

In

ELECTRICAL ENGINEERING

January 2017

KING FAHD UNIVERSITY OF PETROLEUM & MINERALS

DHAHRAN- 31261, SAUDI ARABIA

DEANSHIP OF GRADUATE STUDIES

This thesis, written by **MUHAMMAD SHARJEEL JAVAID** under the direction his thesis advisor and approved by his thesis committee, has been presented and accepted by the Dean of Graduate Studies, in partial fulfillment of the requirements for the degree of **MASTER OF SCIENCE IN ELECTRICAL ENGINEERING.**

Dr. Mohammad Ali Abido
(Advisor)

Dr. Ali Ahmad Al-Shaikhi
Department Chairman

Dr. Ibrahim Mohamed El-Amin
(Member)

Dr. Salam A. Zummo
Dean of Graduate Studies

Dr. Ali T. Al-Awami
(Member)

9/2/17
Date

This thesis is dedicated to my parents and siblings.

ACKNOWLEDGMENTS

All praise is due to ALLAH and peace be upon the Prophet ﷺ and his family, his companions (may ALLAH be pleased with them) and his followers.

With immense respect, I would like to extend my deepest gratitude to my family because without their prayers, love, positive reception and affection I would not have been able to achieve my desired goal in life. I will always be thankful to them for their continuous moral and emotional support and ever-needed prayers. It has been my honor to be able to work with Dr. Muhammad A. Abido. I would like to admire his supervision, suggestions and guidance right from the beginning till the end of this research. His constant motivation helps me to produce quality work. I would like to thank my committee members: Dr. Ibrahim El-Amin and Dr. Ali Al-Awami for their useful response, advice and the time they spent reviewing this thesis. I am very obliged to King Fahd University of Petroleum & Minerals for providing me an opportunity to pursue my graduate degree.

I would also like to appreciate all the support that I received from the Electrical Engineering Department in carrying out this research. I would like to thank all my friends and all the seniors at KFUPM for providing the moral support, pleasant atmosphere and unforgettable moments.

TABLE OF CONTENTS

LIST OF TABLES

LIST OF FIGURES

LIST OF ABBREVIATIONS

DC ES: Direct Current Electric Spring

DFT: Discrete Fourier Transform

DSM: Demand Side Management

DSP: Digital Signal Processor

ES: Electric Spring

ESS: Energy Storage System

EV: Electric Vehicle

FACTS: Flexible AC Transmission Systems

FLC: Fuzzy Logic Controller

GA: Genetic Algorithm

IEEE: Institute of Electrical and Electronics Engineers

PCC: Point of Common Coupling

PEV: Plug-in Electric Vehicle

PI: Proportional Integrator Controller

PLL: Phase Locked Loop

PQ: Power Quality

PV: Photovoltaic

PWM: Pulse Width Modulation

RMS: Root Mean Square

RTP: Real Time Pricing

SSSC: Static Synchronous Series Compensator

STATCOM: Static Synchronous Compensator

SVC: Static Var Compensator

VSC: Voltage Source Converter

Symbols are explained wherever they are used and whenever necessary.

ABSTRACT

Full Name : Muhammad Sharjeel Javaid

Thesis Title : Electric Spring Control for Smart Grid Performance Improvement

Major Field : Electrical Engineering

Date of Degree : January 2017

Electric spring is a novel smart grid technology which is based on power electronic based switching components. It has multitude of benefits associated with its widespread use at distribution level, which includes enhanced voltage stability, reduction in power imbalance and improved power quality. With ever increasing need of incorporating renewable energy sources and inclusion of electric vehicles in the existing power grid, certain power quality issues arise. Electric spring (ES) offers a viable solution to these problems. A new generation of electrical loads is also proposed recently, known as smart loads, which is the outcome of integrating electric spring in series with a non-critical load. This research is focused to unveil the positive impact of this device in improving smart grids attributes including power quality (PQ), and demand side management (DSM) along with its ability to reduce neutral current and voltage fluctuations. This work also presents novel control techniques based on mathematical formulations that suggest definite improvements in the existing control strategies in terms of response parameters and computational efficiency. Moreover, this work also proposes the use of ES for addressing the adverse effect of heavy electric vehicles penetration. A laboratory scale hardware prototype is also developed to act as the proof-of-concept of proposed models and theories. Hardware results are found to be in congruence with

those obtained from simulation models, ensuring the efficacy of theoretical framework.

ملخص الرسالة

الاسم الكامل: محمد شرجيل جاويد

عنوان الرسالة: التحكم في النابض الكهربائي لتحسين أداء الشبكات الذكيةالذكية

التخصص: الهندسة الكهربائية

تاريخ الدرجة العلمية: يناير 2017

تعتبر النوابض الكهربائية من التقنيات الحديثة المستخدمة في شبكات الطاقة الذكية والتي تعتمد في تشغيلها على إلكترونيات القوى والمفاتيح الكهربائية. تستخدم هذه النوابض في شتى المجالات المتعلقة بشبكات توزيع الطاقة الكهربائية، كزيادة ثبات الجهد الكهربائي و تقليل عدم التوازن بين القوى الكهربائية باللإضافة إلى تطوير كفاءتها. عند توصيل مصادر الطاقة المتجددة والسيارات الكهربائية بالشبكة الكهربائية، تنشأ بعض المشاكل المتعلقة بكفاءة وجودة الشبكة الكهربائية. هذه المشاكل يمكن حلها عن طريق استخدام النابض الكهربائي. أيضًا، عند توصيل النابض الكهربائي بأحمال كهربائية غير حساسة، ينشأ بما يسمى بالأحمال الكهربائية الذكية. هذه الأحمال تعتبر جيل جديد وحديث الوجود من الأحمال الكهربائية.

في هذا البحث، سيتم التركيز على دراسة الأثار الإجابية للنابض الكهربائي من ناحية تطويره لمختلف جوانب شبكات الطاقة الذكية. تشتمل هذه الجوانب على كفاءة القوة الكهربائية و إدارة الأحمال الكهربائية، و التقليل من تذبذبات التيار وفرق الجهد المحايدين. بالإضافة إلى ذلك، هذا البحث يقدم تقنيات تحكم حديثة مبنية على معادلات رياضية. هذه التقنيات بالتأكيد ستطور من تقنيات التحكم الموجودة حاليًا من حيث إستجابة العوامل الرياضية والكفاءة الحسابية. يطرح هذا البحث أيضًا دراسات تتعلق بإستخدام النابض الكهربائي لمعالجة الآثار المتعلقة بتوصيل السيارات الكهربائية بشبكات الطاقة. ومن أجل إثبات النظريات والمفاهيم المطروحة في هذا

البحث، تم عمل نموذج أولي ملموس في المعمل. وبعد مقارنة نتائج الدراسات المأخوذة من المعمل بالنتائج المستخرجة من نماذج المحاكاة في الحاسوب، تم التثبت من تطابقهما مما يدل على كفاءة العمل النظري المطروح في هذا البحث.

.

CHAPTER 1

INTRODUCTION

1.1 Background

The ever increasing demand of green energy has encouraged the renewable sources to play the pivotal role in power sharing of future power systems, so that not only the cost of per unit energy would be reduced but environmental friendly energy can also be produced. These benefits of such energy resources are accompanied with the drawback of dynamic behavior of power produced. Eventually, problems arise in power balance and its quality. Voltage fluctuations become common due to intermittent nature of wind and solar energy. Under this situation, power electronic devices give rise to control methodologies which can propose promising solution to these problems. Load side management can also be achieved with the help of more sophisticated conventional strategies and telecommunication technology.

One of the emerging, innovative, and recent technologies in smart grid area is the electric spring (ES). Since 1660s, when the British scientists Robert Hooke described the principle of the mechanical spring, there were no serious attempts during these three centuries to extend the principle of the mechanical spring to an electrical concept. ES has great potential in stabilizing future smart grid by regulating the main voltage despite the fluctuation of the output power of the intermittent renewable energy sources. It can be

integrated with home appliances allowing the load to follow the intermittent generation of renewable energy sources. This is unlike the previous idea that depends on generating enough energy to cover the load demand either completely or partially.

An ES can be considered as a controlled voltage source connected in series with the noncritical load to form a new combination of smart load. This smart load is connected in parallel with critical load where power and voltage should remain constant. Non critical load is necessary for the operation of ES, as it acts as a damper. Noncritical load is a special type of load which can be operated within a limit of fluctuating voltage. Examples of such loads include refrigeration, air conditioning and lighting loads. On the other hand the critical load, across which the voltage is required to remain constant, gets the desired voltage, and so power absorbed by critical load also remains constant, allowing the noncritical load power to vary as per the generation. Ultimately, ES maintains the load demand balance while increasing voltage stability.

ES operation is similar to that of a mechanical spring. It can be said that three different operations of ES are analogous to the three cases of mechanical spring (neutral, mechanical push and mechanical pull). ES can be modeled by a current controlled voltage source. This current is responsible for the voltage boosting and voltage reduction operation of this device which eventually leads to maintaining of power balance within the system.

The major difference between ES and reactive power compensators is the fact that conventional compensators are typical output feedback, output control systems which tends to regulate the output of the system based on the feedback fed to the controller from

the output terminal. Whereas, ES uses input feedback input control strategy. It takes feedback signal from the input side of the system and tries to regulate it to a certain reference value. This slight change allows the controller to regulate input which is connected to critical load, while the output voltage (connected to noncritical load) is left unregulated. The mentioned approach is different from other flexible ac transmission systems (FACTS) devices. For example in static synchronous compensator (STATCOM) and static var compensator (SVC) the usual shunt voltage control is used to regulate the point of common coupling (PCC) voltage whereas ES uses different strategy to provide reactive power support. This feature gives the opportunity to use electric spring not only for voltage regulation but also for reducing power imbalance.

1.2 Thesis Motivation

The actual interest behind this work lies in the repercussions of using conventional power generation units which burn fossil fuels for their operation. Global warming, which is the direct consequence of using such electric generation units, has drawn the attention of power systems researchers to come up with an idea of green environmental friendly energy sources. Hence many countries' governmental energy policies are being revised to incorporate low carbon emission energy systems to bring down the alarmingly high rate of carbon content in atmosphere and global warming.

Now, the integration of renewable energy sources have created severe stability and power quality issues which are inevitable due to their functionality. The problem arises when the penetration of renewable sources is increased beyond limit. Under these circumstances,

an ES will play the role at distribution level. Loads are needed to be classified into two types; noncritical and critical loads based on their operating voltage and power limits.

The imbalance between power generation and consumption in grids can lead to issues relating to grid reliability, resiliency and stability. Both theoretical and empirical studies have shown that the variability and uncertainty of future renewable power generation and consumption can pose great challenges to the control of the local bus voltage and line frequency [1]. The issues of bus voltage fluctuation and frequency deviation are found to be more prominent in isolated power networks and microgrids. The causes of the power imbalance can be imputed, but are not limited, to the intermittent power generation of renewable energy sources, load fluctuation and generator tripping.

Different solutions have been studied and developed to cope with the aforementioned issues to suit various applications, including FACTS, energy storage system (ESS), power reverse banks, etc. Apart from these solutions implemented at the power transmission level, the distributed voltage and frequency control approach on the distribution level is an emerging control scheme for enhancing the stability and reliability of power systems. Time scheduling and load shedding are commonly adopted for controlling the demand side real power consumption. In this research, usability of ES is explored in detail to eradicate above mentioned problems.

Therefore, this work is motivated to explore the applications of ES in improving the overall performance of smart grid which can be otherwise deteriorated by the heavy induction of renewable plants.

1.3 Thesis Objectives

The aim of this research is to develop and test ES as a new smart grid technology in order to mitigate the drawbacks associated with renewable sources integrations. Controllers are designed to regulate ES performance for the purpose of demand side management, improving power quality and mitigating voltage fluctuation. The objectives of this study include:

1. Model and characterize single phase ES.
2. Comparatively analyze ES with other reactive power compensators.
3. Develop a fuzzy logic based controller to improve the transient response of ES
4. Extend single-phase ES to its three-phase implementation for neutral current mitigation.
5. Design a controller for ES that offers household voltage regulation in the widespread presence of EV.
6. Development of a lab based prototype for the experimentation of ES to verify its applicability.

1.4 Thesis Methodology

The achievement of thesis objectives can be divided into the following steps:

Task 1: Technology assessment and literature survey

- Assessing technological advances in development and scope of ES
- Surveying application of ES in improving characteristics of smart grid.

Task 2: Developing and testing on Matlab Simulink

- Developing single phase ES in Simulink environment.
- Design input feedback based fuzzy controller to control the output of ES inverter.

Task 3: Implementing three-phase electric spring

- Investigating the use of ES in the domain of three-phase.
- Design a controller for three-phase ES that can mitigate neutral current.

Task 4: ES application for mitigating voltage drop caused by electric vehicles

- Model a distribution network incorporating ES and electric vehicles.
- Design a controller for ES to regulate mains voltage during peak loading time.

Task 5: Building the laboratory prototype

- Build prototype for smart load.
- Build prototype of proposed control strategies controlling ES.

Task 6: Investigation and evaluation of laboratory prototype performance

- Experimental investigation of the smart load prototype.
- Experimental investigation of the control strategy prototype.

1.5 Thesis Contribution

Primary contribution of this research revolves around novel applications of ES in improving smart grid performance with novel and more efficient control schemes. ES linearization followed by application based mathematical formulation is also a new proposition in this domain. Unique phasor diagrams are plotted for neutral current

mitigation explaining the operation of ES. Another major contribution can be accounted as the development of experimental prototype of ES with laboratory based components. Simple instrumental steps resulting in major contributions are listed below.

1. A novel control approach based on fuzzy logic is proposed to control ES for the purpose of voltage regulation.
2. A simple and direct control scheme based on mathematical modeling of a typical power system has been proposed to mitigate neutral current caused by unbalanced three-phase loads.
3. A new application of ES involving reduction in voltage drop caused by high penetration of electric vehicles is proposed.
4. Another application of ES is presented in which presence of ES ensures the availability of constant power for a load irrespective of its offered impedance.
5. For obtaining experimental results, spatially optimized portable voltage and current senor board has been developed with an onboard chipset for inverter drive and power module.

1.6 Thesis Breakdown

The basis of the research problem and the foundation of the thesis area are presented in this current chapter (Chapter 1). It also includes the discussion of objectives and research methodology. Chapter 2 details the literature review and highlights the past work that has been conducted in this field of consideration. It keeps the focus on ES since its advent to the recent advancements that have been proposed in the past couple of years. Chapter 3 deals with the introduction and modes of operation of ES. It also includes the

conventional control topology to perform voltage regulation and demand side management. From Chapter 4 to Chapter 7, various applications of ES with unique control schemes have been discussed. In Chapter 4 fuzzy based controller is proposed and implemented for the purpose of voltage regulation and its results are compared with those obtained from PI controller. Chapter 5 discusses the operation of ES for dealing with the problem of neutral current mitigation. Next, in Chapter 6 the new technique of compensating voltage drop caused by sudden and simultaneous Plug-in electric vehicles (PEV) charging is introduced and explained. Details of experimental setup, followed by its assembling are provided in Chapter 7. It also highlights the equivalence between the results of simulation model and hardware prototype for the application of constant power load applications. In the end, Chapter 8 concludes the findings and suggests the future work.

CHAPTER 2

LITERATURE REVIEW

The imbalance between power generation and power consumption in power grids can lead to issues relating to grid reliability, resiliency and stability. Both theoretical and empirical studies have shown that the variability and uncertainty of future renewable power generation and power consumption can pose great challenges to the control of the local bus voltage and line frequency [1]. The issues of bus voltage fluctuation and frequency deviation are found to be more prominent in isolated power networks and microgrids. The causes of the power imbalance can be imputed, but are not limited, to the intermittent power generation of renewable energy sources, load fluctuation and generator tripping.

Different solutions have been studied and developed to cope with the aforementioned issues to suit various applications, including flexible ac transmission systems (FACTS), energy storage system (ESS), power reverse banks, etc. Recently, an automatic demand response technology, called the electric springs (ES) has been proposed. This technology solved the critical challenge of achieving grid voltage control and power grid stability in distribution networks connected to intermittent renewable power sources. So far, three types of ES have been developed. The first two types of ES are connected in series with non-critical loads (series-type ES) to form smart loads that are adaptive to the availability of power generation, with the first type handling only reactive power and the second type handling both active and reactive power [4]. The third type of ES can be incorporated

into any bidirectional grid-connected AC-DC power converters. without an association to any non-critical load. (And is known as the shunt type ES)

2.1 Fundamentals and Basic Analysis

Electric spring (ES) is basically a power electronic based reactive power compensator which is proposed for demand side management and voltage stability in smart grid. Its basic operation, analogy to mechanical spring and operating conditions are presented in [1], [2]. The circuit of ES is practically implemented in [3] . All details are given for a 10 kVA power system which is connected to an intermittent renewable source. Control algorithms to drive ES are successfully tested on the physical model of ES.

The steady state model of ES is analyzed mathematically in [4], where equations of different controllers are given along with its analytical detail. It has been shown that mathematical analysis validates the experimental result signifying the importance of ES concept. In [4],[5] theoretical platform is established for further work to rely on and strong basis is developed to justify ES as a voltage regulation and frequency stabilizing smart device. In [6], mathematical bases are explored to characterize ES connected to various types of loads. Experimental validity is also given to support the proposed basis. It is found that ES can be used with a wide range of loads to perform its required task of voltage regulation and demand side management. The traditional control paradigm of having power generation to follow power demand has to be reversed [7]. Future power grids must have the loads adaptive to the availability of power generation, particularly when renewable power such as wind and solar power becomes substantial. Researchers in the power systems community have responded to this new challenge with various

demand-side management methods such as scheduling of delay–tolerant power demand tasks [8], use of energy storage to alleviate peak demands [9], RTP [10] and direct load control or on-off control of electric loads [11]

The first reporting of the impact caused by widespread integration of ES at distribution level was first reported by [12]. It proposes the concept of connecting ESs with multiple loads in the smart grid and proves its effectiveness by regulating voltage at each point of their application and by displaying an enhanced overall system's stability. The proposed control algorithm allows the system to work in coordinated way without any conflict among their shares. Therefore, each noncritical load is experiencing a less deviant voltage waveform.

ES technology offers viable solution to demand side management problems in smart grid as well. Simple and accurate averaged dynamic model for ES has been developed in [13], [14] which can be incorporated in large scale of power system for simulation studies. In this model, the dynamic of DC link voltage is ignored and considered as a constant voltage. Comparing the experimental and simulation results shows the validation of this model for collective operation when it is distributed in power system. In addition, the results show the effectiveness of the dynamic model for different load power factor and different proportions of critical and non-critical loads.

Analysis of ES with a relatively advanced controller is done in [15], where the phase angle of a predefined reference in proportional resonant controller is realized. Analysis of critical operating functions of electric spring is carried out with various critical loads. Geometric relationships along with associated vector diagrams are examined for voltage

calculations. Voltage at PCC is regulated to required value whereas the phase angle between current and ES voltage is also determined. Experimental verification is also given to verify the effectiveness of this controller.

2.2 Experimental Validity and Power Quality

Three practical experiments have been carried out in [1] to investigate the performance and the capability of the ES to perform voltage regulation to the main voltage and allow the load demand to follow the power generation. However, in the first experiment, the ES is connected in series with the non-critical load and fed by a standard AC power supply to test the ES performance in neutral, capacitive and inductive modes by measuring its voltage and current. In the second experiment, the critical and non-critical resistive loads are fed by an unstable AC power supply like wind turbines simulator and power plant taking into consideration two cases when the ES is enabled and disabled in the power system. ES is programmed to perform voltage boosting function only to regulate the main voltage and low the non-critical load to follow the generation. In the third experiment, ES is connected in power distribution system and cable impedance is also considered in this case. ES works for voltage boosting and voltage reduction.

Different scenarios for ES have been described in [12] where ES is connected with different types of loads such as resistive, capacitive inductive and constant power loads. The models of the load characterization are derived mathematically and verified by practical experiments.

Several applications of ES have been discussed in [4]-[12]. General steady state analysis is performed to investigate the ability of the ES for real and reactive power

compensation. ES voltage can be controlled by changing the modulation index value. Consequently, the voltage of the series connected load is dynamically changed. So, the amount of current, flowing in the circuit, changes. As a result, the amount of power delivery to grid varies and noncritical load takes part in power compensation. Practical experiments are performed using different types of loads to verify the derived models of steady-state analysis. These experiments have been carried out for two cases, the grid delivers only real power and both the resistive and inductive or capacitive loads in series with ES are connected to the grid. The ES is responsible for reactive power compensation either by generating reactive power in case of an inductive load or absorbing the reactive power in case of capacitive load. In second case, both of the grid and the ES supply positive or negative complex power to the load.

Droop control scheme has been used to control ES for parallel operation in power distribution network [6]. It has a feature that the voltage reference of the ES is automatically adjusted according to the location of the ES in the distribution system due to its decentralized control. A power system has been simulated with traditional AC generator and intermittent renewable energy source at different locations of ES. Electrical loads are connected to investigate the behavior of the ES as voltage regulator and power compensator with and without droop control scheme. Each experiment is divided into three sections: with ES, ES with traditional controller and ES with droop control. According to the result, the main voltage of the feeder remains stable in both cases with and without droop control, but ES doesn't operate in a coordinated manner without droop control. However, the droop control scheme has capability to solve these issues.

It was reported that the ES can reduce the storage capacity requirements in the power system in future smart grid [16]. The electric spring is shown to be an emerging technology proven to be effective in i) stabilizing smart grid with substantial penetration of intermittent renewable energy sources and ii) enabling load demand to follow power generation. The subtle change from output voltage control to input voltage control of a reactive power controller offers the electric spring new features suitable for future smart grid applications. In this work, the effects of such subtle control change are highlighted, and the use of the electric springs in reducing energy storage requirements in power grid is theoretically proven and practically demonstrated in an experimental setup of a 90 kVA power grid. Unlike traditional STATCOM and Static VAR Compensation technologies, the electric spring offers not only reactive power compensation but also automatic power variation in non-critical loads. Such an advantageous feature enables non-critical loads with embedded electric springs to be adaptive to future power grid. Consequently, the load demand can follow power generation and the energy buffer and therefore energy storage requirements can be reduced as shown in [9]

The charging and discharging rates of the battery with ES is much less than without ES. For power quality improvement, a new control scheme has been proposed [17]- [18]. The new controller scheme contains multiple resonant controller and second order generalized integrator to improve the power quality by enabling ES and so eliminating the transmission line harmonics [17]. When the dc link capacitor is replaced by a battery, ES can work in eight different modes. These modes are inductive and capacitive modes, resistive and negative resistive modes, inductive plus resistive and capacitive plus resistive modes, and inductive plus negative-resistive and capacitive plus negative

resistive modes. The input controller is designed for ES with a battery. Hence, the ES is capable of working as a power factor corrector for different RL and RC loads [19].

Distributed voltage control (ES) and single point voltage control (STATCOM) have been compared with respect to the total voltage regulation and also, total requirement of reactive power capacity [20],[21]. ES and STATCOM models are implemented in MATLAB/SIMULINK using controllable voltage source. The only difference is that the ES is connected in series with the non-critical load. Simple case study is implemented using an ES and a STATCOM at a time. This study is extended for both IEEE 13-bus feeder and on a part of distribution network of Hong Kong [20]. The results show that the effectiveness of ES for total voltage regulation along the transmission line is better than the STATCOM. In addition, ES requires less reactive power capacity than STATCOM. The capability if the ES depends mainly in the ratio of the critical and non-critical load.

Power imbalance reduction of three phase power system in the building is a new potential of ES [22],[23]. The second generation of distribution voltage control which includes a battery at the DC terminal of the ES is used. This may lead to some ES limitations that the maximum output voltage of the inverter (ES) is the maximum voltage value of a battery. In this case, the phase angle varies within 0°-360°. Imbalance current of the transmission line can be reduced when the ES re-distribute the power of non-critical loads. Practical and simulation study verified the capability of ES to reduce the power imbalance in the buildings making it adaptive to any internal load changes and also regulate the external main voltage for any disturbances [22]. In [24], type I ES is used in three phase loads to mitigate neutral current due to the unbalanced load which is a severe power quality issue. ES is programmed such that it becomes able to nullify or reduce the

three phase load imbalance, which eventually turns out to be an effective method of reducing problems related to excessive neutral current.

Several advance schemes to the instantaneous output voltage of single phase inverter were introduced in the literature. Some of these controllers are current and voltage controllers, repetitive controllers, deadbeat controllers and d-q controllers [25]–[28]. These controllers aim to improve the dynamic response and zero steady-state error performance of the power system.

2.3 Recent Applications of ES

Recently, more advanced and complicated application of ES has been reported [29]- [30]. It is previously stated that ES can provide active and reactive power compensation. Due to the limited storage capacity of the battery, [29] explores a new control scheme for the third version of the electric springs to operate under the physical constraints of the state-of-charge of the battery for microgrid stability applications. Such a scheme has been tested in an experimental prototype and a power grid simulator to illustrate the use of the scheme in battery's monitoring, charging/discharging management and output power control.

In [29] a modified control scheme with the inclusion of the battery management system (BMS) for the third version of the ES is proposed. Among various battery models, the hybrid model, as used in [31], has been proposed due to relatively increased accuracy as it accounts for the recovery effect, which is important for the dynamic tracking of the state-of-charge. Reference [30] implements a general battery model together with a modified dead zone control circuit with a hysteresis band embedded in the existing

active-reactive power decoupling control scheme for ES-3. Experimental and simulation results have demonstrated that the proposed control method can preserve the original ability of ES-3 on regulating both grid voltage and utility frequency while providing an effective way for managing the state-of-charge of the battery system. With the automatic charging and discharging strategy integrated in the active power control loop, the ES is expected to improve the quality of grid in the long term with higher stability. ES-3 employs AC/DC converter with battery storage and without association with noncritical load [32]

Micro-grids fed with small synchronous generators and intermittent renewable power sources are generally considered as weak power grids unless very large energy storages are incorporated as the energy buffer. Auxiliary techniques are needed to improve their stability when transient interrupts occur. In [33], the 3-phase Electric Spring (ES) is studied to improve the stability of the micro-grid in transient operations. The power compensation characteristics of the 3-phase ES are firstly analyzed. The linear relationships between decoupled d and q components of ES voltage and real and reactive power of smart load enable the ES to conduct frequency and voltage regulation simultaneously. The droop control is further developed to coordinate the operation of multiple ESs distributed along a distribution line. The transient stability issues of the micro-grid under study are analyzed in detail.

Droop control is a well-established scheme to coordinate the operations of multiple parallel generators in micro-grids [34]–[38]. The same philosophy can be adopted in load management of micro-grid, and adaptive loads enabled by ES can contribute to the regulation of micro-grids. Based on this incentive, a novel droop control is introduced

and examined to harmonize the operation of distributed ESs. Simultaneously, the power of noncritical loads can be shed and boosted when ESs operate in different modes. The power compensation characteristics of 3 phase ESs make it possible to decouple voltage and frequency regulation simultaneously. Simulation results of [33] indicate that ESs with the proposed droop control can react swiftly to fast transient changes of microgrids including unintentional islanding, intentional islanding, and sudden load changes.

Issues pertaining to widespread integration of ES into the system are reported in [39]–[41]. When multiple stable systems are combined into one system, the newly formed hybrid system has a certain possibility to be unstable. Such a natural phenomenon has been verified in the fields of chemistry and biology over the last century. The use of electric springs (ES), which must be implemented in large quantity over the power grids, can also suffer from the same issue if specified designs are not carried out. In [42], a method of tuning Kp and Ki of the PI controllers of the ES to ensure the overall system stability in a weak grid is investigated. The method is based on the concept of relative stability and is achieved through the aid of simulation. Both simulation and experimental results validate that as the number of ES in the weak grid increases, more stringent values of Kp and Ki are required to achieve system stability. Apparently, a corresponding relationship between the optimal tuning of Kp and Ki of the PI controllers and the maximum number of ES installed in the weak grid exists. If the optimal values of Kp and Ki are adopted, a maximum number of ES can be stably installed over the grid. Another advanced controller which uses fuzzy logic to tune Kp and Ki of both DC link and regulated voltage is presented in [43].

In [44]–[50] each grid-tied inverter is connected to the grid with a low impedance to achieve stability. However, the circumstance is changed if multiple inverters are connected to the grid in parallel. The stability of the system is then dependent on the total system's impedance. Parallel oscillation of the system between the inverters may occur [44]. Furthermore, if the number of inverters is increased, the total capacitance of the system will be increased, which means that the resonant frequency will decrease. If the resonant frequency falls below the band frequency, the system will be unstable [46]. For multiple ES, such a phenomenon can also happen and there is possibility of system instability, which can severely affect the power quality of the electricity used by consumers and ruin the original purpose of ES in terms of stabilizing local node voltages supplying critical loads. More importantly, if the amplitude of the oscillation is significant and does not cease within the permitted period, the whole power system may blackout. Therefore, it is necessary to investigate the stability property of multiple ES when installed in the power grids and to provide the corresponding design solution. In [42], the small-signal model and the stability analysis for multiple ES in both strong and weak grids are provided. A tuning method of the PI controller of the ES in achieving stability for multiple ES implementation in a weak grid is provided based on the analysis, simulation results, and experimental results. Radial Chordal Decomposition method is mathematically presented and used to decouple power angle and voltage control of ES in [30].

2.4 DC Electric Spring

A significant research is going on integrating renewable energy source to Direct Current distributed power systems and Direct Current microgrids. The power quality and voltage

stability are critical issues if a renewable energy sources possess a major share in the DC grid. [51] presents an electric active suspension technology known as the DC electric springs for the first time to stabilize and enhance the power quality in DC microgrids. An introduction is given to the basic characteristics and operating modes of a DC electric spring. Also, other concerned problems that adversely affect the power quality of the DC grid, including system fault, harmonics, voltage droop and the bus voltage instability, are briefly addressed.

Reference [52] presents a control scheme that is applied on the shunt-type electric springs (ES), which is used to strictly regulate the grid voltage for ensuring local voltage stability and to mitigate the utility frequency deviation. The operating method of the shunt-type ES is discussed. A laboratory-scale 1 kW experiment has been done to verify the proposed control scheme and to validate the feasibility of applying the method on a power system [52]. When controlling the real and reactive power of the ES, a conflict exists between the voltage and frequency control [53] as both the voltage and frequency are nonlinear functions of the real and reactive powers of the ES. In the proposed control method, such a conflict is eliminated through the implementation of different bandwidths in the control of the voltage and frequency control loop such that they are decoupled from one another. In realizing this control, the primary target is given to the fast regulation of the local grid voltage. This is because the fluctuation of the voltage can more easily affect the normal operation of critical electrical facilities such as motors and telecommunication equipment. A lower priority is given to the frequency control due to the following reasons: (i) the normal frequency deviation in an emerging power system is typically only within a few percent [54] and (ii) the dynamic response of the system frequency is slow

because it is relying on the inertia constant of generators. Hence, a frequency control on ES with slow response is sufficient to handle the mitigation of frequency variation. For these reasons, the presented control scheme is designed to provide a fast response to bus voltage fluctuation and a relatively slow response to frequency deviation due to the relatively large rotor inertia of generation units.

A control paradigm of the third version of electric springs is provided in [55] to eliminate the contradiction between frequency control and voltage control found in pervious control schemes. Experimental results from a 1-kW laboratory setup verified the feasibility of the control scheme. The control method has been applied on a 2.8 MW micro power system to further confirm its validity. The shunt-type electric springs with the proposed control method is potentially applicable to existing distributed renewable energy systems such as PV micro-inverters embedded with battery storage. In [55] difference between the series and shunt DC electric spring applied to the DC grids are addressed. Operating modes and topologies of both the series ES and shunt ES are systematically defined. The experiments have probed that both types are effective mechanism of achieving DC bus voltage regulation, PCC harmonic compensation and fault ride through function

Shunt ES is proved to be better for harmonic compensation application as it does not consume energy when performing harmonic filtering and the shunt ES with its quicker dynamic response, is more suitable for handling fault than the series ES.

2.5 Discussion

This literature survey has revealed certain shortcomings which are yet to be addressed and several gaps which are yet to be filled. Since the advent of this specific connection topology of an inverter, most of the attempts to explore the applications of ES have been covered in this survey. However, there are certain control schemes which can be enhanced for better transient response. In addition to this, latest problems incurred by power systems due to EVs can be solved by using distributed ES. Shortcomings incurred during the literature review and proposed modifications are discussed below:

So far, PI controller has been reported in literature for voltage regulation. However, it has been established that for performance reasoning and to avoid complexities incorporated by nonlinearities in the system, a linguistic rule approach can be used. Fuzzy logic controller (FLC), determines the control signal by evaluating simple linguistic rules, without requiring any mathematical modeling of given system. FLC requires designer's experience and well inferred input-output relationship for better performance. Another approach which combines the effect of PI controller and FLC (by applying Fuzzy Logic to obtain gain constants of PI controller) is suggested as another alternative, known as Adaptive PI.

As discussed, ES has been used to reduce three phase load imbalance. An independent control of three phase ES with control parameters being evaluated using Genetic Algorithm (GA) has been suggested previously. The accuracy of GA is highly dependent on initial population size and training data. The large convergence time and finite set of training data limits their usage for real time applications. Moreover, GA based controller makes the system unnecessary complicated which results in reduced computational

efficiency. In another attempt, three-phase ES is connected to system via isolation transformer with a controller based on impedance estimation. This approach is direct and convenient but it lacks depth and significant simulation results. In order to address these shortcomings, a novel and direct approach based on system's mathematical model, runtime impedance estimation and electric spring voltage feedback has been proposed in this thesis.

It has been known that voltage profile of a distribution network is adversely affected by heavy and imminent penetration of EVs. Voltage profile is regulated by both active and reactive power management while introducing a communication scheme among EVs. On the downside, reactive power control will require modification in available EVs' inverter control. Moreover, this approach has certain limitations in terms of reactive power transfer based on battery's storage capacity. For communication between EVs, an enhanced infrastructure is required. Under this scenario, design of ES for voltage support is proposed as a viable alternative.

In order to substantiate the theoretical propositions, a laboratory scale prototype is developed to validate simulation results.

CHAPTER 3

THEORY AND CONVENTIONAL CONTROL OF ELECTRIC SPRING

This chapter includes the details pertaining to fundamental theory of ES. In the beginning, its analogy to mechanical spring is explored followed by establishing the basis of categorizing any electrical load into critical or noncritical load. Subsequently, three different types of ES are explained which enables the discussion of all modes of operation of ES. In the next section, conventional control topology for voltage regulation is presented and its implementation on a typical simulation model is detailed. Basically, this chapter provides the starting point for the development of consequent controllers and novel applications of ES.

3.1 ES Fundamentals

3.1.1 Analogy to Mechanical Spring

In late 2012, a research group from Hong Kong proposed ES as an alternative tool for DSM, independent of communication protocol. In analogy to mechanical spring, the concept of electrical spring is introduced [1]. Establishing its basis on the famous Hooke's law, electric spring provides the support, stability and storage capability as its mechanical counterpart. In the simplest form, ES is a power electronic based device in which a controller provides control signal to an inverter. The waveform of inverter is

integrated to the power system in such a manner that the whole topology presents the replica of mechanical spring. The following equations govern the fundamentals of ES:

$$q = \begin{cases} CV_a \text{ inductive mode} \\ -CV_a \text{ capacitive mode} \end{cases} \tag{3.1}$$

$$q = \int i_c dt \tag{3.2}$$

where q is the charge stored in the capacitor, C is the capacitance and V_a is the voltage across the capacitor.

In equation (3.2), it can be seen that charge stored in the capacitor is the function of current i_c flown into the capacitor. This realization establishes that ES can be modeled by a current controlled voltage source. This current is responsible for the voltage boosting and voltage reduction operation of this device which eventually leads to maintaining of power balance within the system.

Figure 3.1 and Figure 3.2 show the current controlled voltage device as discussed above. Smart load is formed after embedding a noncritical load in series with ES. This load is necessary for the operation of ES, as it acts as a damper. Noncritical load is a special type of load which can be operated within a limit of fluctuating voltage. Examples of such loads include refrigeration, air conditioning, and lighting loads. On the other hand, the critical load, across which the voltage is required to remain constant, gets the desired voltage. Therefore, the power absorbed by critical load remains constant, allowing the noncritical load power to vary as per the generation. Ultimately ES maintains the generation-load balance while increasing voltage stability.

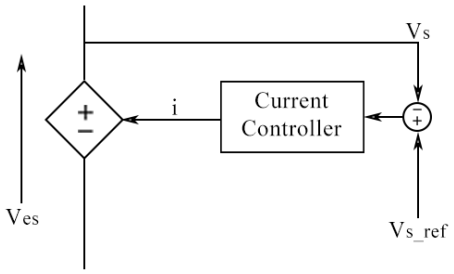

Figure 3.1 An electric spring representation as controller voltage source

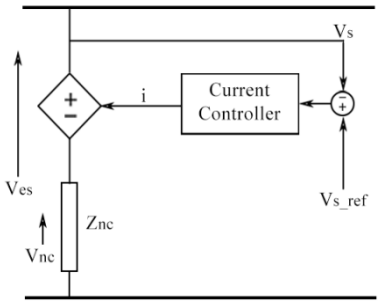

Figure 3.2 Smart load formation by integrating ES with noncritical load

3.1.2 Load Characterization

Noncritical loads refer to electrical equipment and appliances that can be subjected to fairly large variation of mains voltage. Examples of such loads are air conditioning, hot water, refrigeration and lighting. These loads can operate, without significant losses in their functionality, under a voltage variation of ±20% of nominal value [3].

Critical loads refer to electrical equipment and appliances that require a well regulated voltage. Examples are life supporting medical equipment and computer controlled systems. Voltage across the terminals of these loads is supposed to be at nominal value in a strict sense. It is to be noted that in this work, voltage across critical load has a broader meaning in the sense that it also covers the connotation of voltage at PCC.

Hong Kong statistics are being shown in Figure 3.3 which depict that noncritical loads contribute to about 50% of the total power consumption in commercial buildings.

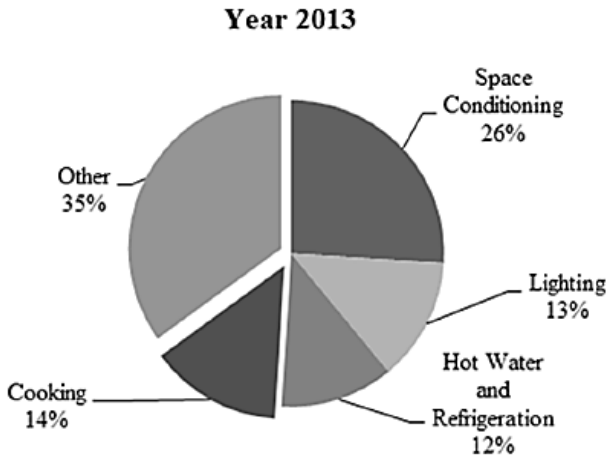

Figure 3.3 Typical energy usage in commercial buildings

3.1.3 Types of Electric Spring

Researchers have proposed three versions of ES. The first version of ES has a capacitor on the DC side of inverter and hence it can only provide or absorb reactive power primarily to perform voltage regulation and DSM. In the second version, capacitor is replaced by a DC source (for example regulated solar cell, electric vehicle battery, or a regular lead acid battery), which results in eight modes of operation of ES (detailed in Section 3.4). Active power exchange becomes possible in the second version of ES. Active suspension concept, as provided by the first two versions of ES, can be used with a shunt type ES to form the third version of ES. Basically, it is an input-feedback bidirectional grid connected power converter. It does not need a noncritical load connected in series. The categorization and operating limits of critical and noncritical loads are discussed in next section.

Schematics of three versions of ES are shown in Figure 3.4.

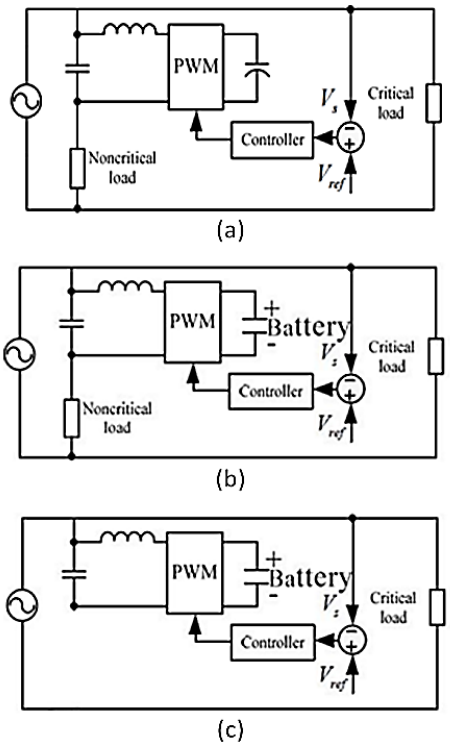

Figure 3.4 Basic circuit implementation of (a) first, (b) second and (c) third version of ES.

3.1.4 Operating Modes of Electric Spring

It has been established from previous discussion that ES is a power electronic interface that generates an AC voltage profile $V_{es}(t)$ to act as a series compensator to modify the applied voltage of the actual load $V_{nc}(t)$thus directly affecting the composition of real and reactive powers flowing to the load. It can be embedded in electric appliances, forming a new generation of smart loads adaptive to the power grid. When massively distributed over the power grid, they could provide highly distributed and robust support for the smart grid, similar to the arrays of mechanical springs supporting a mattress. The smart load is connected to an AC power source with $V_s(t)$ which may represent a strong or a weak power source on a grid network with or without transmission impedance. In this study, we adopt the general assumption that both the power source and the load are

capable of bidirectional power flow, meaning that they can both act as a power source (negatively resistive) or a power sink (resistive).

For a typical load Z of the following types: resistor R, resistor and inductor RL, or resistor and capacitor RC, there are eight possible types of power (voltage) compensation which the ES can support, namely:

1) inductive power ($+jQ_{es}$) compensation;
2) capacitive power ($-jQ_{es}$) compensation;
3) positive real power ($+P_{es}$) compensation;
4) negative real power ($-P_{es}$) compensation;
5) inductive plus positive real power ($+jQ_{es} + P_{es}$) compensation;
6) inductive plus negative real power ($+jQ_{es} - P_{es}$) compensation;
7) capacitive plus positive real power ($-jQ_{es} + P_{es}$) compensation;
8) capacitive plus negative real power ($-jQ_{es} - P_{es}$) compensation

Where P_{es} and Q_{es} are the real and reactive power supplied or absorbed by ES respectively.

In the case of inductive power compensation, the ES emulates the characteristic of an inductor such that it has an inductive voltage drop and it introduces an inductive load power component into the system. The same analogy applies to capacitive power compensation. For positive and negative real power compensations, the ES behaves, respectively, as a positive load resistor (real power sink) that absorbs and negative load resistor (real power source) that injects real power into the system. For inductive plus positive or negative real power compensation, the ES emulates an inductor with,

respectively, a positive or a negative resistor. The same analogy applies to the remaining types of power compensation. A phasor illustration of the three power quantities for the eight possible types of power compensation described previously is depicted in Figure 3.5a-h.

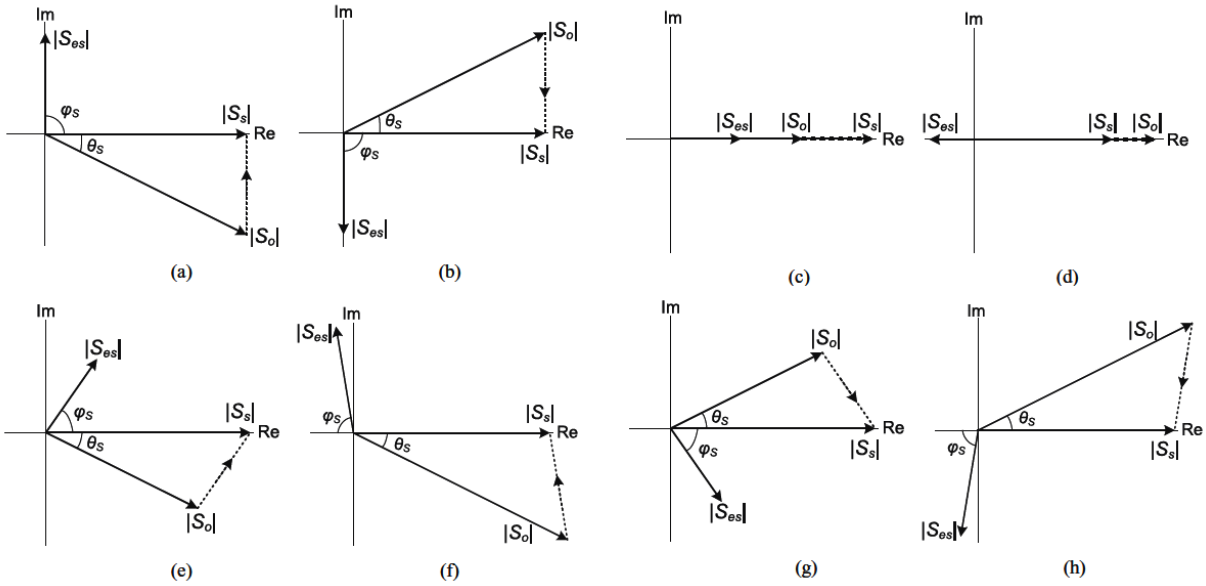

Figure 3.5 Phasor illustration of the three power quantities for different cases of power compensation. (a) Inductive, (b) capacitive, (c) positive real, (d) negative real, (e) inductive plus positive real, (f) inductive plus negative real, (g) capacitive plus positive real, and (h) capacitive plus negative real power (voltage) compensations [4]

where $|S_s|$, $|S_0|$, and $|S_{es}|$, are the magnitudes of the complex power of the power source, the load, and the ES, respectively, and θ_s, and φ_s are the displacement angles of the respective powers with reference to $|V_s|\angle 0$.

3.2 Conventional Control Strategy

This section provides the detailed signal routing of conventional controller based on a closed loop system. The controller feeds a sinusoidal signal to PWM generator of electric spring inverter.

$$V_{pwm} = m \times \sin(\omega t + \phi) \quad (3.1)$$

Modulation index 'm' is obtained by reading the mains voltage, converting it into rms value using DFT and comparing it with the reference rms voltage. This error signal is fed to PI controller which tries to bring the error to zero. After incorporating saturation block, the output of PI is brought between 0 and 1 which will serve as the modulation index to the PWM generator. For phase shift, current is measured from the same branch where ES is installed. The phase of this current is measured using Phase Locked Loop (PLL). In order to get ϕ, 90 degrees are either added to or subtracted from this signal depending on the sign of difference between reference voltage and measured mains voltage to finalize the phase shift of the modulated sinusoidal input for the PWM generator.

Once both signals are obtained, a sinusoidal of amplitude 'm' and phase shift 'ϕ' is generated which is fed into PWM generator of a full bridge inverter which eventually generates the required voltage to maintain the mains voltage and to let the voltage across the noncritical load to vary accordingly. Full bridge inverter increases complexity while modeling but it reduces the number of capacitors and hence less designing is required. Schematic of used inverter is shown in Figure 3.6. If DC voltage of the inverter is represented by V_{dC} , and m represents the modulation signal then output peak voltage is given by

$$V_{ac\,p} = m \times V_{dc} \quad (3.2)$$

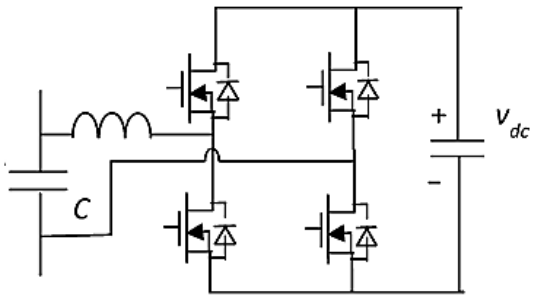

Figure 3.6 Full H bridge inverter topology used in control of single-phase ES [7]

In this manner, voltage across the critical load is regulated. The block diagram of this control strategy is shown in Figure 3.7.

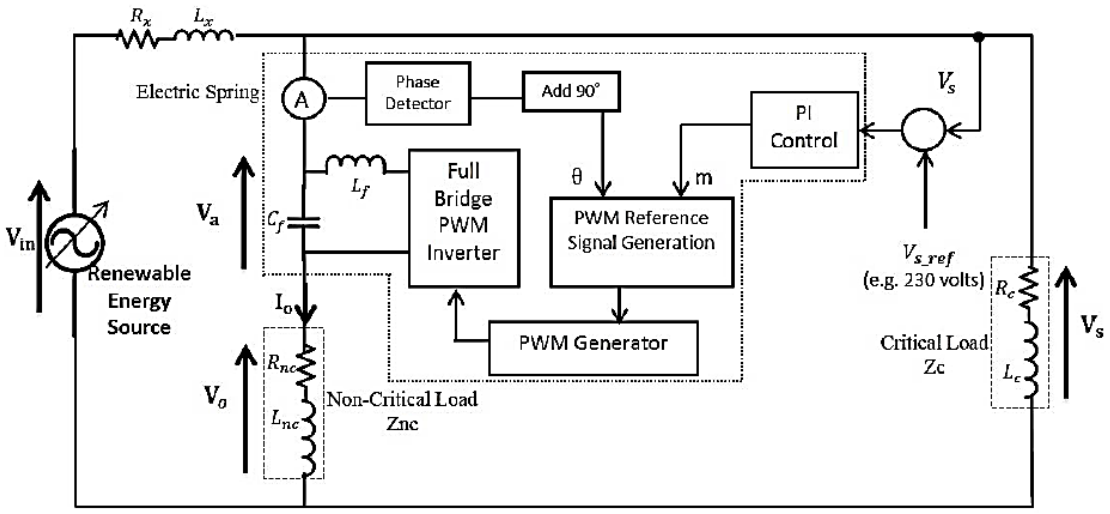

Figure 3.7 Block diagram for control signal of ES (for the testing of voltage fluctuation only)

3.3 Simulation Model

MATLAB simscape toolbox and Simulink environment is used for simulating the proposed control on ES. It is to be noted that in both parts resistive loads are considered for simplicity. Figure 3.8 contains the schematic of the simulation model implemented in Simulink. Table 3.1 contains the simulation parameters details.

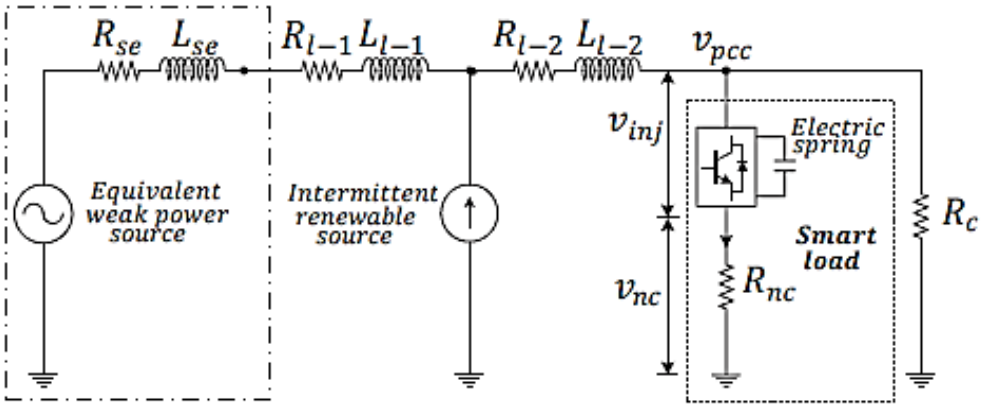

Figure 3.8 Schematic of power network implemented in Simulink

Table 3.1 Details of Simulation Parameters

Voltage of weak power source	110 volts
Lumped line resistance	10Ω
Renewable energy source current	10 A
Frequency of system	60 Hz
Inverter filter inductance	3.8mH
Inverter filter capacitance	13.2μF
Noncritical load	53Ω
Critical load	51Ω
Kp of ES	1.2
Ki of ES	0.05
V_{DC} of inverter	50 Volts
Sampling time of simulation	5 μs

3.4 Results and Discussion

For testing the voltage fluctuation control loop, simulation is carried out such that ES was bypassed by short circuiting for first 2.5 seconds. After 2.5 seconds, it is connected in

series with the noncritical load. Random fluctuations in supply voltage are considered for 5 seconds of simulation time. RMS value of supply voltage changes after every 0.1 second. It can be seen in Figure 3.9 that before enabling ES, the voltage across ES is zero and critical load is facing voltage fluctuation which is highly undesirable. But after 2.5 seconds, when ES comes into action, it stabilizes the fluctuations by providing reactive power support. Voltage across noncritical load is also presented, which essentially follows the pattern of supply voltage for first 2.5 seconds but then noncritical load starts to compensate for critical load and bears even severe voltage fluctuations, as it is designed to operate within ±20% of nominal voltage level, and hence the limits for ES operation is set. ES design specification must consider its operating range which is defined by dc bus voltage and modulation index. In this case, noncritical load is operated within the allowed voltage range and so ES remains within its operating range. Thus it can be said that ES is reducing the voltage fluctuation for critical load which will automatically result in demand supply balance.

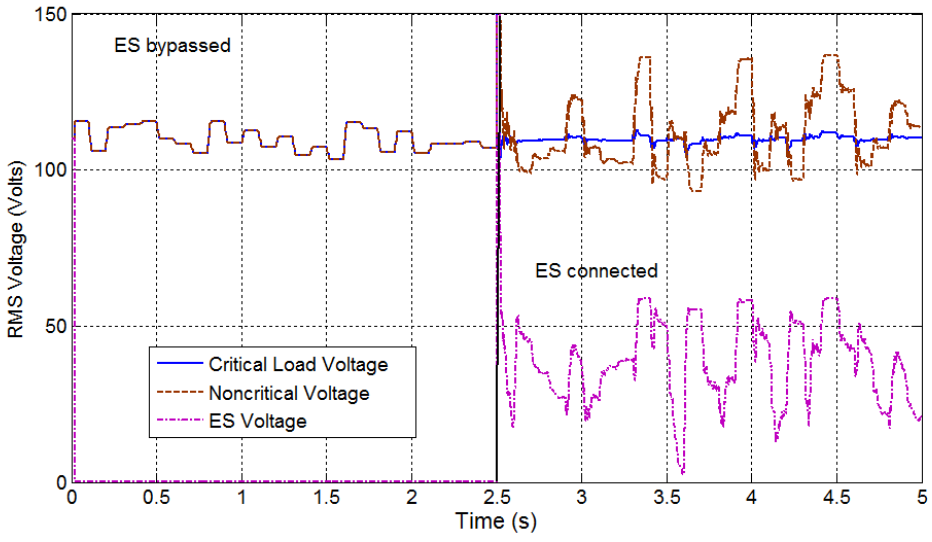

Figure 3.9 Critical load, Noncritical load and ES voltage before and after enabling ES at 2.5 seconds

In Figure 3.10, real power consumed by each load is shown. Before activation of ES, both loads follow the same pattern of power production. Although noncritical load can withstand such power fluctuations, critical load are required to be supplied with constant power. It can be seen that after ES starts operating, it keep the critical load power consumption to be constant, while noncritical load compensates for the remaing power production, keeping demand supply balance.

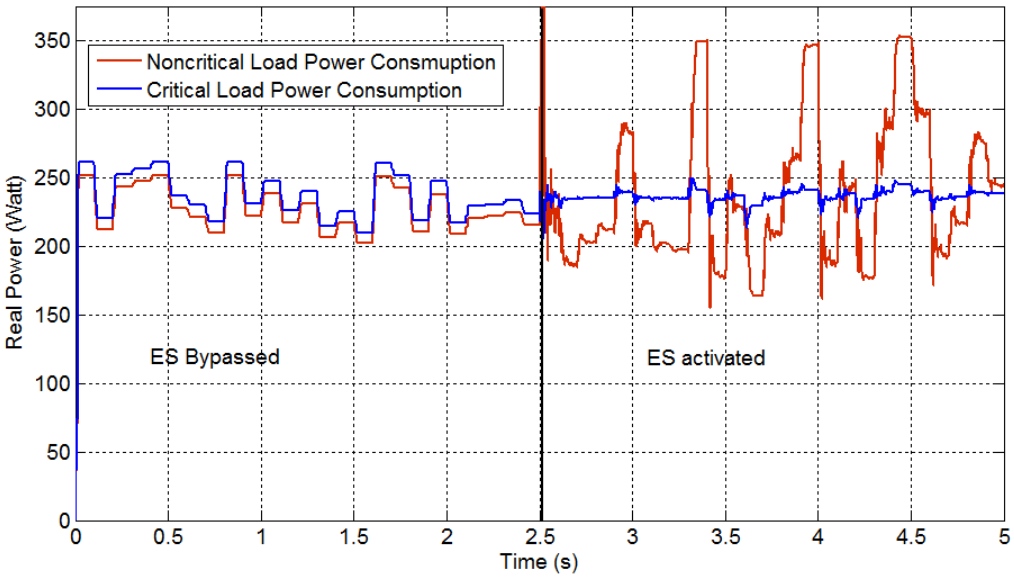

Figure 3.10 Critical load and ES real power consumption before and after enabling ES at 5 seconds

Reactive power compensation is shown in Figure 3.11. When ES is supplying reactive power to increase voltage level at PCC, it works in capacitive mode. The moments in which ES operates in capacitive mode during the simulation are shown by all negative values of reactive power of ES, whereas the positive values of reactive power shows the operation in inductive mode.

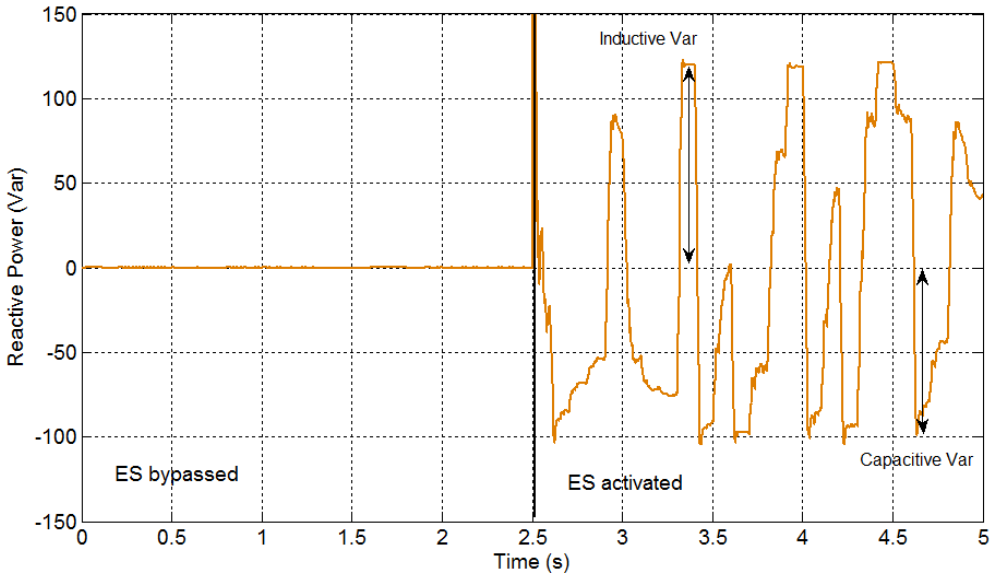

Figure 3.11 Reactive power supplied or absorbed by ES for voltage regulation

Basically, in this chapter primary features of ES are highlighted and simulated on Matlab Simulink. Results obtained substantiate the mathematical equations and theoretical analogies, making it a considerable device to be used in future. Voltage fluctuations are successfully neutralized using conventional control strategy. The dynamic performance of ES is found satisfactory. In next chapter, fuzzy based controllers are designed and implemented to perform voltage regulation.

CHAPTER 4

FUZZY LOGIC BASED CONTROL OF ELECTRIC SPRING FOR VOLTAGE REGULATION

This chapter presents a novel control scheme for electric spring based on fuzzy logic to regulate mains voltage. Simulations are carried out for ES based on conventional PI controller, fuzzy logic controller and adaptive PI (fuzzy PI) and their transient responses are analytically compared. Primarily, a weak grid connected system is modeled with a substantial contribution from renewable energy source. Smart load with a controller based on PI is integrated with the system for the purpose of voltage regulation. Later, the PI controller is substituted with fuzzy logic controller and adaptive PI controller to perform the same task. The proposed controller schemes target an improvement in the dynamic response of the smart load. The transient response of smart load is investigated in sudden voltage variation caused by the presence of renewable energy source

4.1 Controller Designs

In this chapter, design of conventional PI controlled ES is presented first. This is followed by the design of fuzzy logic controller and adaptive PI controller. The output of all three schemes is fed into the PWM generator of ES inverter.

Modulation index ‘m’ is obtained by reading the mains voltage, converting it into rms value using DFT and comparing it with the reference rms voltage. This error signal is fed to the proposed controller schemes (conventional PI, FLC, and adaptive PI), each of

which tries to bring the error to zero. After incorporating saturation block, the output of controller is brought between 0 and 1 which will be served as the modulation index to the PWM generator. For phase shift, current is measured from the same branch where ES is installed. The phase of this current is measured using PLL. In order to get ϕ 90 degrees are either added to or subtracted from this signal, depending on the sign of difference between reference voltage and measured mains voltage to finalize the phase shift of the modulated sinusoidal input for the PWM generator. This control scheme is shown in the Figure 4.1.

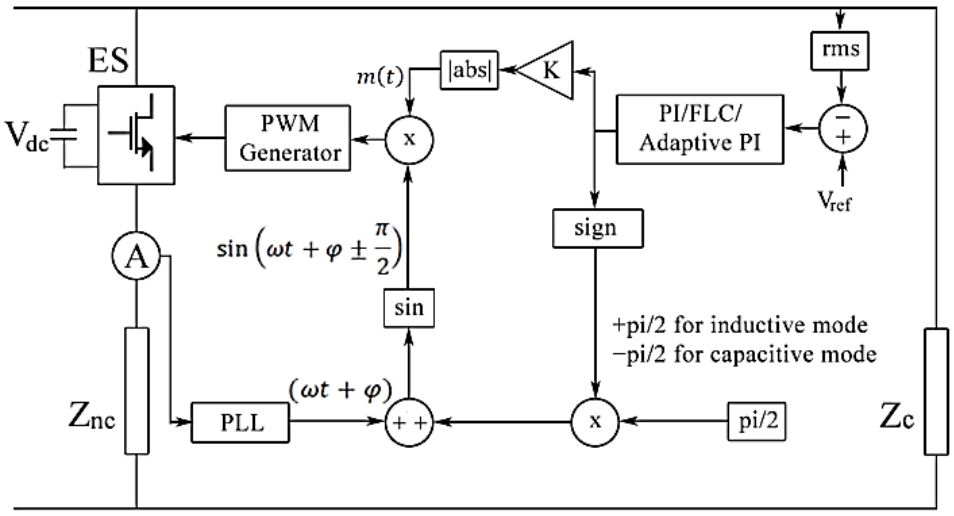

Figure 4.1 Basic control scheme of ES

Once both signals are obtained, a sinusoidal signal of amplitude ‘m’ and phase shift ‘ϕ’ is generated which is fed into PWM generator of full bridge inverter which eventually generates the required voltage to maintain the mains voltage and to let the voltage across noncritical load to vary accordingly. Full bridge inverter increases complexity while modeling but it reduces the number of capacitors and hence less designing is required [7].

$$V_{pwm} = m \times \sin(\omega t + \phi) \tag{4.1}$$

4.1.1 PI Controller

For conventional controller, error signal is fed to the PI block governed by following equation.

$$u(t) = K_p e(t) + K_i \int_o^t e(\tau) d\tau \tag{4.2}$$

The output of PI controller is a weighted sum of the input signal and the integral of the input signal. K_p is the gain constant for proportional part, whereas, K_i is the gain constant for integral part. The proportional and integral gain parameters that could be determined by GA as done in [14] or by linearized analysis of smart load. Another systematic way to tune PI gain constants is known as Ziegler Nichols method [56]. It is a heuristic method to obtain proportional, integral and derivative gains of a PID controller. It involves following steps:

- The integral (K_i) and (K_d) derivative gains are set to zero
- The proportional gain (K_p) is then increased (from zero) until it reaches the ultimate gain (K_u), at which the output of the control loop has stable and consistent oscillations.
- K_u and the oscillation period (T_u) are used to set the proportional, integrator, and derivative gains depending on the type of controller used

Table 4.1 shows the ratios used to determine the gain for each type of controller.

Table 4.1 Gain Parameters Determination using Ziegler Nichols Method

Ziegler Nichols Method			
Controller Type	K_p	$1/K_i$	K_d
P	$0.5K_u$	-	-
PI	$0.45K_u$	$T_u/1.2$	-
PD	$0.8K_u$	-	$T_u/8$
PID	$0.6K_u$	$T_u/2$	$T_u/8$

This method gives an acceptable result for some purposes, but not optimal for all applications. This tuning rule is meant to give best disturbance rejection.

4.1.2 Fuzzy Logic Controller

It has been reported that for performance reasoning and to avoid complexities incorporated by nonlinearities in the system, a linguistic rule approach can be used. Fuzzy logic controller (FLC), determines the control signal by evaluating simple linguistic rules, without requiring any mathematical modeling of given system. FLC requires designer's experience and well inferred input-output relationship for better performance [57].

Fuzzy logic is a convenient way to map an input space to an output space. Mapping input to output is the starting point for the design of FLC. It works by translating the experienced human's inference in to fuzzy rules that what output should be produced for a particular range of input. Fuzzy rules involve simple 'if then' rules and linguistic assignment to the certain ranges of input and output variables. Figure 4.2 is a block diagram of a simple fuzzy system.

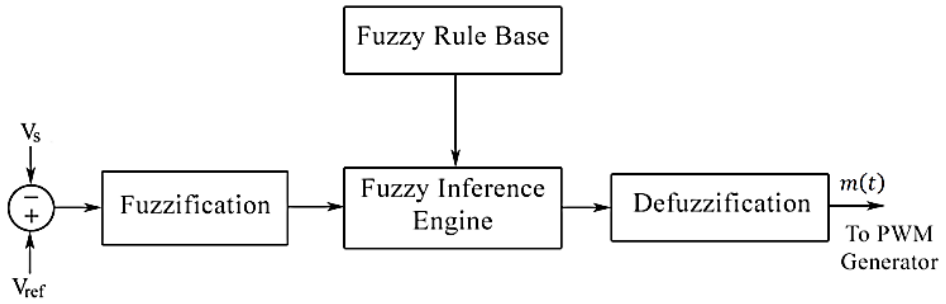

Figure 4.2 Fuzzy logic controller schematic

For the presented case, input variables comprise of error and change in error. Both are defined by triangular membership function. Rules are presented in Table 4.2, where 'E' and 'dE' represent 'error' and 'change in error' respectively. 'NB' and 'NS' are symbols for 'negative big' and 'negative small', whereas, 'PS' and 'PB' are used for 'positive small' and 'positive big' respectively. Zero state is denoted by 'Z'. Mamadani type of Fuzzy inference system is used with centroid defuzzification method [83].

Table 4.2 Fuzzy Rule Base

dE \ E	**NB**	**NS**	**Z**	**PS**	**PB**
NB	NB	NB	NS	NS	Z
NS	NB	NS	NS	Z	PS
Z	NS	NS	Z	PS	PS
PS	NS	Z	PS	PS	PB
PB	Z	PS	PS	PB	PB

4.1.3 Adaptive PI Controller

In adaptive PI controller, the values of K_p and K_i are determined by Fuzzy rule base on runtime. Both gain values are determined by a separate and independent fuzzy inference

system with the sole purpose to bring the error signal to zero. The schematic of adaptive fuzzy control is shown in Figure 4.3. In this case, input variables are defined by triangular membership function whereas output variable are determined by Gaussian membership function as reduced overshoot has been anticipated with it. Here also Mamadani type of Fuzzy inference system is used with centroid defuzzification method.

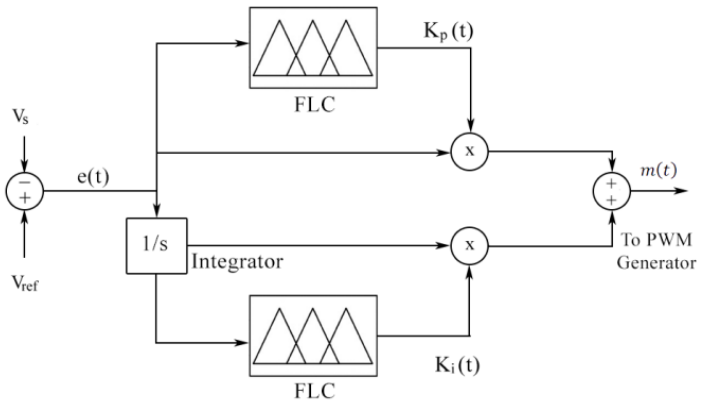

Figure 4.3 Adaptive PI controller

4.2 Simulation Model

MATLAB Simscape Toolbox and Simulink environment is used for simulating the proposed control on ES. Figure 4.4 contains the schematic of the simulation model implemented in Simulink. Table 4.3 enlists the specifications of simulated power system.

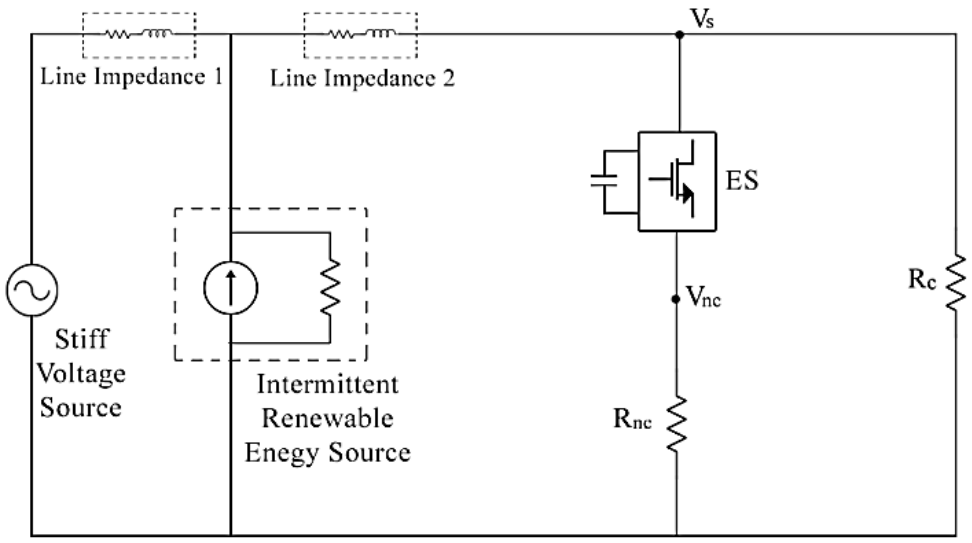

Figure 4.4 Simulation model for voltage regulation

Table 4.3 Detailed Specification of Simulated Power System

System and Loads	
Frequency	60Hz
Open Circuit Voltage of Stiff Voltage Source	190V
Nominal System Voltage V_s	110V
Line Impedance 1	0.6Ω
	2.4mH
Line Impedance 2	0.1Ω
	1.22mH
Renewable Energy Source	Base Reactive Power Injection: 1100 Var
Non-critical Load R_{nc}	50Ω
Critical Load R_c	52Ω
Electric Spring Specifications	
Inverter Type	Single Phase Full Bridge Inverter
Switching Frequency	20kHz
Regulated DC Bus Voltage	300V
DC Bus Capacitance	6000μF
Low-pass Filter Inductance	500μH
Low-pass Filter Capacitance	13.2μF

A stiff voltage source that is weakly connected to the system is modeled by a constant voltage source and high line impedance. From literature it has been adapted that almost 50% of the loads in the system are classified as noncritical loads and rest are critical loads, therefore, critical and noncritical loads are taken as 52Ω and 50Ω respectively. For renewable energy source modeling, a current source with very high parallel impedance is used with a base reactive power profile of 100Var. Inverter of ES is a single phase full bridge inverter with DC bus voltage regulated at 300V. Sampling time of simulation model is 50μs

4.3 Results and Comparison

All three controllers are implemented on following two cases.

- The reactive power injection from the renewable energy source is increased form 1100Var to 1400Var causing a decrement in mains voltage.
- The reactive power injection from the renewable energy source is decreased from 1100Var to 880Var causing an increment in voltage

In Figure 4.5 and Figure 4.6, first case is discussed. It is shown that without ES, system voltage is reduced to 91.25V. It tends to come back to nominal voltage with ES connected to the system. Zoomed region in Figure 4.5 shows the difference between the responses of all three controllers of ES. Conventional PI controller has larger settling time (0.6s) but less overshoot (6.4V) as compared to adaptive PI controller, which has more overshoot (12.3V) but settling time is less (0.3s). With FLC, it can be seen that there is a steady state error but overshoot and settling time are the least. Voltage (rms) across ES terminals is shown in Figure 4.6 for all three controllers. As expected, adaptive

PI based ES reaches the steady state earlier than PI based ES, whereas FLC based ES has lower steady state value. The change in reactive power causing this disturbance in system voltage level is shown in Figure 4.7.

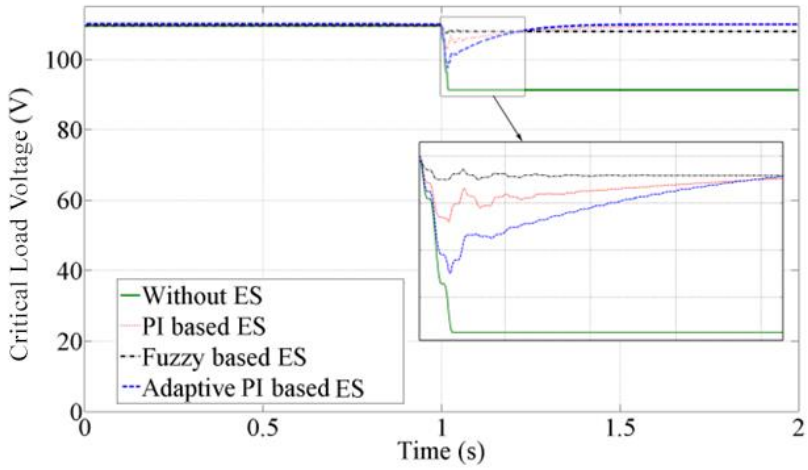

Figure 4.5 Critical load voltage when reactive power injection is increased to 1400Var creating a voltage decrease (ES operating in capacitive mode)

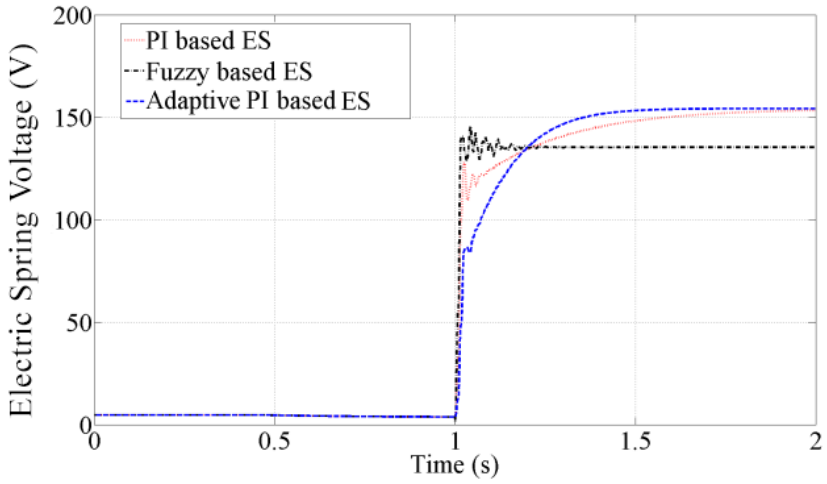

Figure 4.6 Electric spring voltage when reactive power injection is increased to 1400Var creating a voltage decrease (ES operating in capacitive mode)

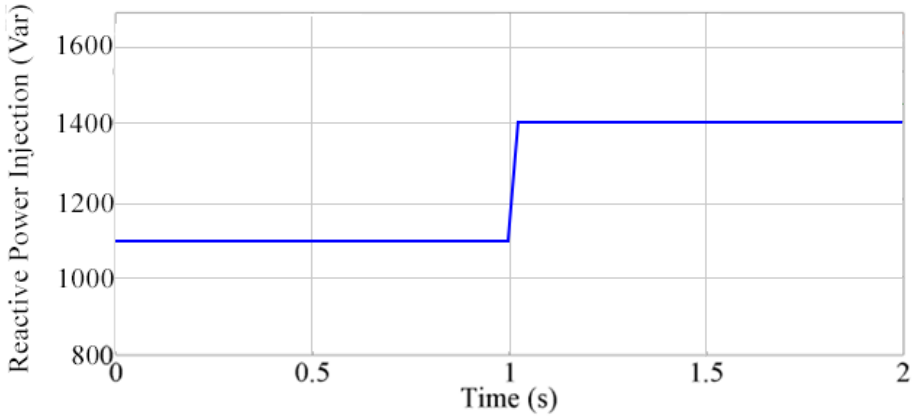

Figure 4.7 Increment in reactive power injection from 1100Var to 1400Var which causes a decrement in main voltage

In Figure 4.8 and Figure 4.9, the second case is discussed. Under this scenario, ES is operated in inductive mode. It tends to decrease voltage across critical load, which was supposed to be increased due to change in reactive power injection from renewable energy source, as shown in Figure 4.8. It is noted that all three proposed controllers are working well for bringing down the voltage to its nominal value. Zoomed area shows the detailed comparison of response of all three controllers. Figure 4.9 shows the ES terminal voltage for all three controllers, when ES is operating in inductive mode. This disturbance is caused by change in reactive power from its base value to 880Var, as shown in Figure 4.10.

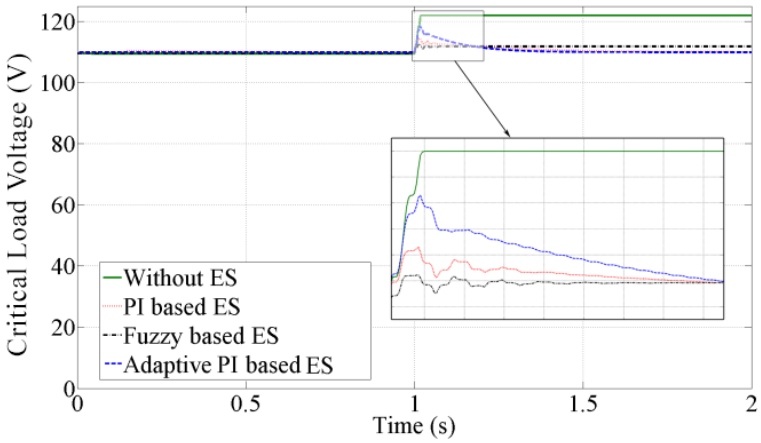

Figure 4.8 Critical load voltage when reactive power injection is decreased to 880Var creating a voltage increase (ES operating inductive mode)

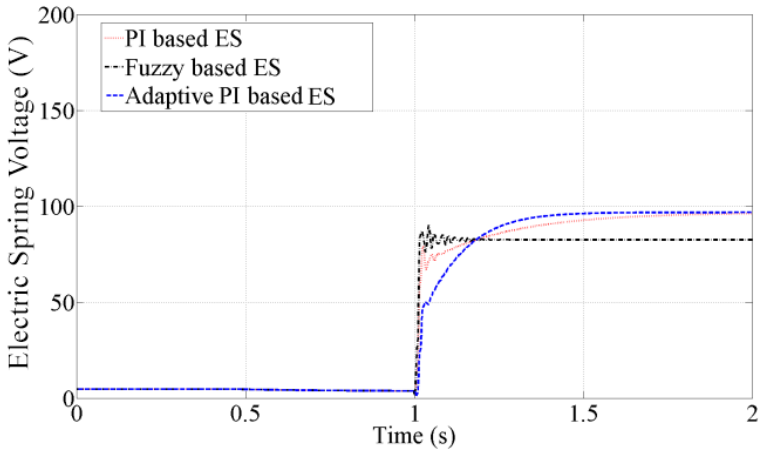

Figure 4.9 Electric spring voltage when reactive power injection is decreased to 880Var creating a voltage increase (ES operating inductive mode)

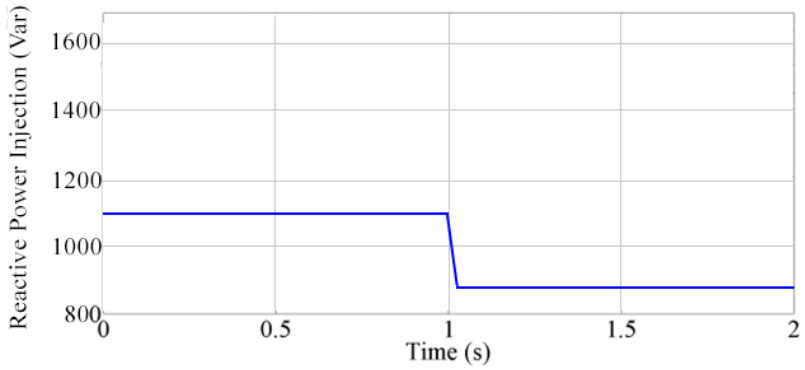

Figure 4.10 Decrement in reactive power injection from 1100Var to 880Var which causes an increase in main voltage

4.4 Conclusion

In this chapter, ES has been operated using FLC and adaptive PI controller for the first time. Three controllers are designed and implemented to operate ES for voltage regulation. Fundamentals proposed controllers are presented followed by simulation model and results indicating the efficacy and comparison of all three controlling techniques. It has been found that each controller has its own pros and cons. PI controller offers less overshoot but settling time is higher, whereas adaptive PI has more overshoot with reduced settling time. FLC controller gives steady state error with improved settling time. It can be said that adaptive PI controller gives the best combination of response parameters. Thus, it is recommended as an alternative to the other two controllers due to its ability to attain steady state faster than conventional PI controller with zero steady state error.

CHAPTER 5

ELECTRIC SPRING FOR NEUTRAL CURRENT MITIGATION

In this chapter, a novel control scheme for three-phase ES is proposed and its mathematical basis is formulated. Theory of operation is illustrated by a phasor diagram. The proposed controller will allow the ES to mitigate neutral current under the condition of unbalanced three phase loads. Simulation results are carried out to support the theoretical framework. A typical three-phase unbalanced power system is used to show the efficacy of the developed controller. The performance of proposed controller is evaluated under dynamic loading condition.

5.1 Background

Power imbalance in three phase four wire system due to unbalanced load is a major concern for sophisticated power systems. Neutral current, a direct consequence of unbalanced loads, has a deteriorating effect on key components of power system such as induction motors, electric drives and voltage source inverters [58]. Adverse effect of neutral current also includes increased system loss and reduced system efficiency [59]. Moreover, unbalance line currents result in asymmetric voltage drops in the network, causing an overall reduction in power quality [60]. To resolve this major concern several methods have been used [61]. Three-phase to single phase static or rotary converter is sometimes used to feed single phase load. Another way to mitigate neutral current is to

use rotating equipment to absorb negative sequence component [63]. Three-phase to single phase transformer is also used to serve this purpose. All these conventional methods are less efficient and costly [61]. With the advent of modern power electronic devices, new solutions are developed to improve power quality and reduce neutral current. Shunt active filter has been used as reactive power compensator to reduce load imbalance [62]. A mixture of several techniques can be used, where active filter is used to redistribute real power, keeping total real power constant, and on the other hand positive, negative and zero sequence components are compensated independently or together. Such techniques are presented and evaluated [62]–[66].

In [22]–[24] ES has been used to reduce three phase load imbalance. Reference [22], [23] presents an independent control of three phase ES with control parameters being evaluated using GA, whereas, in [24] three phase ES is connected to system via isolation transformer in a built environment with a controller based on impedance estimation. GA based controller makes the controller unnecessary complicated which results in reduced computational efficiency. The approach used in [24] is direct and convenient but it lacks depth and significant simulation results.

In the following sections, a novel control scheme, based on run time impedance measurement, is proposed to mitigate neutral current from unbalanced three-phase system. Mathematical analysis is also given and corresponding simulations are carried out to substantiate the theoretical framework. Simulation results show the efficacy of presented technique under various unbalanced loading conditions.

5.2 Proposed Control Scheme

5.2.1 Three-phase Extension of Electric Spring

Single phase ES can be extended to three-phase ES as shown in Figure 5.1. Here the placement of star connected noncritical and critical loads is illustrated in a typical three phase power system. A controller sends switching signals to three-phase inverter of ES based on the measurement taken from different nodes in the circuit. Controller can be programmed to achieve various tasks. It is shown that controller is programmed such that each phase of ES generates a voltage which brings the balance in overall impedance of the load.

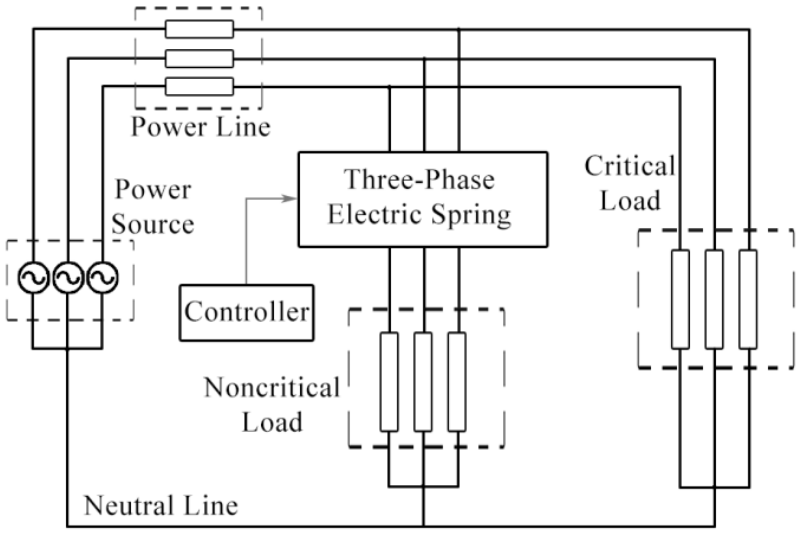

Figure 5.1 Circuit diagram of typical three-phase power system with ES

5.2.2 Theoretical Framework

In the following derivation, it is considered that critical loads tend to be unbalanced three-phase loads whereas noncritical loads always remain balanced. Neutral current will be mitigated if source sees same impedance for each of the three phases. Therefore, ES is

required to balance the equivalent impedance of the network. In case of balanced critical loads, ES will not operate and equivalent impedance as seen at the point of common coupling (PCC) is given by

$$Z_{eq_{a,b,c}} = Z_c || Z_{nc} \tag{5.1}$$

Where,

$$Z_c = Z_{c_a} = Z_{c_b} = Z_{c_c} \tag{5.2}$$

In above equations Z_{c_a}, Z_{c_b}, Z_{c_c} represents the critical load impedances of phase A, phase B and phase C, respectively. Z_{nc} represents the phase impedance of noncritical load. In this analysis noncritical load will be a balanced load for all cases, therefore, each phase impedance is indicated by Z_{nc}. When critical load is unbalanced, $Z_{c_a} \neq Z_{c_b} \neq Z_{c_c}$, it is suitable to determine the average impedance of unbalanced loads $Z_{c_{avg}}$.

$$Z_{c_{avg}} = \frac{Z_{c_a} + Z_{c_b} + Z_{c_c}}{3} \tag{5.3}$$

For unbalanced loads, ES will come into action. It redistributes real power among each phase, such that the total impedance as seen by the source is balanced out. Now the equivalent impedance of each phase is given by:

$$Z_{eq_{a,b,c}} = Z_{c_{avg}} || Z_{nc} = Z_{c_{a,b,c}} || (Z_{nc} + Z_{ES_{a,b,c}}) \tag{5.4}$$

where $Z_{ES_{a,b,c}}$ is the impedance offered by ES in response to unbalanced loads for corresponding phases. Solving (5.4) for $Z_{ES_{a,b,c}}$ results in:

$$Z_{ES_{a,b,c}} = \frac{Z_{nc}^2(Z_c - Z_{c_{a,b,c}})}{Z_{nc}Z_{c_{a,b,c}} + Z_{c_{avg}}Z_{c_{a,b,c}} - Z_{nc}Z_{c_{avg}}} \quad (5.5)$$

The vector voltage that has to be produced by ES (denoted by $V_{ES_{a,b,c}}$) in order to achieve load balancing is determined by voltage divider rule, as shown below:

$$V_{ES_{a,b,c}} = \left(\frac{Z_{ES_{a,b,c}}}{Z_{ES_{a,b,c}} + Z_{nc}}\right) V_{pcc_{a,b,c}} \quad (5.6)$$

where V_{pcc} is the corresponding phase voltage at point of common coupling.

5.2.3 Phasor Diagram

Figure 5.2 shows the phasor diagram associated with proposed control strategy. Noncritical load is considered to be a balanced three phase load, whereas critical loads are unbalanced. This can be seen on Figure 5.2a. Without ES, noncritical load phase currents $I_{nc_{a,b,c}}$ are equal in magnitude and symmetric in phase. On the other hand, critical load phase currents $I_{c_{a,b,c}}$ are unbalanced and hence causing the net current $I_{A,B,C}$ to be unbalanced (Figure 5.2b). When ES is connected with the system, it rearranges the real power distribution by controlling the current of noncritical load branch, which enables the net current vectors to be symmetric and balanced, eventually resulting in neutral current mitigation.

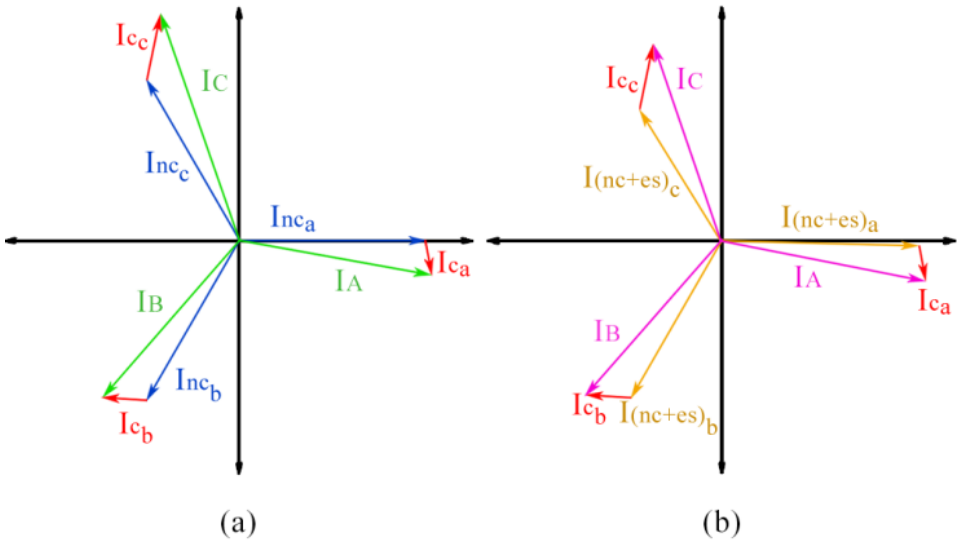

Figure 5.2 Vector diagram of currents of an unbalanced system (a) without and (b) with ES

5.3 Control Scheme Implementation

MATLAB Simscape Toolbox and Simulink environment is used for simulating a typical three-phase unbalanced power system and the designed controller on ES.

5.3.1 Flow Diagram

Figure 5.3 illustrates the steps of computation performed by the proposed controller. Based on current and voltage readings, impedance of each phase of noncritical load is estimated followed by determining average phase impedance. Impedance required to offer by each phase of ES is calculated using equation (5.5). Reference voltage of each phase of ES is set to the value computed by equation (5.6), which allows ES to redistribute real power among three phases, and hence achieving neutral current mitigation.

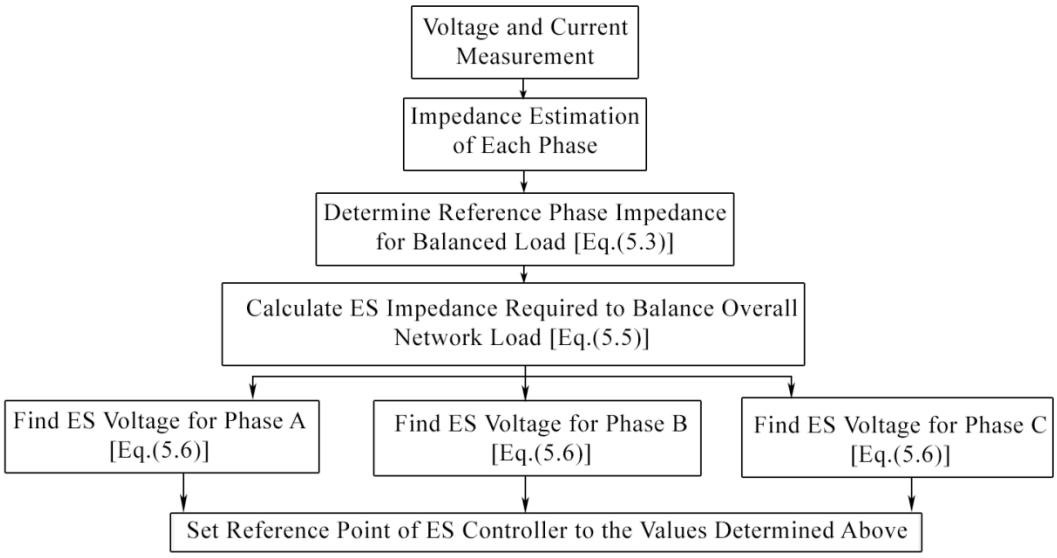

Figure 5.3 Flow chart of control algorithm of three-phase ES

5.3.2 Simulation Model Details

Simulated power system network is illustrated in Figure 5.4. Both critical and noncritical loads are star connected with a stiff balanced source feeding the loads at 220V and 50 Hz. Detailed specifications of the balanced noncritical load and unbalanced critical loads are given in Table 5.1. Sampling time of simulation model is 50µs.

Table 5.1 System's Impedance Specifications

	Phase A	Phase B	Phase C
$Z_c(\Omega)$	2+11.05j	4+8j	4.5+4j
$Z'_c(\Omega)$	1.5	1.2+3.1j	0.5+12.5j
$Z_{nc}(\Omega)$	2	2	2
V_S (V)	$220\angle 0$	$220\angle 240$	$220\angle 120$

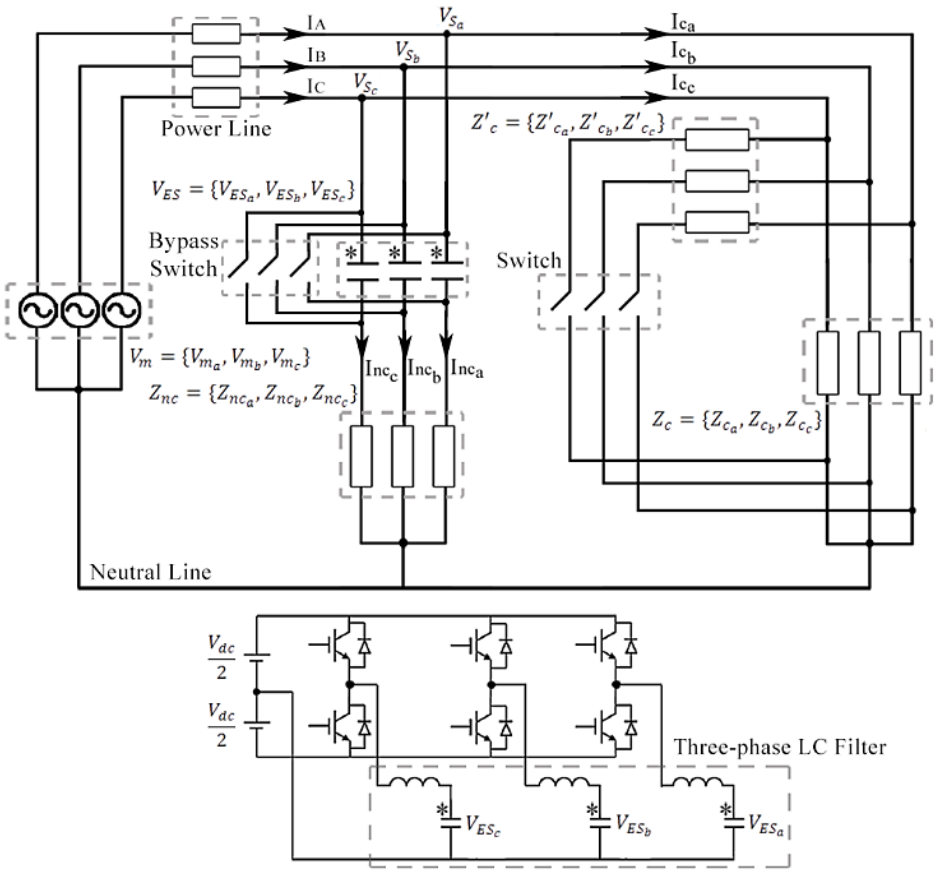

Figure 5.4 Simulation diagram of power system with unbalanced critical load and dynamic loading

5.4 Results and Discussions

Two simulation scenarios are presented. First the impact of ES in the system is shown. This is followed by dynamic loading condition test. These simulation scenarios are listed below:

- To check the impact of ES, an unbalanced three phase system will be simulated for 0.4s. ES will come into action at 0.2s.
- In next simulation, there are four intervals in the total simulation time of 0.8s. First interval ranges from 0s to 0.2s during which ES is bypassed and only one

three-phase critical load Z_c is connected to the system. In second interval, which ranges from 0.2s to 0.4s, ES is operational to mitigate neutral current caused by unbalanced Z_c. Later, in third interval ES is bypassed again, and three-phase load is changed by connecting Z'_c in parallel with Z_c. In last interval, ES is activated to mitigate the increased neutral current.

Results of first scenario are presented in Figures 5.5-5.8. Simulation is carried out for 0.4s in an unbalanced three phase circuit. For first 0.2s, ES is bypassed using a bypass switch as shown in Figure 5.4. In Figure 5.5, it can be seen that without ES, net current driving the load is unbalanced ($I_A = 115.7\angle 350.4°$ A, $I_B = 122\angle 229.7°$ A and $I_C = 138.6\angle 110°$A). Neutral current for initial 0.2s is given by $21.68\angle 124.34°$ and is shown in Figure 5.6. After 0.2s of simulation, the bypass switch is opened enabling ES operation. Conforming to the theoretical analysis, neutral current is mitigated to $0.4\angle 8°$. It can be noted that in Figure 5.5 after 0.2s, all three phase currents have same magnitude with a phase difference of almost $120°$ ($I_A = 123\angle 348°$ A, $I_B = 123\angle 229°$ A and $I_C = 123\angle 108°$A).

Figure 5.7 and Figure 5.8 illustrate the waveform of voltages across ES and noncritical load. Voltage across each phase of ES terminals is approximately same as calculated by equation (5.6). The voltage at noncritical load, which is vector subtraction of $V_{ES_{a,b,c}}$ from $V_{S_{a,b,c}}$, is represented in Figure 5.8.

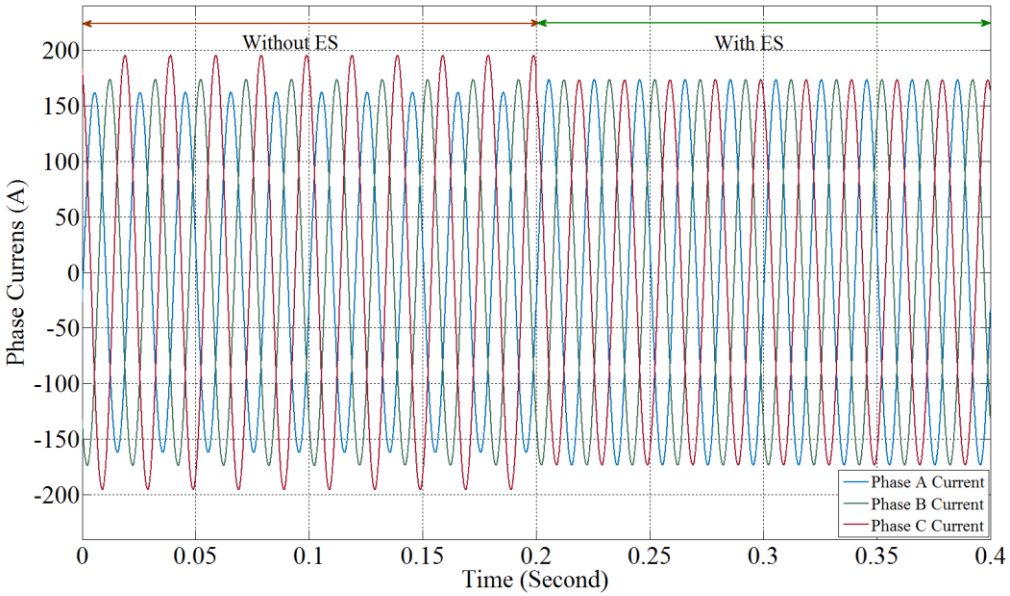

Figure 5.5 Supplied current waveform of each phase before and after activating three-phase ES

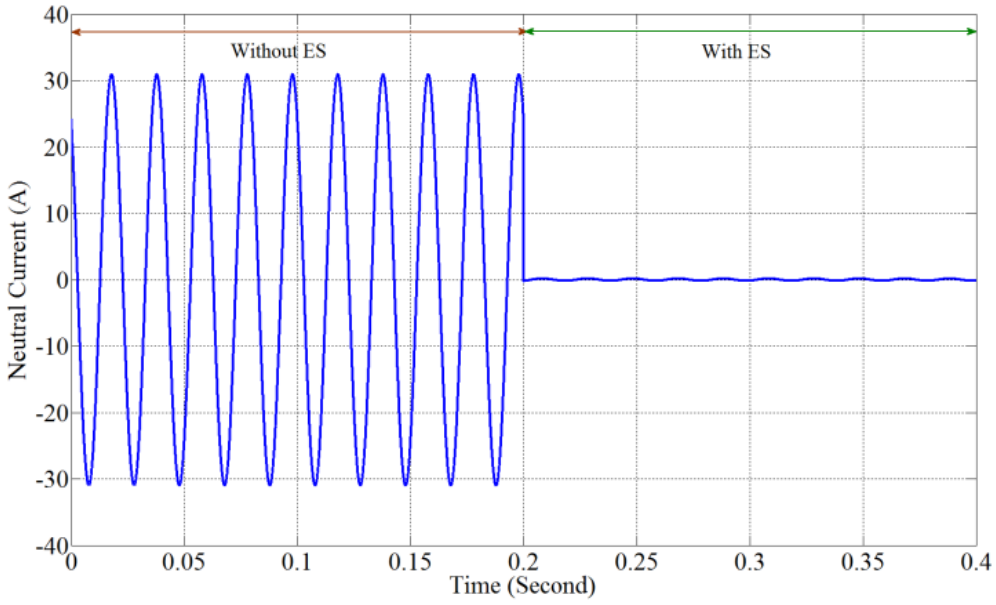

Figure 5.6 Neutral current waveform before and after activating three-phase ES

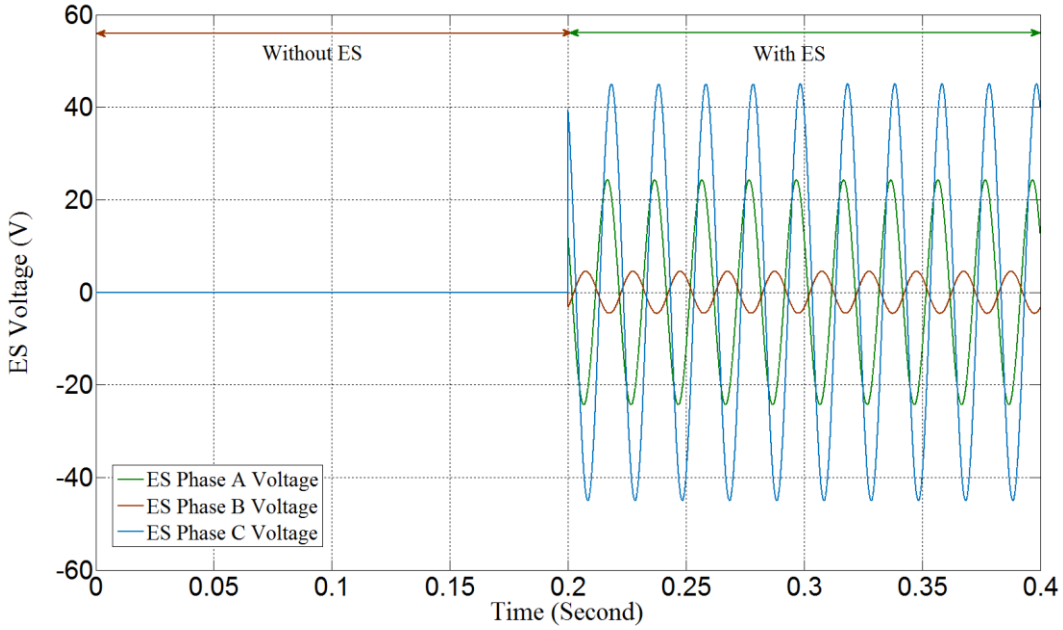

Figure 5.7 Three-phase voltage of ES load before and after activating three-phase ES

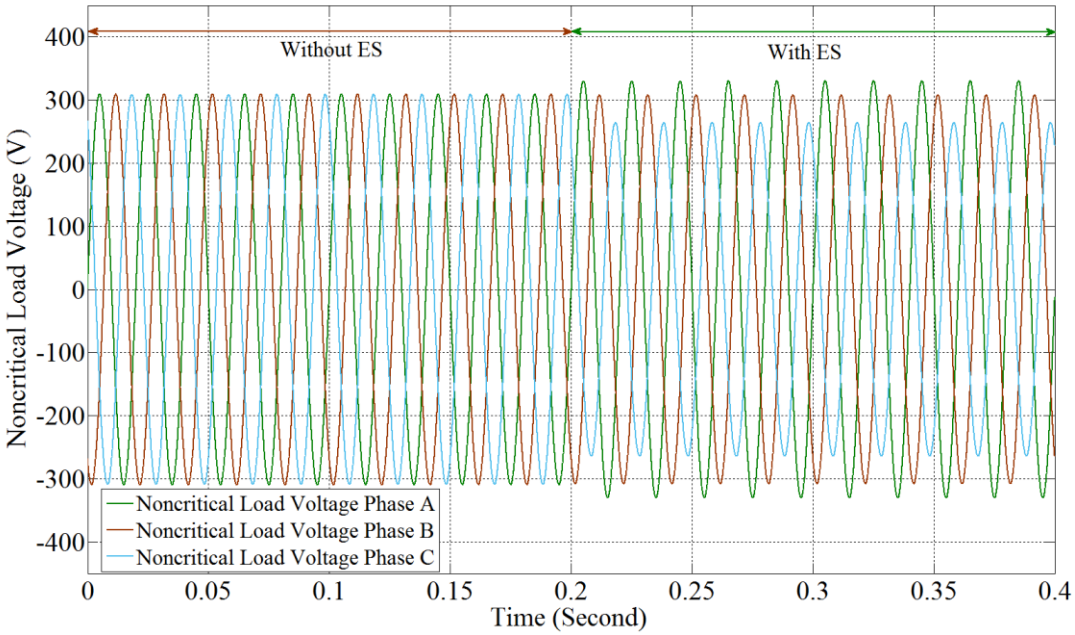

Figure 5.8 Three-phase voltage of noncritical load before and after activating three-phase ES

It is important to note that after connecting ES, voltage across noncritical load is unbalanced and so is the current of each phase of that branch but net current is balanced and so neutral current is mitigated. In other words it can be said that ES redistributes power in each branch of noncritical load such that the adverse effect of unbalanced critical load is eliminated.

In second scenario, dynamic loading conditions and adaptability of ES to sudden load change is tested. Simulations are carried out for 0.8s, as depicted in Figures 5.9-5.11. For first 0.4s, system is simulated with same settings and therefore, similar results are obtained. After 0.4s an additional three-phase critical load Z'_c is connected in parallel to existing load as shown in Figure 5.4. It can be seen in Figure 5.9 that neutral current of the system is increased from 21.68A to 89.19A. But after 0.6s, ES is again activated which brings the neutral current back to 0.72A.

Under dynamic load changing, concept of active power distribution to mitigate neutral current is presented below. Active and reactive powers supplied and/or absorbed by ES during the simulation runtime is illustrated in the Figure 5.10. Time intervals in which ES is bypassed have necessarily zero real and reactive powers, whereas, in remaining time intervals, real and reactive power is supplied and/or absorbed as determined by the control algorithm.

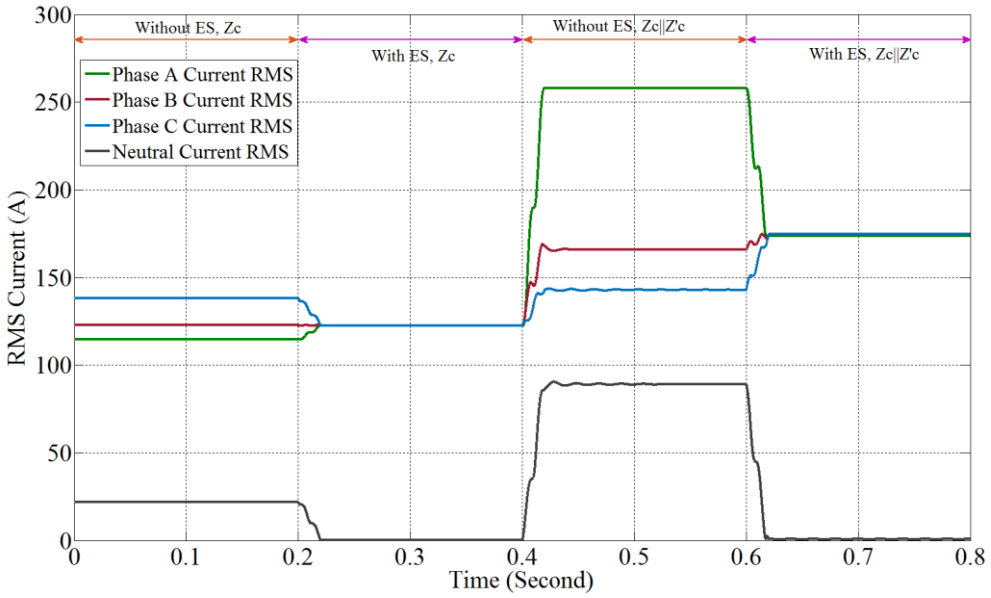

Figure 5.9 RMS phase and neutral currents before and after changing three-phase critical load

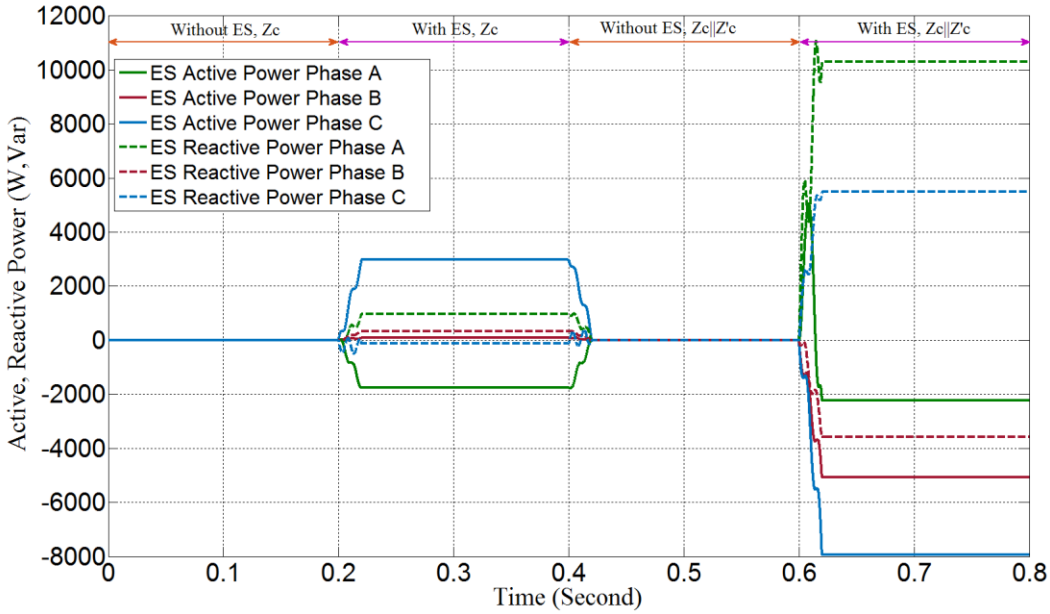

Figure 5.10 Active and reactive power absorbed and/or supplied by ES

As a result, each phase of noncritical load absorbs different real power when ES is operational. On the other hand, when ES is bypassed (0s-0.2s and 0.4s-0.6s), each phase of noncritical load consumes same real power of 24.2kW, as shown in Figure 5.11. Consequential results are obtained for the curves of active power absorbed by noncritical

load. It is to be noted that since noncritical load is considered to be resistive, only real power consumption is observed.

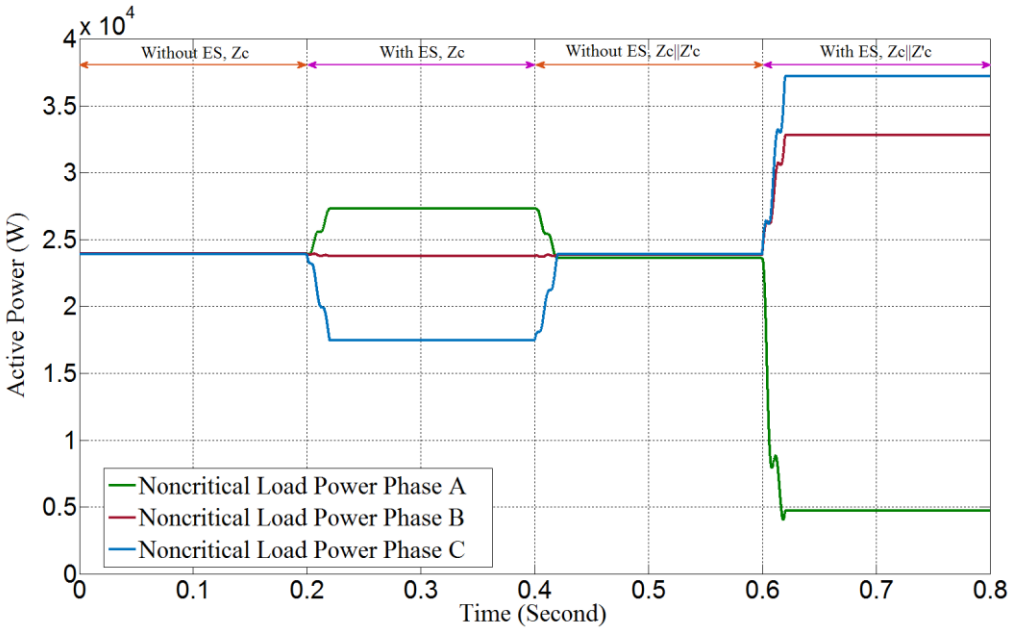

Figure 5.11 Active power absorbed by each phase of noncritical load

5.5 Conclusion

In this chapter, an impedance estimation based control technique is developed to drive ES for neutral current mitigation. Concept behind this approach is presented first by mathematical equations and then explained by phasor diagram. MATLAB Simulink based simulations are performed under dynamic loading condition. It is found that proposed control approach is successful in balancing the unbalanced three-phase load. Under dynamic loading, smart load is able to detect the change and respond accordingly. Therefore, a same physical a same physical device can be used to perform wide range of tasks including voltage regulation, power factor correction and neutral current mitigation depending on the control algorithm used to operate ES.

CHAPTER 6

ELECTRIC SPRING CONTROLLER FOR DISTRIBUTION NETWORK LOADED BY ELECTRIC VEHICLES

6.1 Background

In this chapter, voltage drop caused by electric vehicles (EVs) incorporation is dealt with a relatively new concept of electric spring (ES). A novel control scheme is developed to operate ES in order to support the voltage across a distribution network. Mathematical basis behind the control scheme is presented along with the associated phasor diagram. A typical distribution network is realized and proposed controller on ES is tested under dynamic integration of EVs.

An alarming rise in global warming, CO_2 emissions and greenhouse effect has encouraged the use of environmental friendly means of energy production and consumption. Battery powered zero emission electric vehicles (EVs) are expected to reduce the growing concerns over CO_2 emissions caused by current transportation system running on fossil fuels. Although contemporary vehicles are still considered to be the dominant source of transportation, but issues like inconsistent oil price and carbon emission have become the prime reasons of worldwide inclination towards EVs. Plug-in

electric vehicles (PEVs) are proven to be more environmental friendly than both hybrid and battery EVs [67].

EVs can be charged by plugging into electrical outlets available at home, commercial charging stations or community centers. To accommodate the additional load caused by an enormous number of EVs on current distribution system, certain measures are required to be taken. To predict the change in load demand caused by EVs, several models have been reported [68]–[70]. By 2030, it is expected that EVs will make 5% of the total electrical load of Belgium [71]. However, simultaneous charging of multitude of EVs can cause severe problems in the existing distributions systems including increased power loss, voltage drop and overloading of feeder and transformers. These issues reduce system reliability and efficient operation of electrical devices and hence are considerable for both system operator and consumers. System operator promotes the charging of EVs in night to reduce network overloading in peak hours and to keep the operation of base power plants uninterrupted avoiding additional generator startup resulting in improved overall efficiency [72]. Adverse effects of EV integration on load curve are discussed in [68], [73]. In [74], [75] losses in the distribution system caused by EVs are minimized by appropriate charging schedules. Reference [76] presents an adaptive EV charging controller implemented in real time digital simulator, whereas [77] proposes an adaptive voltage-feedback controller for an onboard EV charger.

Voltage profile of a distribution network is adversely affected by heavy and imminent penetration of EVs. Various techniques have been reported to reduce the voltage drop caused by EVs integration [71], [78]–[80]. EVs are modeled as PQ buses implying that they can provide reactive power for voltage support using the self-commutation of EVs

inverter. In [71], [78], a fleet of 300 EVs is integrated in IEEE-14 bus system as PQ bus and voltage is regulated using reactive power control. This approach along with queuing theory and stochastic power demand is also used in [81]. Load flow studies with constraints on power generation (wind farm) and power demand (EVs) have been reported in [82]. On the other hand, a typical distribution system is implemented in [80], [83] . Voltage profile is regulated by both active and reactive power management while introducing a communication scheme among EVs to enhance the performance. But on the downside, reactive power control will require modification in available EVs' inverter control. Moreover, this approach has certain limitations in terms of reactive power transfer based on battery's storage capacity. For communication between EVs, an enhanced infrastructure is required.

It can be said that although electric vehicles offer a viable mean of commuting, their widespread penetration can have adverse effects on the current electrical distribution networks due to voltage drop and overloading of distribution transformers. In this work, a novel control scheme is proposed and implemented to support the voltage profile of a typical distribution network loaded by electric vehicles. Electric spring, a real/reactive power compensator, is driven by the proposed controller in order to provide voltage support under dynamic loading conditions. It has been suggested that reference voltage to be produced by electric spring is continuously determined and then compared with the instantaneous voltage across electric spring terminal in a closed loop configuration. The proposed controller is tested under various loading conditions to evaluate its overall performance. Results show that electric spring can be successfully used to fix the

problem of voltage drop caused by the sudden and simultaneous charging of EVs without modifying EVs inverter control and communication infrastructure.

6.2 System Fundamentals

Since real power transfer is necessary for this application, second version of ES is used. Average switching model, as discussed in Chapter 3, is put to use here again. This enables ES to operate in one of the two modes shown in Figure 6.1.

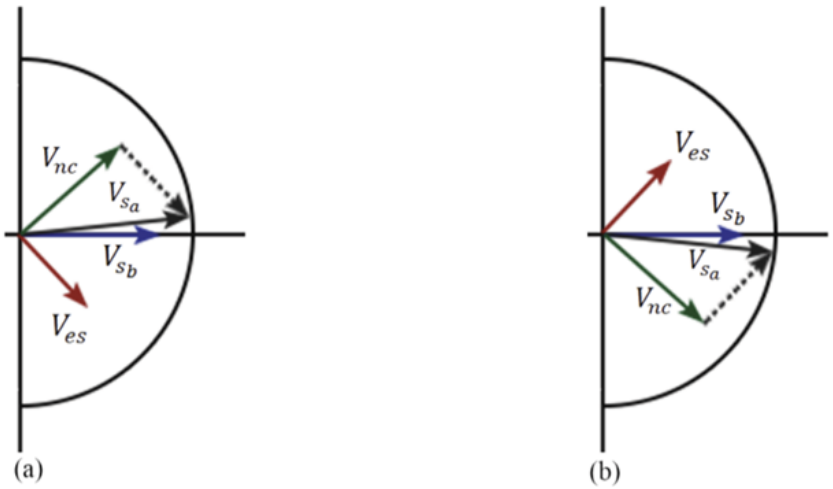

Figure 6.1 Phasor representation of two modes; (a) capacitive plus positive real power and (b) inductive plus real power of second version of ES as used by the controller

As far as EV modeling is considered, EV is usually modeled by an inverter connected with a battery. Usually chemical storage devices are used as a battery in an EV. In its simplest form, EV is modeled as a load which consumes real power while charging according to state of charge and battery dynamics. Schematic of an EV model is shown in Figure 6.2.

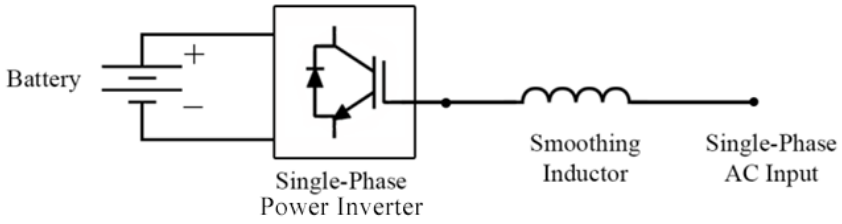

Figure 6.2 Single-phase inverter based ES schematic

6.3 Proposed Controller Design

6.3.1 Theoretical Framework

In the following derivation, it is considered that common household loads are categorized into two categories based on their operating voltage range, critical and noncritical loads. The purpose of proposed controller is to use ES such that it offers impedance which reverts back the net current flowing into a node to its initial value (before EV plugging). Basically, ES redistributes power between itself and noncritical load. Without plugging in EV, the combined load of a household is given by equation (6.1), where Z_c and Z_{nc} represent critical and noncritical load respectively.

$$Z_{eq} = Z_c || Z_{nc} \tag{6.1}$$

When EV is plugged in to the system, it can be modeled as parallel time-varying impedance Z_{ev} depending on battery charging capacity and state-of-charge [80]. In this derivation, instantaneous effect of EV is taken into account. Now the net impedance seen from a node is the parallel combination of three types of load (critical, noncritical and electric vehicle), as shown by equation (6.2).

$$Z_{eq} = Z_c || Z_{nc} || Z_{ev} \tag{6.2}$$

As soon as controller detects the change in overall impedance, it activates ES to offer the required impedance Z_{es} such that the total impedance can be brought back to its previous value. This is shown in equations (6.3) and (6.4).

$$Z_c || (Z_{nc} + Z_{es}) || Z_{ev} = Z_{eq} \tag{6.3}$$

$$Z_c || (Z_{nc} + Z_{es}) || Z_{ev} = Z_c || Z_{nc} \tag{6.4}$$

Solving (6.4) for Z_{es} results in:

$$Z_{es} = \frac{Z_{nc} Z_c Z_{c1}}{Z_{c1} Z_{nc} + Z_c Z_{c1} - Z_{nc} Z_c} - Z_{nc} \tag{6.5}$$

Where,

$$Z_{c1} = Z_c || Z_{ev} \tag{6.6}$$

The vector voltage that has to be produced by ES (denoted by V_{es_ref}), in order to achieve voltage regulation, is determined by voltage divider rule, as shown below:

$$V_{es\_ref} = \left(\frac{Z_{es}}{Z_{es} + Z_{nc}} \right) V_s \tag{6.7}$$

where V_s is the desired node voltage in the distribution line.

6.3.2 Block Diagrams

Figure 6.3 illustrates the steps of computations performed by the proposed controller. Based on current and voltage readings, impedance at each node is monitored. Once a major change is detected in the impedance level, the controller activates ES. Updated impedance value is used by the controller to compute the impedance that is required to be

offered by ES using equation (6.6). Reference voltage of each household's ES is set to the value computed by equation (6.8), which allows ES to offer impedance that brings back the impedance of the node to previous value, eventually reducing the line loss and increasing the node voltage.

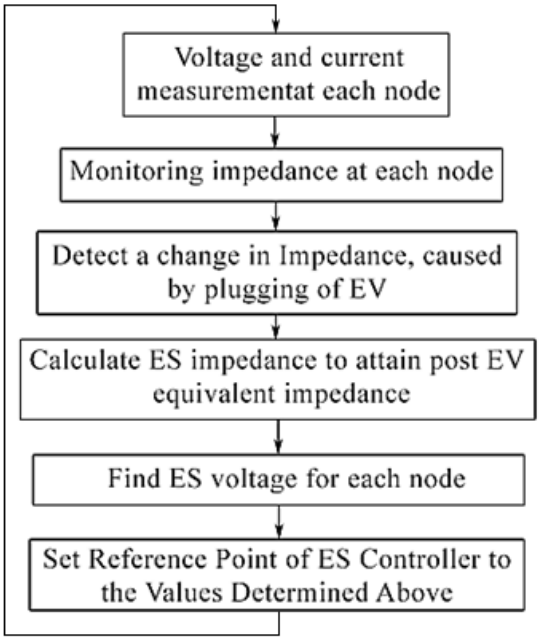

Figure 6.3 Flow chart of proposed control algorithm

Reference voltage of ES, as determined above, is decomposed into its magnitude and phase. This reference magnitude is compared with the instantaneous voltage magnitude of ES, and the error signal is fed into PI controller, followed by a saturation block to keep the amplitude of modulation signal between 0 and 1. On the other hand, phase of the reference signal is added to that of mains voltage, and corresponding sinusoidal wave is generated. Finally, the modulation signal is fed into PWM generator to produce switching pulses that will eventually drive the single-phase full-bridge inverter as discussed in Chapter 5. A simplified model of this closed loop control scheme is shown in Figure 6.4.

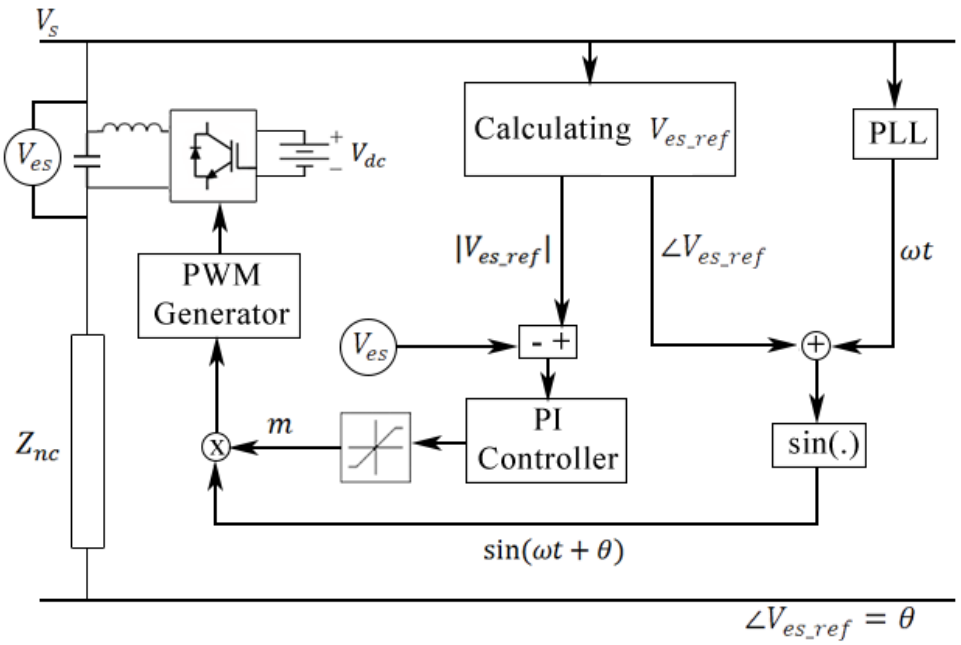

Figure 6.4 Closed loop control scheme for ES

6.4 Simulation Details

MATLAB Simscape Toolbox and Simulink environment is used for validating the functioning of proposed controller. A typical distribution network is developed with five primary nodes (#1~#5) connected with a distribution substation (#S) as shown here in Figure 6.5.

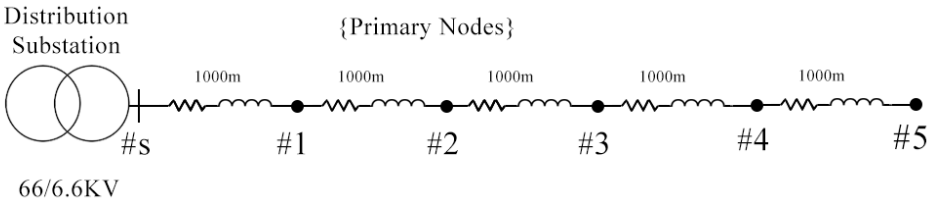

Figure 6.5 Primary feeder model

Voltage at distribution substation is set to be 6.6kV. In this work, the farthest node (#5) is considered since it will have the worst effect of EV integration. Each primary node has several number of pole transformers which is providing electricity connection to four

secondary nodes, 40 meters apart from each other (#5a~#5d for 5th primary node). First primary node is depicted in Figure 6.6.

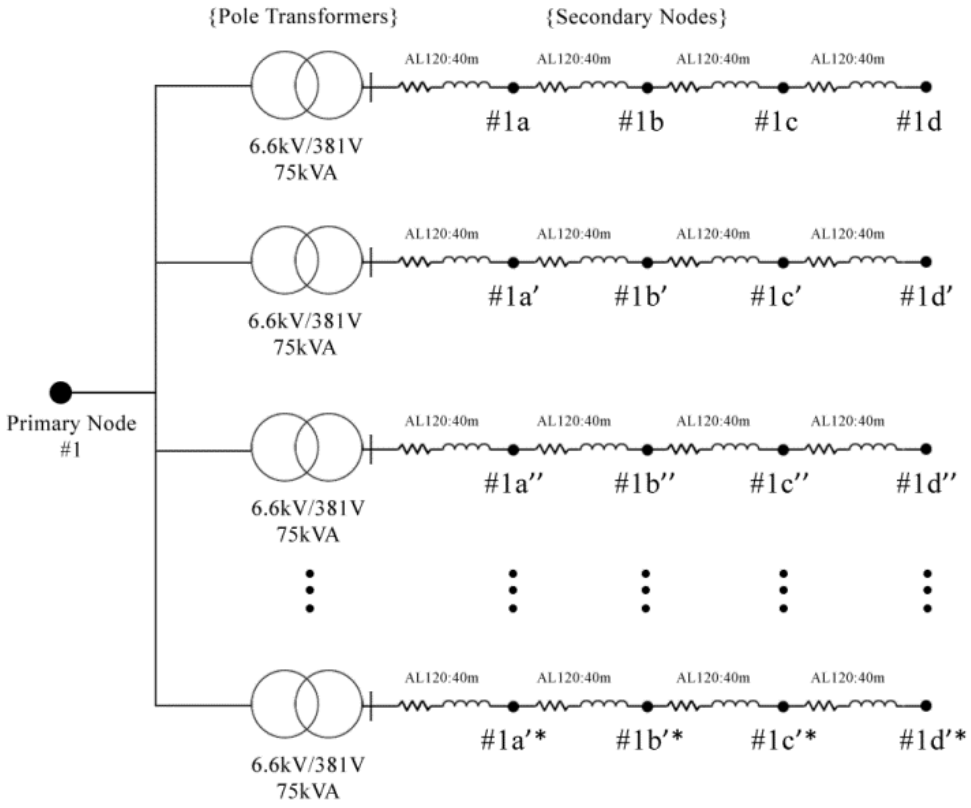

Figure 6.6 Secondary nodes and distribution network

It is assumed that each node comprises of four houses with an average real power consumption of 2.8kW. This power consumption can be categorized into noncritical and critical load power consumption. It can be safely estimated that 60% load of a normal house hold has the tendency to be operated under wide range of voltage and hence can be considered as noncritical load. Loads of each household at a certain node are categorized as shown in Figure 6.7. System parameters and ES details are enlisted in Table 6.1.

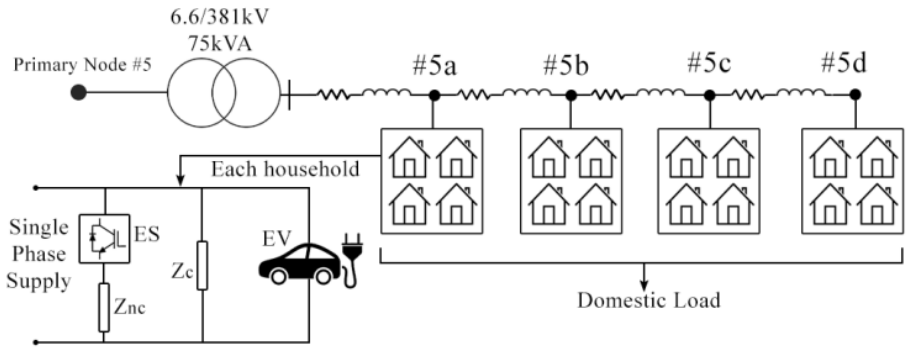

Figure 6.7 Load characterization and ES placement

Table 6.1 System's Specifications

Distribution System			
Pole Transformer	6.6kV/381V	Δ/Y	75kVA
Phase Voltage (Base Value)	230Vrms		
Fundamental Frequency	50Hz		
Noncritical Load at Secondary Nodes	30Ω		
Critical Load at Secondary Node	50Ω		
Maximum Power Consumed by EV	3.3kW		
Secondary nodes Wire Impedance	AL120: Z=(0.253+j0.348)Ω/km		
ES Parameters			
Inverter Type	Single-phase, IGBT, Full Bridge		
DC Link Voltage	200V		
Filter Inductor	0.5mH		
Filter Capacitor	13.2μF		
K_p	0.01		
K_i	7		

6.5 Results and Discussions

In this chapter, multiple simulations are carried out to evaluate the significance of ES in a realistic distribution system, detailed in previous section. These simulations are categorized as follows:

- Steady state voltage profile for three loading conditions (without ES and EV, with EV only, with EV and ES)

- ES response on dynamic loading of the network
- Effect of EV battery characteristics

First of all, voltage levels at each secondary node of primary node #5 are calculated under three different loading conditions using load flow program, as shown in Figure 6.8. It can be seen that without EV integration, node voltage levels are near minimal permissile value of 0.95pu, whereas when fully discharged EVs are connected simultaneously at each node (worst case scenario); voltage profile sees a significant drop down to the least value of 0.91pu (at#5d). But when proposed ES topology is widely distributed in the area, voltage drop will be significantly compensated. Even the farthest node (#5d) will see a voltage of 0.96pu, which is above the nominal value.

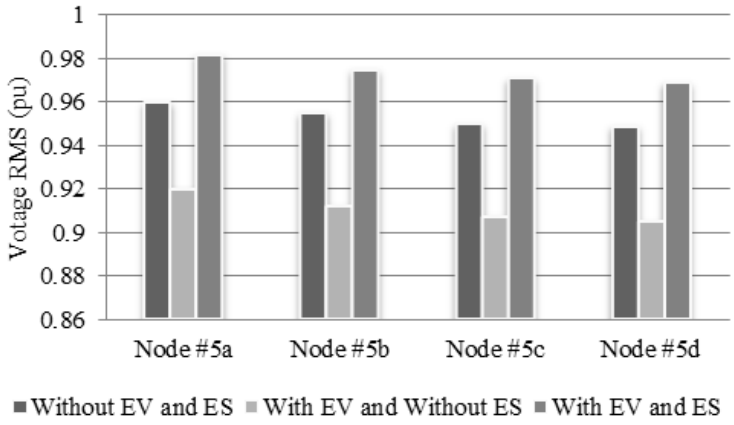

Figure 6.8 Voltage profile of secondary node #5 on three different scenarios

Next, the system is simulated for dynamic loading condition. EVs are plugged-in at each secondary node after predefined time-intervals (20s, 35s, 50s, and 60s at node #5a, #5b, #5c and #5d respectively). Voltage profile at node #5d represents certainly the lowest value, and is shown by solid line in the Figure 6.9. However, for a distribution system supported by ES, voltage levels at each node stay well-regulated (shown in dashed line).

The proposed controller activates ES available at a node at the instant when EV at the respective node is connected. Thus, when node #5a was loaded by EV, all of a sudden, ES associated with node #5a comes into action and tries to play its part, irrespective of the loading condition of remaining network. This feature of proposed scheme makes the controller independent of communication protocols.

Figure 6.10 and Figure 6.11 illustrate the dynamic response of active power associated with the operation of ES. It also demonstrates how ES redistributes the real power between ES and noncritical load to achieve the desired task of voltage regulation. In this case, simulation is run for 1s and EV is integrated with node #5d at 0.5s. Without ES, total power consumption sees a rise after 0.5s, while voltage level is dropped at that node due to higher current requirement. Whereas with ES, it can be seen that after steady state, ES provides a real power of 750Watt, causing a real power reduction of 21% in total power.

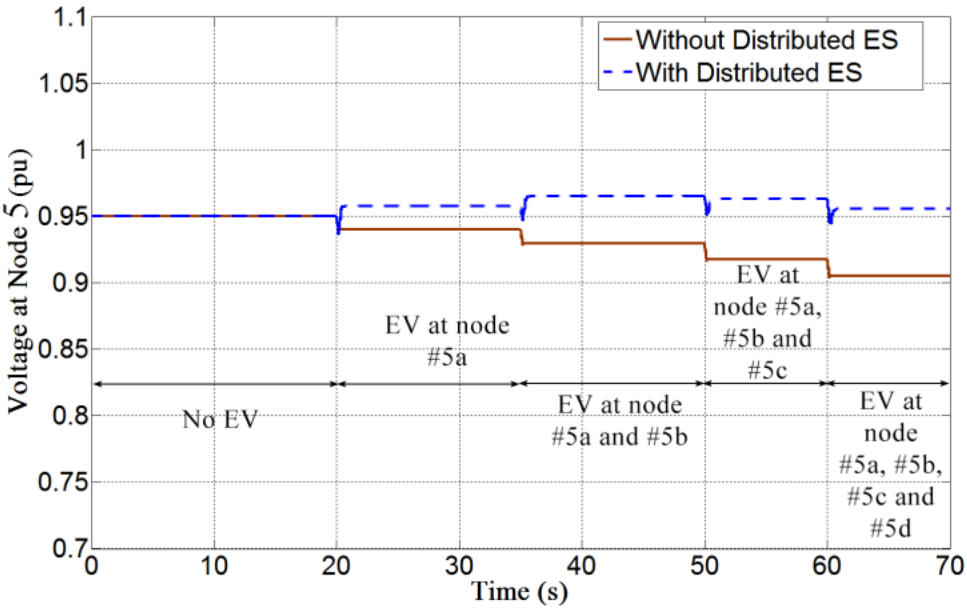

Figure 6.9 Voltage at node #5d when system is loaded by EV with/without ES

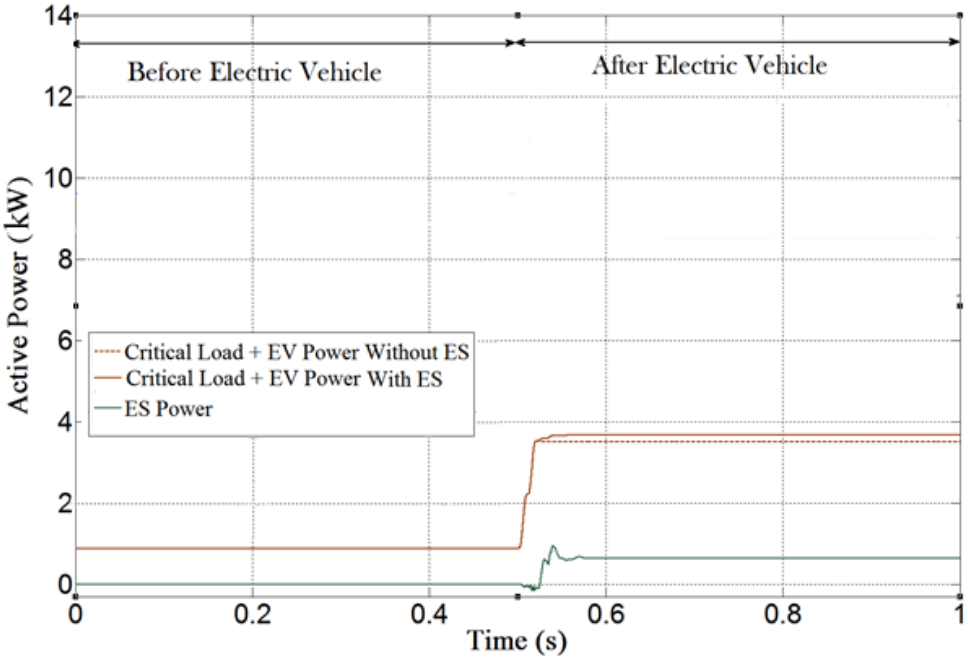

Figure 6.10 Power curves of ES, noncritical load and critical+EV load, when EV is connected at 0.5s, with and without ES

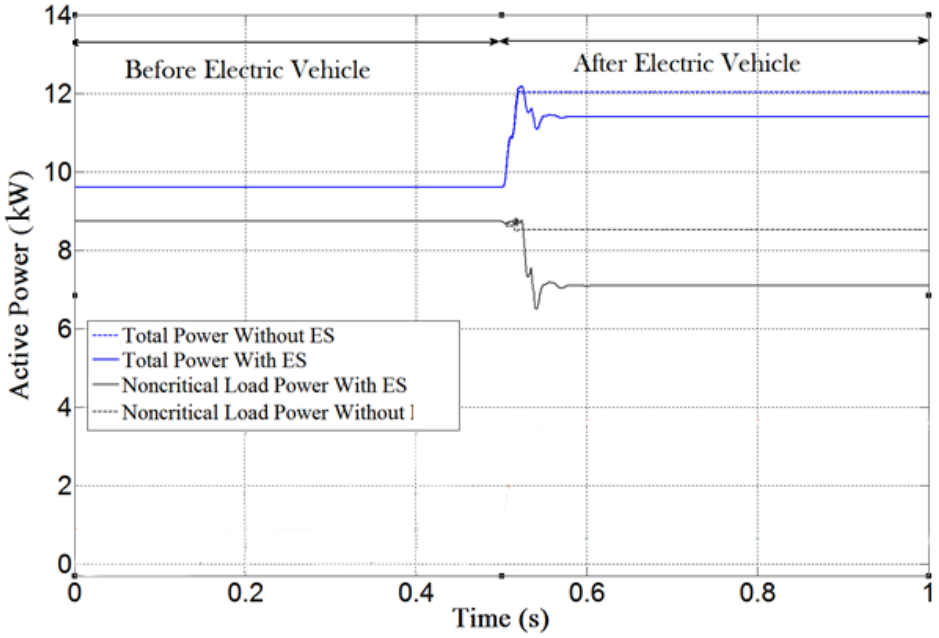

Figure 6.11 Power curves of ES, noncritical load and critical+EV load, when EV is connected at 0.5s, with and without ES

6.6 Conclusion

Thus, in this chapter, a novel application of ES has been proposed in which ES is used to support the severe voltage drop caused by huge penetration of EV in the existing distribution system. The theory behind the operation of proposed controller is mathematically formulated and explained graphically. Proposed scheme is successfully tested and simulated in a typical distribution system. To ensure the effectiveness of ES for this particular applicaion, system is dynamically loaded at different time intervals. It has been found that the proposed controller offers an efficient way to overcome the problem of reduced voltage caused by heavy induction of EV in distribution networks without need of communication infrastructure.

CHAPTER 7

HARDWARE IMPLEMENTATION OF ELECTRIC SPRING FOR CONSTANT POWER APPLICATION

This chapter presents a new control scheme for electric spring to ensure constant power across the loading element of variable impedance. Design and mathematical analysis of the proposed controller are provided followed by hardware prototype implementation. A novel application of electric spring is introduced in which it drives a load at constant power. It has been suggested that reference voltage to be produced by electric spring is continuously determined and then compared with the instantaneous voltage across electric spring terminal in a closed loop configuration. Results of both open and closed loop configurations are analyzed for simulation model. An experimental prototype is also developed to validate the simulation results for both cases. It has been found that hardware results are congruent with those obtained from simulation model, hence ensuring the efficacy of theoretical framework.

7.1 System Modeling

For modeling purpose, three electrical components – a stiff voltage source, ES, and a variable load – are connected in series as shown in Figure 7.1. ES, itself, is a single-phase full-bridge inverter driven by a PWM generator and a regulated DC source. Output is smoothened by an LC filter as shown.

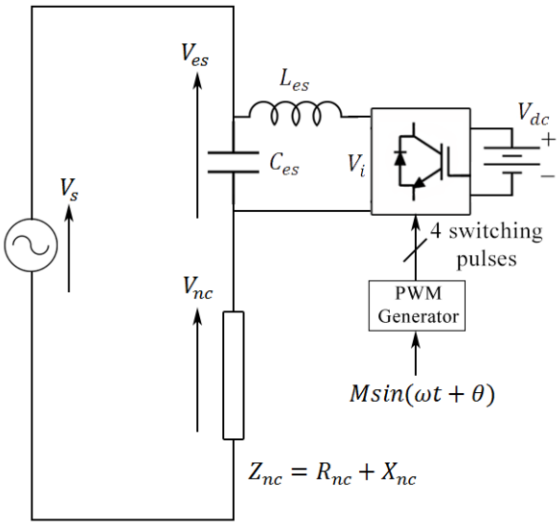

Figure 7.1 Circuit diagram of ES connected in series with voltage source and variable impedance load

Here also, second version of ES (with battery on its DC side) is used due to the requirement of both real and reactive powers transfer for this application. Averaging model is summarized below for the sake of convenience.

Full bridge rectifier's terminal voltage is given

$$\mathrm{V_i(t) = V_{dc}S_{PWM} - V_{dc}\overline{S_{PWM}}} \tag{7.1}$$

Where $\mathrm{S_{PWM}}$ and $\overline{\mathrm{S_{PWM}}}$represents the switching signal controlling the on-off cycles of switches. If $\mathrm{T_s}$ represents the sampling frequency and n represents the order of harmonics, equation (7.1) can be decomposed into fundamental and high frequency components as follows.

$$\mathrm{V_i(t) = V_{1i}(t) + \sum_{n=1}^{\infty} a_n cos\left(\frac{2\pi n}{T_s}t\right) + \sum_{n=1}^{\infty} b_n sin\left(\frac{2\pi n}{T_s}t\right)} \tag{7.2}$$

Averaging above equation for one cycle gives,

$$V_{i\_avg}(t) = \frac{1}{T_s}\int_{o}^{T_s} V_{1i}(\tau)d\tau + \sum_{n=1}^{\infty} a_n \cos\left(\frac{2\pi n}{T_s}t\right) + \sum_{n=1}^{\infty} b_n \sin\left(\frac{2\pi n}{T_s}t\right) \qquad (7.3)$$

The first term is the fundamental frequency (50 Hz) component of $V_i(t)$ averaged over one switching time period. Assuming the switching frequency is much higher than the fundamental frequency, this term is effectively a DC component. The second term would result in a sinusoidal function with high frequency.$V_i(t)$ undergoes a sharp attenuation due to low-pass characteristics of LC filter. Thus the terminal voltage of full-bridge inverter can be approximated to fundamental frequency component and can be represented by following relationship.

$$V_{1i}(t) = V_{dc}m(t) \qquad (7.4)$$

Where $m(t)$ is the modulation signal driving PWM generator and is given by

$$m(t) = M\sin(\omega t + \theta) \qquad (7.5)$$

Equation (7.4) and superposition on circuit of above Figure 7.1 gives

$$V_{es} = \left(\frac{X_c||Z_l}{Z_{nc} + X_c||Z_l}\right)V_s + \left(\frac{X_c||Z_{nc}}{Z_l + X_c||Z_l}\right)mV_{dc} \qquad (7.6)$$

Where $Z_l = R_{es} + X_{es}$ and $Z_{nc} = R_{nc} + X_{nc}$

With $X_{es} = j2\pi fL_{es}$,$X_{nc} = j2\pi fL_{nc}$, and $X_c = \frac{1}{j2\pi fC_{es}}$

In above equations, f is the frequency of the system (50Hz or 60Hz). Laplace transform is applied on the above equation, with zero initial conditions and $X_{nc} = 0$, for the sake of convenience, to obtain the transfer function of the given system as shown below

$$V_{es} = \frac{(sL_{es} + R_{es})V_s + RmV_{dc}}{s^2(LR_{nc}C_{es}) + s(R_{es}R_{nc}C_{es}) + (R_{es} + R_{nc})} \tag{7.7}$$

V_s will remain constant throughout this work as the voltage source is stiff and strongly connected with the system. The block diagram of the transfer function of the system is presented in Figure 7.2.

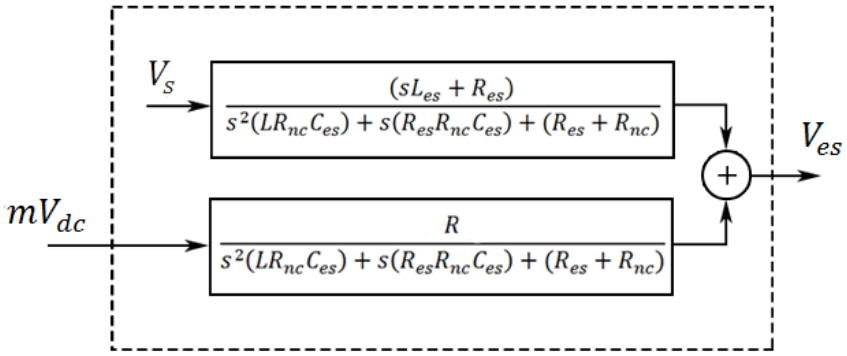

Figure 7.2 Transfer function block diagram

7.2 Controller Configurations

The fundamental operation of ES relies on the following equation

$$V_s = V_{es} + V_{nc} \tag{7.8}$$

Where V_{nc} is the voltage across the variable load terminals. In order to ensure constant power across impedance varying load, its instantaneous impedance is to be determined. If P_{ref} denotes the reference power, the governing control equation for a resistive load will be as follows.

$$V_{es\_ref} = V_s - \sqrt{P_{ref} R_{nc}} \tag{7.9}$$

In the averaging model of full-bridge inverter, a linear relationship is established between amplitude of modulation index and output terminal voltage. However, in practice, this relationship is not straightforward due to several switching nonlinearities, especially when relatively large inductor is used for better filtering. It can be noted that increasing M, does not increase voltage V_{es}, linearly.

To overcome this nonlinearity, two approaches are proposed – open loop configuration and closed loop configuration.

7.2.1 Open Loop Configuration

Nonlinearity is dealt by fitting the linear data around the given curve in the least square sense. After determining the slope (m') and y-intercept (b) of the best-fit line, modulation index amplitude is determined by the following straight line equation (Refer to Figure 7.5).

$$M = \frac{|V_{es\_ref}| - b}{m'} \tag{7.10}$$

Figure 7.3 depicts the sequential block diagram. Slope and y-intercept of straight line are determined from graph. The output $m(t)$ is fed to PWM generator which will generate the required gating pulses to drive ES.

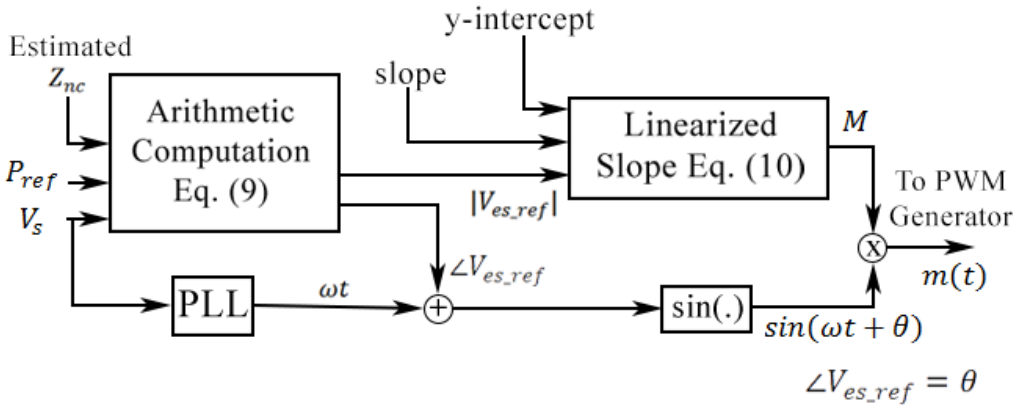

Figure 7.3 Open-loop control sequential block diagram

7.2.2 Closed Loop Configuration

In second approach, reference voltage, as determined by equation (7.9), is decomposed into its magnitude and phase. This reference magnitude is compared with the instantaneous voltage magnitude of ES, and the error signal is fed into PI controller, followed by a saturation block to keep the amplitude of modulation signal between 0 and 1. On the other hand, phase of the reference signal is added to that of mains voltage, and corresponding sinusoidal wave is generated. Finally, the modulation signal is fed into PWM generator to produce switching pulses that will eventually drive the single-phase full-bridge inverter. In this way, a closed loop is completed. The parameters of PI controller that primarily gives the amplitude of the modulation signal can be designed by several methods. In this work, Ziegler Nichols method is used to tune PI controller as discussed in Chapter 4. However, depending on desired specifications, PI controller can be tuned accordingly. If a linear model of system is used, root locus design analysis can also be used. A simplified model of this closed loop control scheme is shown in Figure 7.4.

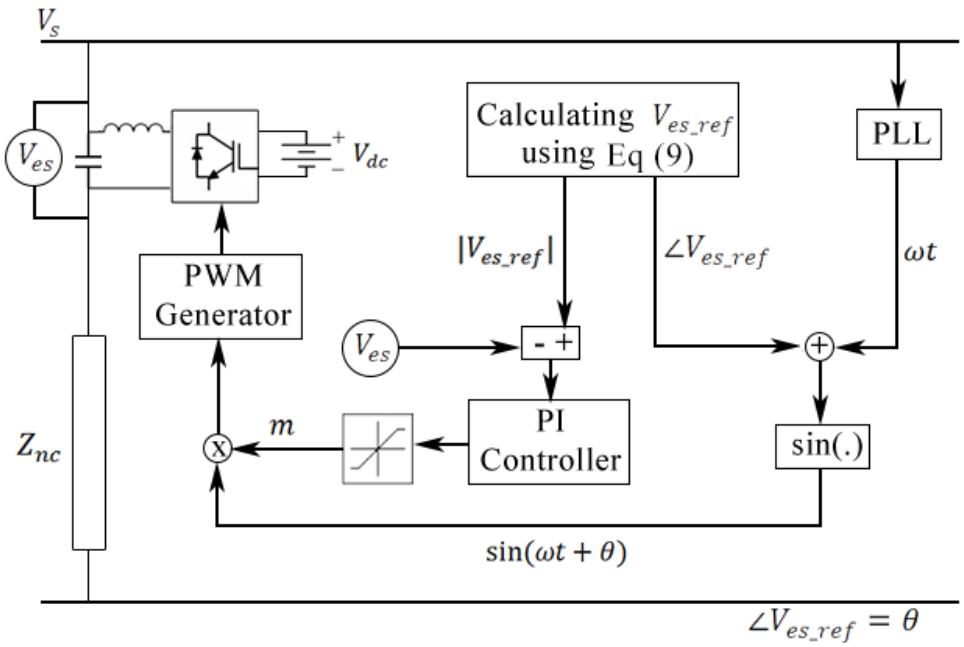

Figure 7.4 Closed-loop control schematic

7.3 Simulation Model and Results

MATLAB Simscape Toolbox and Simulink environment is used for simulating both control approaches. Circuit shown in Figure 7.1 is implemented with the parameters listed in Table 7.1.

Table 7.1 Simulation Model Specifications

Electrical Components	
Voltage Source	110 Vrms
System Frequency	60 Hz
Variable Load Range	100Ω~150Ω
ES Parameters	
Inverter Type	Single-phase, IGBT, Full Bridge
DC Link Voltage	20V
Filter Inductor	1.5mH
Filter Capacitor	200μF
Carrier Frequency	2160Hz
Sampling Time	50μs

Under the above system parameters, nonlinear and linearized curves between M and V_{es} are shown in Figure 7.5. M is increased from 0.4 to 1 at a rate of 0.1, to exclude large nonlinearities.

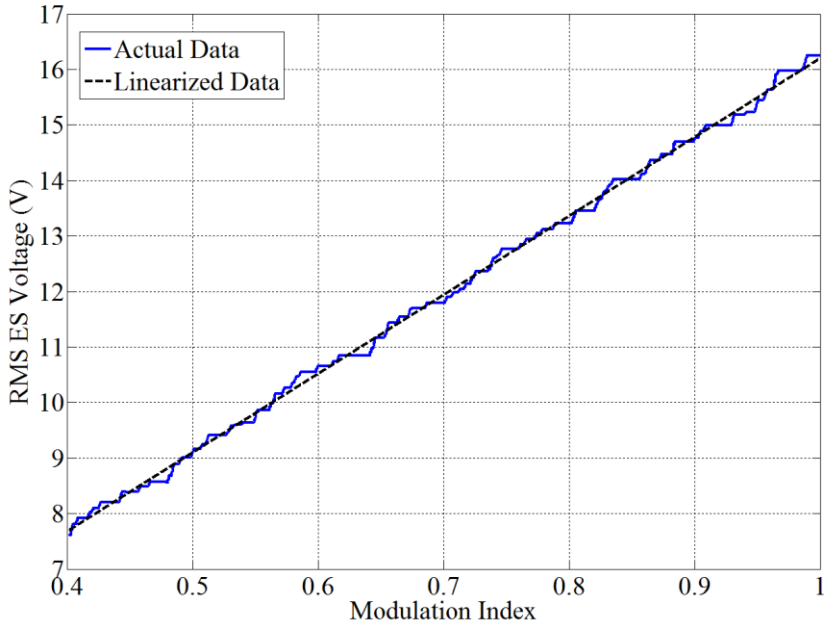

Figure 7.5 Linearization of nonlinear relation between modulation index and output voltage of ES

In open-loop configuration, slope (m′) and y-intercept (b) of linearized data (using least square method) are 14.2 and 1.99, respectively, whereas, the K_p and K_i for closed-loop configuration are found to be 0.025 and 1.71, respectively, using Ziegler Nichols method [56]. Ultimate gain $K_u$is found to be 0.055, whereas period of sustained oscillations T_u is 0.02. Figure 7.6 shows the deviation of consumed real power without ES (dashed), with open-loop controller (solid) and with closed-loop controller (dotted) across the complete range of varying load. It is evident that without ES, power consumption will be directly related to the current being flown into the load. However, with ES, power tends to remain

constant. Better results are obtained with closed-loop configuration. It is to be noted that open loop controller is referred as direct controller in figures.

To observe the transient response of both techniques, load is suddenly changed from 100Ω to 140Ω at 0.5s of simulation time as shown in Figure 7.7.

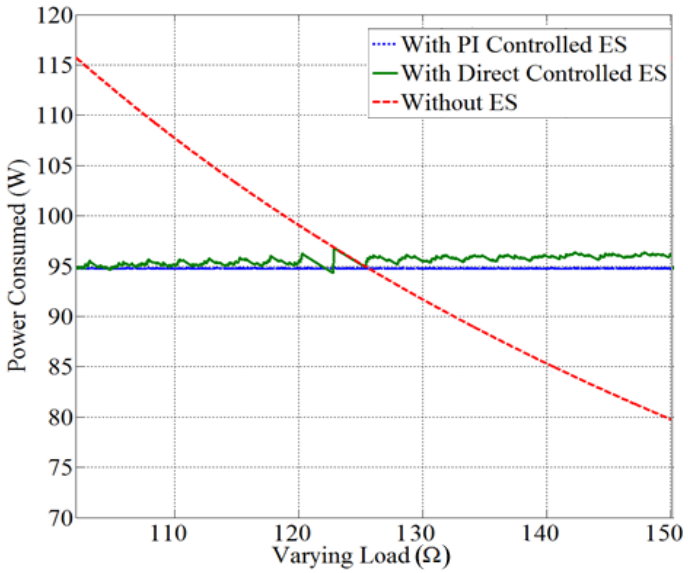

Figure 7.6 Real power consumption curves when load is varied across its range with and without ES

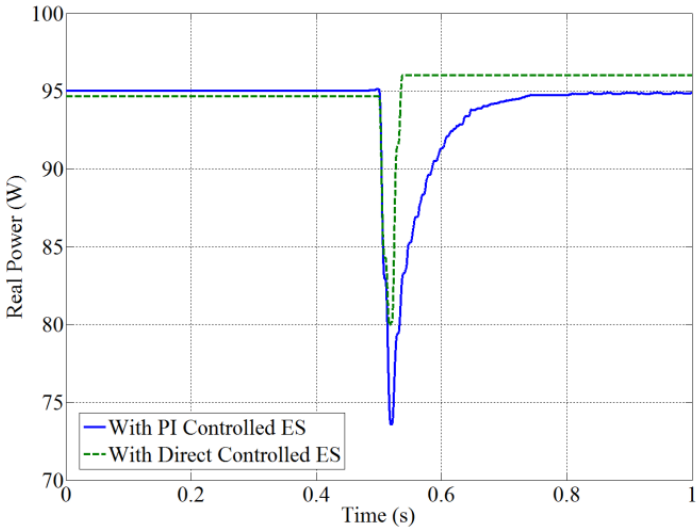

Figure 7.7 Transient response of real power consumption curves when load is suddenly changed from 100Ω to 140Ω at 0.5s for both approaches

Reference power is arbitrary set to 95W. It can be observed that closed-loop controller gives increased overshoot of 47.4% with more settling time (0.15s) as compared to direct approach. On the other hand, direct approach has a steady state error of 1.05%.

For the same simulation, Figure 7.8 shows the voltage at ES terminal. Time range is set from 0.4s to 0.8s to highlight the transient part. ES voltage, load voltage and load current are shown before and after change in load impedance. Transient response for both control approaches is evinced which shows that steady state of ES voltage is achieved swiftly with open loop controller as compared to the one achieved with PI controller. For one cycle ES voltage waveform of PI controller shows an erratic behavior during the transition but later on it gets similar to the waveform obtained using direct approach.

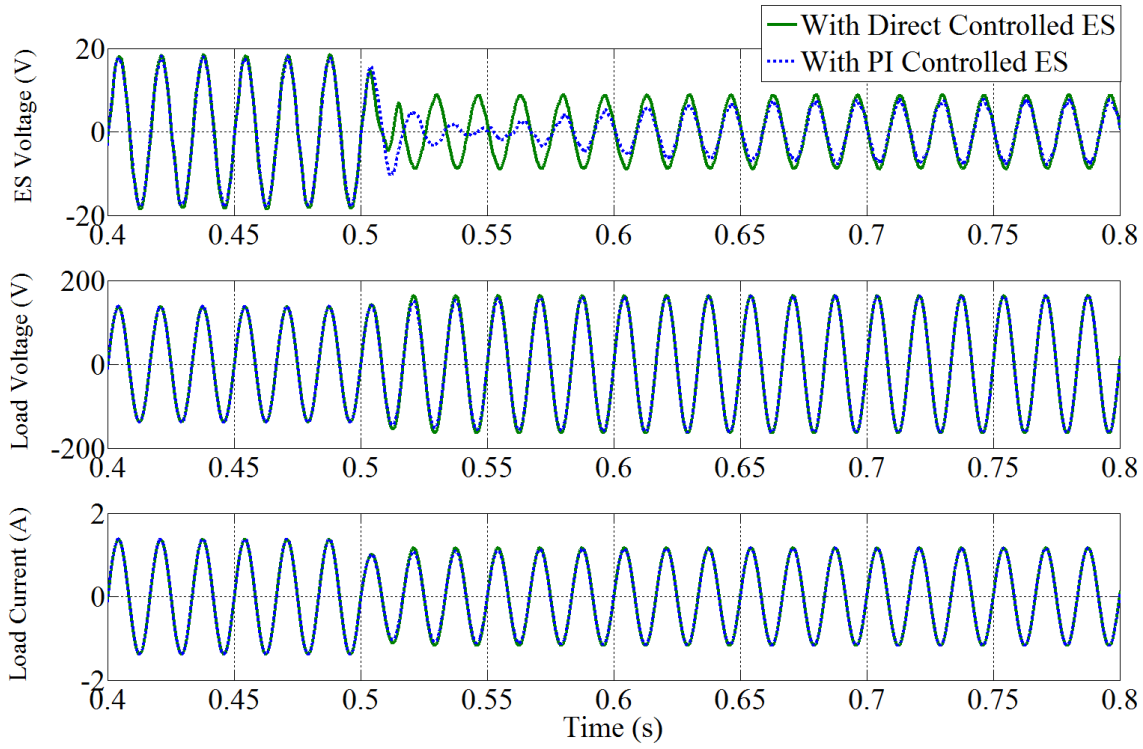

Figure 7.8 Response of ES voltage when load is suddenly changed from 100Ω to 140Ω at 0.5s, with reference power set at 95W

7.4 Hardware Prototype Development

An experimental prototype is developed in Power Quality Lab of King Fahd University of Petroleum and Minerals, Saudi Arabia. Primary components of the hardware setup include programmable Chroma AC source, distribution panel, full-bridge universal inverter, LC filter bank, Chroma programmable load and DC supply. A data sensing and acquisition board is developed using Hall sensors and necessary electronics. For feedback and controller operation, a digital signal processor – dSPACE – is integrated to the system accordingly.

A hardware laboratory scale prototype is developed using controllable source, loads and real time inverter modules to mitigate the harmonics generated by the nonlinear load current. Experimental setup built to investigate the performance of ES is shown in Figure 7.9.

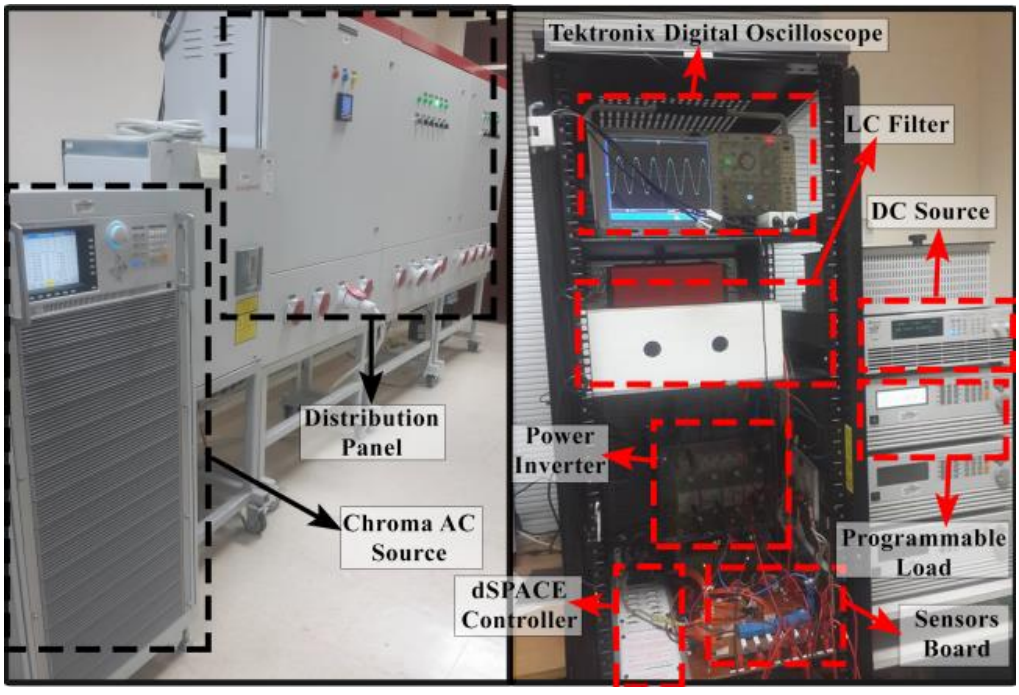

Figure 7.9 Experimental prototype in Power Quality Lab, KFUPM

The three-phase source voltage is generated using programmable AC source. The varying impedance loads are implemented using controllable loads. Tektronix mixed domain oscilloscope MDO4000B is used to display and record the experimental results like source, load and ES currents and three phase source voltage etc. A detailed description of all the equipment used in the experimental setup is given in Appendix A.

7.5 Hardware Results

For compliance with simulation results, hardware parameters are set similar to those mentioned in Table 7.1. In first experiment, impedance of programmable load is swept from 100Ω to 150Ω with a step size of 1Ω. If voltage is kept constant, power consumed by load without ES is inversely proportional to the load resistance; however, with direct control of ES, power tends to track reference power (i.e. 95W). Better response is obtained when a feedback loop and PI controller is introduced as discussed in Section III. It is to be noted that slope and y-intercept (for direct control) and K_p and K_i (for PI control) are kept same as determined in simulations. Power curves for three cases are plotted in Figure 7.10a (simulation results) and in Figure 7.10b (hardware results).

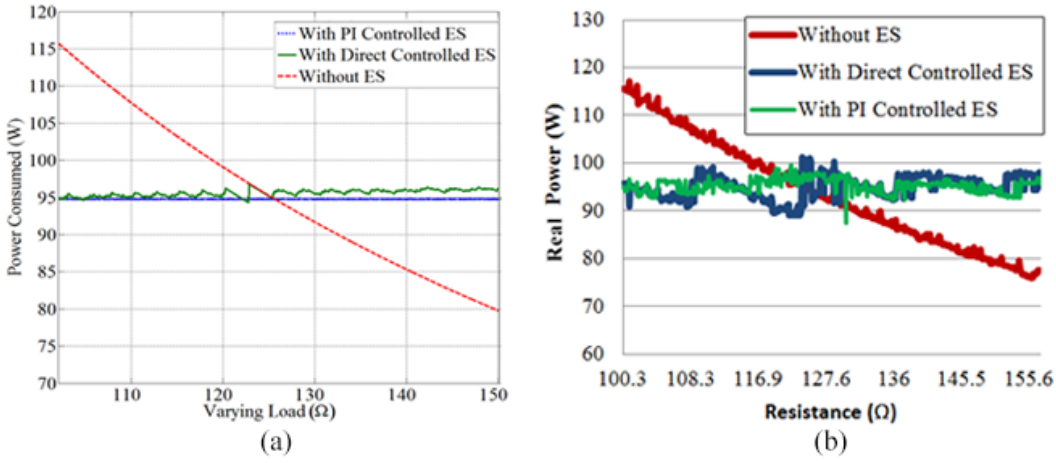

Figure 7.10 Power consumed by load with and without ES, when reference power is set to 95W obtained via (a) simulations and (b) hardware prototype

To compare the transient response of both control approaches, Chroma programmable load is programmed to suddenly change its resistance from 100Ω to 140Ω. Response is recorded in digital form using ADC channel of dSPACE and Control Desk environment, later it is plotted in Figure 7.11b along with the transient responses of both controllers obtained from simulations (Figure 7.11a). In correlation with the simulation results, settling time and overshoot of direct control is better than that of PI based controller by 188% and 0.16s, respectively. Here also, direct control has a state error of 2%; however, with PI controller no steady state error is recorded. In a run time of 0.7s, load undergoes a sudden change at 0.3s.

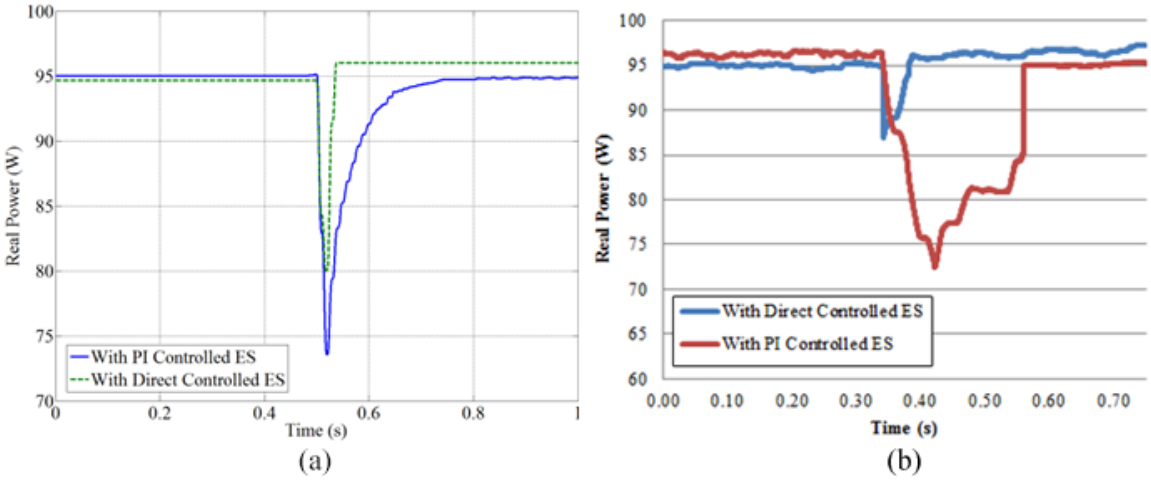

Figure 7.11 Transient response of (a) simulation and (b) hardware prototype when load is changed from 100Ω to 140Ω at 0.3s

To identify the steady-state error present in direct approach due to nonlinearity of inverter response, pictures of LCD screen of programmable load are shown in Figure 7.22, under different loading conditions. Direct control of ES gives a steady state error of 1.53V when load impedance is 100Ω, whereas when load impedance is increased to140Ω, steady-state error increases to 1.57V, as shown in Figure 7.12a of the following figure.

On the other hand, Figure 7.12b represents the case with closed-loop PI controller. For both impedance levels, steady state error is 0.29V, which is due to minor inaccuracy in data acquisition and scaling factor of Hall sensors.

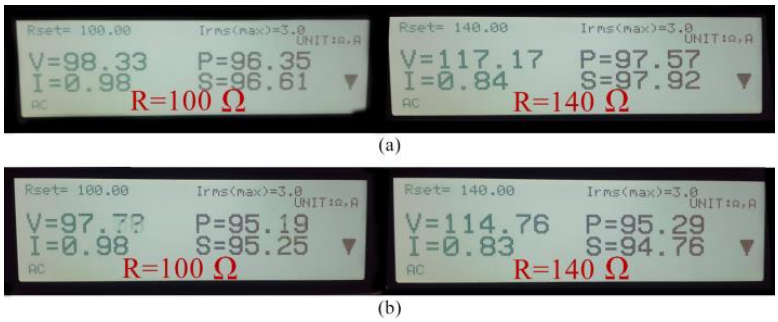

Figure 7.12 Steady-state response comparison for the loads of 100Ω and 140Ω with (a) directly controlled ES (b) PI based control of ES

7.6 Conclusion

Thus in this chapter, an application of ES to provide constant power, irrespective of load impedance, is explored. After introducing the fundamentals of ES, theoretical model of ES is presented based on averaging model. Later, mathematical formulation of the network under study is established. Two control approaches are presented and developed to investigate a typical simulation model and an experimental prototype. It has been found that ES is capable to provide constant power to the load, irrespective of its current requirement. Investigation of both simulation model and hardware setup shows the efficacy of closed-loop controller in terms of steady-state response. However, the direct approach offers less overshoot and settling time.

CHAPTER 8

CONCLUSION AND FUTURE WORK

8.1 Conclusive Remarks

This work specifically looks into the horizon of possibilities for ES to work as a smart power module, widely distributed in the futuristic grid facing both conventional and unconventional power system problems. It has been anticipated that various smart grid performance attributes would be at stake with the world's growing interest in integrating renewable energy sources. So, this research tries to address the concerns directly associated with the ecological advancements in power sector by using a power electronic based switching device known as electric spring.

This thesis is conclusively drawn to following points:

- A comprehensive literature review has been accomplished which includes all proposed advancements of ES since its advent in 2012.
- Previous research on ES modeling and its application as demand side management is further extended to include more applications of ES, in addition to the development of hardware setup.
- Theory of operation of ES is well studied including its comparisons with other real and reactive power compensators, preceded by the discussions of operating modes and versions of ES.

- Novel control approach has been suggested to improve the response of voltage regulation in a power grid heavily equipped by renewable power sources. The dynamic response improvement was found evident with the novel fuzzy control loop.
- Three-phase load imbalance is a major power quality issue which was previously addressed by shunt active filter and other conventional methods. This research has proposed use of ES with novel PI based controller to mitigate neutral current.
- Another application of ES has been explored which deals with the voltage profile support that otherwise would have been dropped when subjected to fleet-based PEVs.
- Laboratory based experimental setup has been developed for ES to test and validate the theories of operation of ES. In doing so, a novel application of ensuring constant power supply to a load, irrespective of its load impedance has been simulated and tested on hardware prototype.
- The obtained results ascertain that ES can offer wide range of applications in addition to the applications discussed in published literature.
- A good agreement has been observed between the experimental results and the simulation results for constant power applications

8.2 Future Work

While investigating the applications and control of ES, several possible work flows were encountered, each of which can be further looked into. In spite of the wide scope of the applications discussed in this research thesis, it can be said that this topic still has ample

research potential and there are numerous topics within ES which can be pursued for a meaningful research. These topics are highlighted below.

- DC microgrids are a prime focus of researcher these days. Keeping this in mind, DC ES can be further investigated with advanced control topology leading to robustness and better dynamic response.
- ES inverter's output has a cross coupling effect. i.e. the amplitude and phase angle of modulation index have cross relational effect on the output of inverters. Dynamic decouplers can be put to use to reduce this coupling effect, and a complete research paradigm can be identified.
- Use of ES to reduce energy storage requirement is investigated only once in literature (according to best of author's knowledge). Obvious room of research is available in this domain, as several optimization techniques can be incorporated with ES to obtain optimized operational strategy for a power plant with enhanced profits and less risk involved.
- Marketing aspect of ES is yet to be explored. At what cost a consumer would agree to sacrifice the perfect operation of his noncritical loads is an intriguing question for the future study of ES.
- Since hardware prototype is ready in PQ lab of KFUPM, neutral current mitigation can be experimentally validated in future along with other applications.

References

[1] S. Y. Hui, C. K. Lee, and F. F. Wu, 'Electric Springs #x2014;A New Smart Grid Technology', *IEEE Trans. Smart Grid*, vol. 3, no. 3, pp. 1552–1561, Sep. 2012.

[2] C. K. Lee, S. C. Tan, F. F. Wu, S. Y. R. Hui, and B. Chaudhuri, 'Use of Hooke's law for stabilizing future smart grid #x2014; The electric spring concept', in *2013 IEEE Energy Conversion Congress and Exposition (ECCE)*, 2013, pp. 5253–5257.

[3] C. K. Lee, B. Chaudhuri, and S. Y. Hui, 'Hardware and Control Implementation of Electric Springs for Stabilizing Future Smart Grid With Intermittent Renewable Energy Sources', *IEEE J. Emerg. Sel. Top. Power Electron.*, vol. 1, no. 1, pp. 18–27, Mar. 2013.

[4] S.-C. Tan, C. K. Lee, and S. Y. Hui, 'General Steady-State Analysis and Control Principle of Electric Springs With Active and Reactive Power Compensations', *IEEE Trans. Power Electron.*, vol. 28, no. 8, pp. 3958–3969, Aug. 2013.

[5] X. Chen, Y. Hou, S.-C. Tan, C.-K. Lee, and S. Y. R. Hui, 'Mitigating Voltage and Frequency Fluctuation in Microgrids Using Electric Springs', *IEEE Trans. Smart Grid*, vol. 6, no. 2, pp. 508–515, Mar. 2015.

[6] C. K. Lee, N. R. Chaudhuri, B. Chaudhuri, and S. Y. R. Hui, 'Droop Control of Distributed Electric Springs for Stabilizing Future Power Grid', *IEEE Trans. Smart Grid*, vol. 4, no. 3, pp. 1558–1566, Sep. 2013.

[7] J. Soni, K. R. Krishnanand, and S. K. Panda, 'Load-side demand management in buildings using controlled electric springs', in *IECON 2014 - 40th Annual Conference of the IEEE Industrial Electronics Society*, 2014, pp. 5376–5381.

[8] A.-H. Mohsenian-Rad, V. W. S. Wong, J. Jatskevich, R. Schober, and A. Leon-Garcia, 'Autonomous Demand-Side Management Based on Game-Theoretic Energy Consumption Scheduling for the Future Smart Grid', *IEEE Trans. Smart Grid*, vol. 1, no. 3, pp. 320–331, Dec. 2010.

[9] F. Kienzle, P. Ahčin, and G. Andersson, 'Valuing Investments in Multi-Energy Conversion, Storage, and Demand-Side Management Systems Under Uncertainty', *IEEE Trans. Sustain. Energy*, vol. 2, no. 2, pp. 194–202, Apr. 2011.

[10] A. J. Conejo, J. M. Morales, and L. Baringo, 'Real-Time Demand Response Model', *IEEE Trans. Smart Grid*, vol. 1, no. 3, pp. 236–242, Dec. 2010.

[11] S. C. Lee, S. J. Kim, and S. H. Kim, 'Demand Side Management With Air Conditioner Loads Based on the Queuing System Model', *IEEE Trans. Power Syst.*, vol. 26, no. 2, pp. 661–668, May 2011.

[12] C. K. Lee, K. L. Cheng, and W. M. Ng, 'Load characterisation of electric spring', in *2013 IEEE Energy Conversion Congress and Exposition (ECCE)*, 2013, pp. 4665–4670.

[13] N. R. Chaudhuri, C. K. Lee, B. Chaudhuri, and S. Y. R. Hui, 'Dynamic Modeling of Electric Springs', *IEEE Trans. Smart Grid*, vol. 5, no. 5, pp. 2450–2458, Sep. 2014.

[14] E. F. Areed and M. A. Abido, 'Design and dynamic analysis of Electric Spring for voltage regulation in smart grid', in *2015 18th International Conference on Intelligent System Application to Power Systems (ISAP)*, 2015, pp. 1–6.

[15] Q. Wang, M. Cheng, Z. Chen, and Z. Wang, 'Steady-State Analysis of Electric Springs with a Novel #x03B4; Control', *IEEE Trans. Power Electron.*, vol. PP, no. 99, pp. 1–1, 2015.

[16] C. K. Lee and S. Y. Hui, 'Reduction of Energy Storage Requirements in Future Smart Grid Using Electric Springs', *IEEE Trans. Smart Grid*, vol. 4, no. 3, pp. 1282–1288, Sep. 2013.

[17] P. Kanjiya and V. Khadkikar, 'Enhancing power quality and stability of future smart grid with intermittent renewable energy sources using electric springs', in *2013 International Conference on Renewable Energy Research and Applications (ICRERA)*, 2013, pp. 918–922.

[18] J. Soni and S. K. Panda, 'Electric spring for voltage and power stability and power factor correction', in *2015 9th International Conference on Power Electronics and ECCE Asia (ICPE-ECCE Asia)*, 2015, pp. 2091–2097.

[19] Y. Shuo, S.-C. Tan, C. K. Lee, and S. Y. R. Hui, 'Electric spring for power quality improvement', in *2014 Twenty-Ninth Annual IEEE Applied Power Electronics Conference and Exposition (APEC)*, 2014, pp. 2140–2147.

[20] X. Luo, Z. Akhtar, C. K. Lee, B. Chaudhuri, S.-C. Tan, and S. Y. R. Hui, 'Distributed Voltage Control with Electric Springs: Comparison with STATCOM', *IEEE Trans. Smart Grid*, vol. 6, no. 1, pp. 209–219, Jan. 2015.

[21] X. Che, T. Wei, Q. Huo, and D. Jia, 'A general comparative analysis of static synchronous compensator and electric spring', in *Transportation Electrification Asia-Pacific (ITEC Asia-Pacific), 2014 IEEE Conference and Expo*, 2014, pp. 1–5.

[22] S. Yan, S.-C. Tan, C.-K. Lee, B. Chaudhuri, and S. Y. R. Hui, 'Electric Springs for Reducing Power Imbalance in Three-Phase Power Systems', *IEEE Trans. Power Electron.*, vol. 30, no. 7, pp. 3601–3609, Jul. 2015.

[23] S. Yan, S.-C. Tan, C.-K. Lee, and S. Y. R. Hui, 'Reducing three-phase power imbalance with electric springs', in *2014 IEEE 5th International Symposium on Power Electronics for Distributed Generation Systems (PEDG)*, 2014, pp. 1–7.

[24] K. R. Krishnanand, S. M. F. Hasani, J. Soni, and S. K. Panda, 'Neutral current mitigation using controlled electric springs connected to microgrids within built environment', in *2014 IEEE Energy Conversion Congress and Exposition (ECCE)*, 2014, pp. 2947–2951.

[25] A. Roshan, R. Burgos, A. C. Baisden, F. Wang, and D. Boroyevich, 'A D-Q Frame Controller for a Full-Bridge Single Phase Inverter Used in Small Distributed Power Generation Systems', in *APEC 2007 - Twenty Second Annual IEEE Applied Power Electronics Conference*, 2007, pp. 641–647.

[26] M. J. Ryan, W. E. Brumsickle, and R. D. Lorenz, 'Control topology options for single-phase UPS inverters', *IEEE Trans. Ind. Appl.*, vol. 33, no. 2, pp. 493–501, Mar. 1997.

[27] Y.-Y. Tzou, R.-S. Ou, S.-L. Jung, and M.-Y. Chang, 'High-performance programmable AC power source with low harmonic distortion using DSP-based repetitive control technique', *IEEE Trans. Power Electron.*, vol. 12, no. 4, pp. 715–725, Jul. 1997.

[28] D. N. Zmood and D. G. Holmes, 'Stationary frame current regulation of PWM inverters with zero steady-state error', *IEEE Trans. Power Electron.*, vol. 18, no. 3, pp. 814–822, May 2003.

[29] T. Yang, K.-T. Mok, S.-C. Tan, and S. Y. R. Hui, 'Control of electric springs with coordinated battery management', in *2015 IEEE Energy Conversion Congress and Exposition (ECCE)*, 2015, pp. 6740–6746.

[30] K.-T. Mok, S.-C. Tan, and S. Y. Hui, 'Decoupled Power Angle and Voltage Control of Electric Springs', *IEEE Trans. Power Electron.*, vol. 31, no. 2, pp. 1216–1229, Feb. 2016.

[31] T. Kim and W. Qiao, 'A Hybrid Battery Model Capable of Capturing Dynamic Circuit Characteristics and Nonlinear Capacity Effects', *IEEE Trans. Energy Convers.*, vol. 26, no. 4, pp. 1172–1180, Dec. 2011.

[32] O. C. Onar, J. Kobayashi, D. C. Erb, and A. Khaligh, 'A Bidirectional High-Power-Quality Grid Interface With a Novel Bidirectional Noninverted Buck #x2013;Boost Converter for PHEVs', *IEEE Trans. Veh. Technol.*, vol. 61, no. 5, pp. 2018–2032, Jun. 2012.

[33] S. Yan, X. Luo, S.-C. Tan, and S. Y. R. Hui, 'Electric springs for improving transient stability of micro-grids in islanding operations', in *2015 IEEE Energy Conversion Congress and Exposition (ECCE)*, 2015, pp. 5843–5850.

[34] J. He, Y. W. Li, and F. Blaabjerg, 'An Enhanced Islanding Microgrid Reactive Power, Imbalance Power, and Harmonic Power Sharing Scheme', *IEEE Trans. Power Electron.*, vol. 30, no. 6, pp. 3389–3401, Jun. 2015.

[35] C.-T. Lee, C.-C. Chu, and P.-T. Cheng, 'A new droop control method for the autonomous operation of distributed energy resource interface converters', in *2010 IEEE Energy Conversion Congress and Exposition (ECCE)*, 2010, pp. 702–709.

[36] J. Hu, J. Zhu, Y. Qu, and J. M. Guerrero, 'A new virtual-flux-vector based droop control strategy for parallel connected inverters in microgrids', in *2013 IEEE ECCE Asia Downunder (ECCE Asia)*, 2013, pp. 585–590.

[37] H. Han, Y. Liu, Y. Sun, M. Su, and J. M. Guerrero, 'An Improved Droop Control Strategy for Reactive Power Sharing in Islanded Microgrid', *IEEE Trans. Power Electron.*, vol. 30, no. 6, pp. 3133–3141, Jun. 2015.

[38] T. L. Vandoorn, B. Meersman, J. D. M. De Kooning, and L. Vandevelde, 'Transition From Islanded to Grid-Connected Mode of Microgrids With Voltage-Based Droop Control', *IEEE Trans. Power Syst.*, vol. 28, no. 3, pp. 2545–2553, Aug. 2013.

[39] X. Chen and Y. Hou, 'Distributed control of multiple Electric Springs in microgrids', in *2015 IEEE Power Energy Society General Meeting*, 2015, pp. 1–5.

[40] Z. Akhtar, B. Chaudhuri, and S. Y. R. Hui, 'Smart Loads for Voltage Control in Distribution Networks', *IEEE Trans. Smart Grid*, vol. PP, no. 99, pp. 1–10, 2015.

[41] Z. Akhtar, B. Chaudhuri, and S. Y. R. Hui, 'Primary Frequency Control Contribution From Smart Loads Using Reactive Compensation', *IEEE Trans. Smart Grid*, vol. 6, no. 5, pp. 2356–2365, Sep. 2015.

[42] Y. Yang, S.-S. Ho, S.-C. Tan, and S. Y. R. Hui, 'Stability design of electric springs in power grids', in *2015 IEEE Energy Conversion Congress and Exposition (ECCE)*, 2015, pp. 6838–6844.

[43] P. Jadhav and M. M. Waware, 'Development and performance analysis of Electrical Spring with intermittent renewable energy sources using advanced controller', in

2015 International Conference on Advancements in Power and Energy (TAP Energy), 2015, pp. 494–499.

[44] Y. A.-R. I. Mohamed and E. F. El-Saadany, 'Adaptive Decentralized Droop Controller to Preserve Power Sharing Stability of Paralleled Inverters in Distributed Generation Microgrids', *IEEE Trans. Power Electron.*, vol. 23, no. 6, pp. 2806–2816, Nov. 2008.

[45] S. V. Iyer, M. N. Belur, and M. C. Chandorkar, 'A Generalized Computational Method to Determine Stability of a Multi-inverter Microgrid', *IEEE Trans. Power Electron.*, vol. 25, no. 9, pp. 2420–2432, Sep. 2010.

[46] X. Lu, K. Sun, L. Huang, M. Liserre, and F. Blaabjerg, 'An active damping method based on biquad digital filter for parallel grid-interfacing inverters with LCL filters', in *2014 Twenty-Ninth Annual IEEE Applied Power Electronics Conference and Exposition (APEC)*, 2014, pp. 392–397.

[47] N. Bottrell, M. Prodanovic, and T. C. Green, 'Dynamic Stability of a Microgrid With an Active Load', *IEEE Trans. Power Electron.*, vol. 28, no. 11, pp. 5107–5119, Nov. 2013.

[48] N. Pogaku, M. Prodanovic, and T. C. Green, 'Modeling, Analysis and Testing of Autonomous Operation of an Inverter-Based Microgrid', *IEEE Trans. Power Electron.*, vol. 22, no. 2, pp. 613–625, Mar. 2007.

[49] M. Borrega, L. Marroyo, R. Gonzalez, J. Balda, and J. L. Agorreta, 'Modeling and Control of a Master #x2013;Slave PV Inverter With N-Paralleled Inverters and Three-Phase Three-Limb Inductors', *IEEE Trans. Power Electron.*, vol. 28, no. 6, pp. 2842–2855, Jun. 2013.

[50] L. Zhang and H.-P. Nee, ‘Multivariable feedback design of VSC-HVDC connected to weak ac systems’, in *PowerTech, 2009 IEEE Bucharest*, 2009, pp. 1–8.

[51] K.-T. Mok, M.-H. Wang, S.-C. Tan, and S.-Y. Hui, ‘DC electric springs - An emerging technology for DC grids’, in *2015 IEEE Applied Power Electronics Conference and Exposition (APEC)*, 2015, pp. 684–690.

[52] K.-T. Mok, T. Yang, S.-C. Tan, C.-K. Lee, and S.-Y. Hui, ‘Distributed grid voltage and utility frequency stabilization via shunt-type electric springs’, in *2015 IEEE Energy Conversion Congress and Exposition (ECCE)*, 2015, pp. 3774–3779.

[53] K. L. Cheng, X. Luo, and C. K. Lee, ‘Reactive power flow control of grid tie inverter to enhance the stability of power grid’, in *2014 IEEE 5th International Symposium on Power Electronics for Distributed Generation Systems (PEDG)*, 2014, pp. 1–8.

[54] R. Doherty, A. Mullane, G. Nolan, D. J. Burke, A. Bryson, and M. O’Malley, ‘An Assessment of the Impact of Wind Generation on System Frequency Control’, *IEEE Trans. Power Syst.*, vol. 25, no. 1, pp. 452–460, Feb. 2010.

[55] M.-H. Wang, K.-T. Mok, S.-C. Tan, and S.-Y. R. Hui, ‘Series and shunt DC electric springs’, in *2015 IEEE Energy Conversion Congress and Exposition (ECCE)*, 2015, pp. 6683–6690.

[56] R. Kofahl and R. Isermann, ‘A Simple Method for Automatic Tuning of PID-Controllers based on Process Parameter Estimation’, in *1985 American Control Conference*, 1985, pp. 1143–1148.

[57] V. Vindhya and V. Reddy, ‘PID-Fuzzy logic hybrid controller for a digitally controlled DC-DC converter’, in *2013 International Conference on Green*

Computing, Communication and Conservation of Energy (ICGCE), 2013, pp. 362–366.

[58] A. von Jouanne and B. Banerjee, 'Assessment of voltage unbalance', *IEEE Trans. Power Deliv.*, vol. 16, no. 4, pp. 782–790, Oct. 2001.

[59] S. George and V. Agarwal, 'A DSP Based Optimal Algorithm for Shunt Active Filter Under Nonsinusoidal Supply and Unbalanced Load Conditions', *IEEE Trans. Power Electron.*, vol. 22, no. 2, pp. 593–601, Mar. 2007.

[60] B. Singh, K. Al-Haddad, and A. Chandra, 'A review of active filters for power quality improvement', *IEEE Trans. Ind. Electron.*, vol. 46, no. 5, pp. 960–971, Oct. 1999.

[61] V. B. Bhavaraju and P. N. Enjeti, 'Analysis and design of an active power filter for balancing unbalanced loads', *IEEE Trans. Power Electron.*, vol. 8, no. 4, pp. 640–647, Oct. 1993.

[62] J. W. Dixon, J. J. Garcia, and L. Moran, 'Control system for three-phase active power filter which simultaneously compensates power factor and unbalanced loads', *IEEE Trans. Ind. Electron.*, vol. 42, no. 6, pp. 636–641, Dec. 1995.

[63] A. Chandra, B. Singh, B. N. Singh, and K. Al-Haddad, 'An improved control algorithm of shunt active filter for voltage regulation, harmonic elimination, power-factor correction, and balancing of nonlinear loads', *IEEE Trans. Power Electron.*, vol. 15, no. 3, pp. 495–507, May 2000.

[64] C.-C. Chen and Y.-Y. Hsu, 'A novel approach to the design of a shunt active filter for an unbalanced three-phase four-wire system under nonsinusoidal conditions', *IEEE Trans. Power Deliv.*, vol. 15, no. 4, pp. 1258–1264, Oct. 2000.

[65] P. Verdelho and G. D. Marques, ‘An active power filter and unbalanced current compensator’, *IEEE Trans. Ind. Electron.*, vol. 44, no. 3, pp. 321–328, Jun. 1997.

[66] W.-C. Lee, T.-K. Lee, and D.-S. Hyun, ‘A three-phase parallel active power filter operating with PCC voltage compensation with consideration for an unbalanced load’, *IEEE Trans. Power Electron.*, vol. 17, no. 5, pp. 807–814, Sep. 2002.

[67] T. K. Au and M. Ortega-Vazquez, ‘Assessment of plug-in electric vehicles charging on distribution networks’, in *2013 IEEE Power Energy Society General Meeting*, 2013, pp. 1–5.

[68] K. Qian, C. Zhou, M. Allan, and Y. Yuan, ‘Modeling of Load Demand Due to EV Battery Charging in Distribution Systems’, *IEEE Trans. Power Syst.*, vol. 26, no. 2, pp. 802–810, May 2011.

[69] J. T. Salihi, ‘Energy Requirements for Electric Cars and Their Impact on Electric Power Generation and Distribution Systems’, *IEEE Trans. Ind. Appl.*, vol. IA-9, no. 5, pp. 516–532, Sep. 1973.

[70] S. Rahman and G. B. Shrestha, ‘An investigation into the impact of electric vehicle load on the electric utility distribution system’, *IEEE Trans. Power Deliv.*, vol. 8, no. 2, pp. 591–597, Apr. 1993.

[71] A. Jimenez and N. García, ‘Power flow modeling and analysis of voltage source converter-based plug-in electric vehicles’, in *2011 IEEE Power and Energy Society General Meeting*, 2011, pp. 1–6.

[72] V. Marano and G. Rizzoni, ‘Energy and economic evaluation of PHEVs and their interaction with renewable energy sources and the power grid’, in *IEEE*

International Conference on Vehicular Electronics and Safety, 2008. ICVES 2008, 2008, pp. 84–89.

[73] D. Wu, D. C. Aliprantis, and K. Gkritza, 'Electric Energy and Power Consumption by Light-Duty Plug-In Electric Vehicles', *IEEE Trans. Power Syst.*, vol. 26, no. 2, pp. 738–746, May 2011.

[74] L. P. Fernandez, T. G. S. Roman, R. Cossent, C. M. Domingo, and P. Frias, 'Assessment of the Impact of Plug-in Electric Vehicles on Distribution Networks', *IEEE Trans. Power Syst.*, vol. 26, no. 1, pp. 206–213, Feb. 2011.

[75] E. Sortomme, M. M. Hindi, S. D. J. MacPherson, and S. S. Venkata, 'Coordinated Charging of Plug-In Hybrid Electric Vehicles to Minimize Distribution System Losses', *IEEE Trans. Smart Grid*, vol. 2, no. 1, pp. 198–205, Mar. 2011.

[76] S. Faddel, A. T. Al-Awami, and M. A. Abido, 'Real time digital simulation of voltage-based controller for electric vehicle charging', in *2016 Clemson University Power Systems Conference (PSC)*, 2016, pp. 1–5.

[77] A. T. Al-Awami, E. Sortomme, G. M. A. Akhtar, and S. Faddel, 'A Voltage-Based Controller for an Electric-Vehicle Charger', *IEEE Trans. Veh. Technol.*, vol. 65, no. 6, pp. 4185–4196, Jun. 2016.

[78] D. P. Montoya and A. E. Díez, 'Power flow steady-state model analysis of grid-connected plug-in electric vehicle charging stations', in *2015 12th International Conference on Electrical Engineering, Computing Science and Automatic Control (CCE)*, 2015, pp. 1–6.

[79] K. Clement-Nyns, E. Haesen, and J. Driesen, 'The Impact of Charging Plug-In Hybrid Electric Vehicles on a Residential Distribution Grid', *IEEE Trans. Power Syst.*, vol. 25, no. 1, pp. 371–380, Feb. 2010.

[80] Y. Mitsukuri, R. Hara, H. Kita, E. Kamiya, N. Hiraiwa, and E. Kogure, 'Voltage regulation in distribution system utilizing electric vehicles and communication', in *Transmission and Distribution Conference and Exposition (T D), 2012 IEEE PES*, 2012, pp. 1–6.

[81] R. Garcia-Valle and J. G. Vlachogiannis, 'Letter to the Editor: Electric Vehicle Demand Model for Load Flow Studies', *Electr. Power Compon. Syst.*, vol. 37, no. 5, pp. 577–582, Apr. 2009.

[82] J. G. Vlachogiannis, 'Probabilistic Constrained Load Flow Considering Integration of Wind Power Generation and Electric Vehicles', *IEEE Trans. Power Syst.*, vol. 24, no. 4, pp. 1808–1817, Nov. 2009.

[83] Y. Mitsukuri *et al.*, 'Study on Voltage Regulation in Distribution System Using Electric Vehicles—Control Method Considering Dynamic Behavior', *J. Int. Counc. Electr. Eng.*, vol. 4, no. 2, pp. 121–129, Apr. 2014.

APPENDIX A

EXPERIMENTAL SETUP COMPONENTS

A.1 Programmable AC Source

Programmable AC source provides powerful functions to simulate the standard power quality disturbances. In this work, Chroma 61511 is used as a grid source for the distribution system as shown in Figure A.1. It can provide up to 300 Vac output voltage and 12 KVA power ratings. It is capable to generate the first forty harmonics and interharmonics ranging from 0.01 Hz to 2400 Hz.

Figure A.1 Programmable AC source Chroma 61511

A.2 Programmable Electronic Load

Programmable electronic loads are designed to simulate the AC/DC loads. The programmable AC/DC load Chroma 63800 is selected to simulate the non-linear rectified loads and load conditions under high crest factor as shown in Figure A.2. It is capable of working under distorted mains voltage. The chroma-63800 can be configured as a constant power source up to 1800W, while as a constant current load up to 45 Arms at the voltage range is 50V – 350 Vrms. Three identical units of chroma-63800 are used separately to simulate the three-phase load.

Figure A.2 Programmable electronic load

A.3 Inverter/Rectifier Module

SEMITEACH – IGBT inverter and rectifier module is used for real time voltage source inverter implementation. This module has three major functions including single and

three-phase voltage source inverter, buck or boost converter and brake chopper. An isolated uncontrolled rectifier is also a part of this system. The basic block diagram of this module is shown in Figure A.3, where a pair of 2200μF DC capacitor is also installed for energy storage purpose. The rectifier input is 230/ 400V while the output may vary up to 600V DC. The input output range of inverter can also varied up to 400V AC and 600V DC with 30A as a maximum current.

In this study, the voltage source inverter and three phase diode rectifier are used. The voltage source inverter is used to inject the nonlinear harmonic current required by the load attached to the dc side of the diode rectifier. The gate pulses are provided to the inverter generated by the dSAPCE controller using amplifier. A DC voltage source of 15 volts is applied to the gate driven circuit of the inverter. The dc bus capacitors are used to store the energy and provide the required nonlinear current while maintaining the certain reference value.

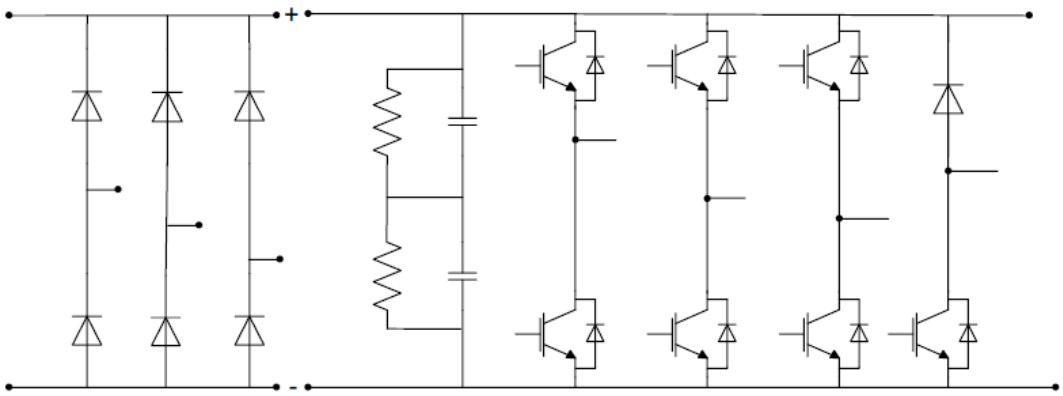

FigureA.3 Block diagram of inverter and rectifier

As a finished portable product, Figure A.4 shows the inverter module.

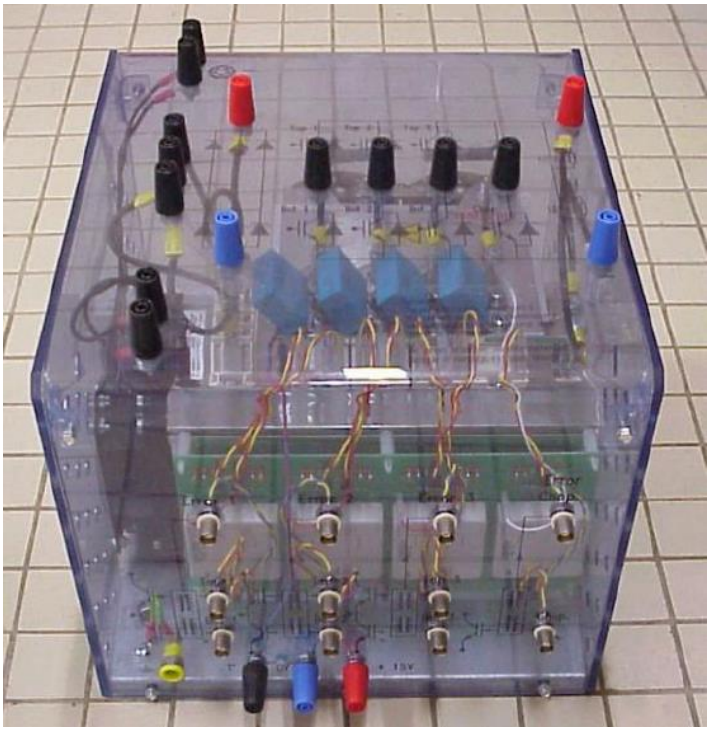

Figure A.4 Real time inverter and rectifier module

A.4 Mixed Domain Oscilloscope

Tektronix 4104B-3 mixed domain oscilloscope is used to record the experimental results as shown in Figure A.5. It is capable of analyzing signals in both frequency and time domain. It can be used a spectrum analyzer. It has four channels that can be used for the measurement of voltage and current signals.

The voltage probe Tektronix TPP-1000 is a 1GHz bandwidth probe used for the measurement of voltage signals up to 300 volts. It offers 10X and 2X attenuation factors. Tektronix TCP0030A probe is utilized for the measurement of source, load and ES current signals. This probe provides the selectable measurement of 5A and 30A with the bandwidth greater than 120 MHz.

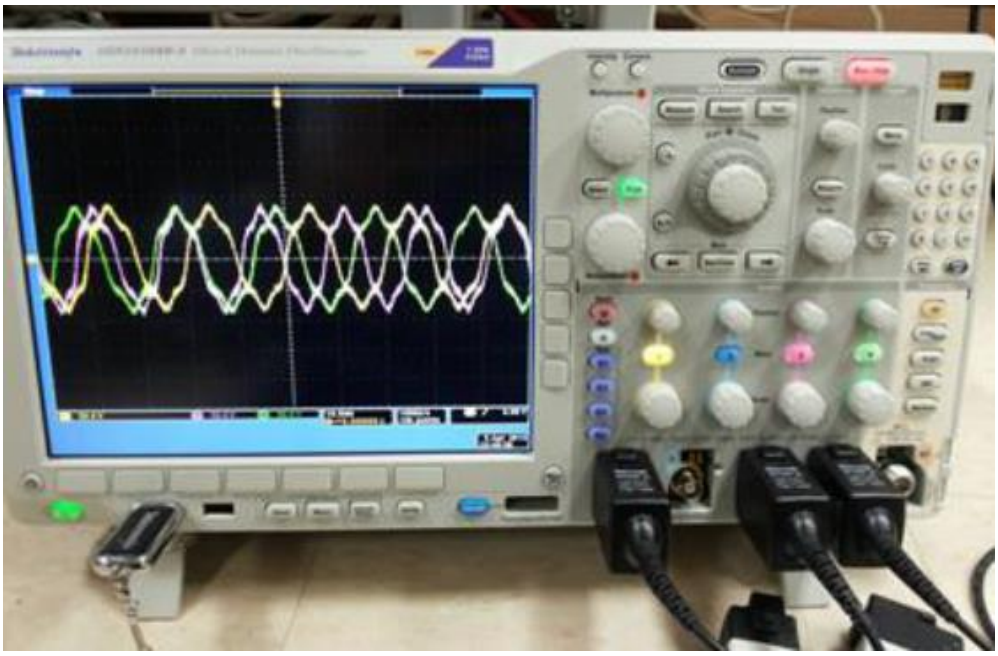

Figure A.5 Mixed domain Tektronix oscilloscope

A.5 Voltage and Current Transducers

Voltage and current transducers are utilized to reduce the voltage and current signals of distribution system, which can be fed to the controller for a possible control action. The dSPACE controller, used in this work has input output range up to ±10V while the actual voltage and current ratings are much higher. So, voltage and current transducers are used to make the input voltage and current signals compatible with the controller I/O range.

(a) Voltage Transducer

SoCan SCB 2 sensor is used as a voltage transducer for the real time measurement of voltage signal. It can measure DC, AC and pulsed voltage signals from 10 to 1500 V using the Hall Effect. The basic block diagram of the current transducer is shown in Figure A.6. The terminals HT+ and HT- represent the signal phase connection terminals of supply voltage. The user specified resistor R is used as an input resistors to limit the

input current less than 10mA at the primary side. The current conversion ratio of the SoCan SCB 2 is 2500:1000. The resistor RM is used as a measurement resistor. The value of RM should be carefully selected so that the output voltage will remain the range less than ± 10V. The voltage terminal ±Vc represents the terminal of the supplied dc voltage of ±15V. An example is illustrated below to explain the functionality of voltage transducer.

Suppose Vs = 230 V

Input Resistor = R = 47000 Ω

Measurement Resistor =R_L = 500 Ω

Primary current =230/47000 = 4.8936mA

Secondary current = 2.5 x primary current = 12.234 mA

Output Voltage = Secondary current x Measurement Resistor = 6.11V

It can be seen that for a supply voltage of 230V, the transducer output voltage is 6.11 volts, which is far less than 10 Volts. Therefore, the transducer output can be fed to the dSPACE controller. In this work, input resistor of 47kΩ is used for the three-phase voltage measurement while 94kΩ is used for the dc bus side with a 500Ω as a measurement resistor.

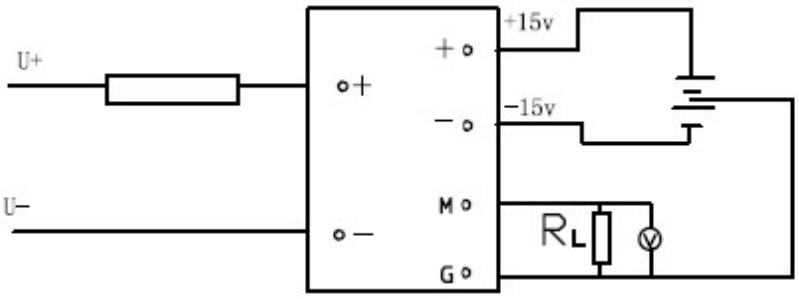

Figure A.6 Circuit diagram of voltage transducer SoCan SCB 2

This voltage sensor works on the principle of closed-loop Hall Effect, The magnetic flux created by the primary current is balanced by a complementary flux produced by driving a current through the secondary windings. A hall device and associated electronic circuit are used to generate the secondary (compensating) current that is an exact representation of the primary current. SoCan SCB2 sensor is used shown in Figure A.7

Figure A.7 Voltage transducer SoCan SCB2

(b) Current Transducer

Current transducers are utilized to transform the high rated current signals into the low valued voltage signals in the distribution system, which can be fed to the controller for a possible control action.

SoCan SCK3 sensor is used as a current transducer for the real time measurement of source load and ES current. It is a closed loop sensor, which can measure DC, AC 145 and pulsed current signals up to 50A using the Hall Effect. A single-phase wire is passed

through the sensor to induce the current in the sensor coil. The output of this sensor is an AC voltage signal, which can be easily used in any industrial controller like dSPACE. The basic block diagram of the current transducer is shown in Figure A.8, where Ip represents the measured current. The voltage terminal ±Vc represents the terminal of the supplied DC voltage of ±15V. The resistor RM is used as a measurement resistor. The value of RM should be carefully selected so that the output voltage will remain the range less than ± 10V. SoCan SCK3 sensor is shown in Figure A.9.

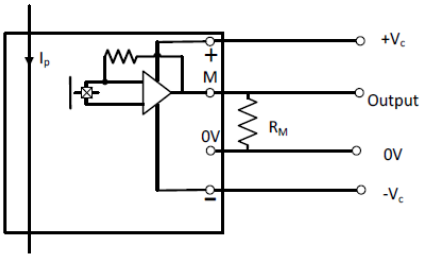

Figure A.8 Circuit diagram of current transducer SoCan SCK3

Figure A.9 Current transducer SoCan SCK3

A.6 Inverter Drive

The digital output of the dSPACE controller is in the range of ±10V, while the gate pulses input required by the real time inverters are ±15V. Therefore, a double gain amplifier is designed using the hex inverter TTL logic integrated circuit SN7416. The schematic diagram of the hex inverter circuit is shown in Figure A.10. This TTL hex inverter has a minimum breakdown voltage of 15 volts. A 15 volts DC supply is provided

at the V_{cc} terminal. The output level can be adjusted using pull up resistors. This TTL hex inverter can sink maximum current up to 30mA.

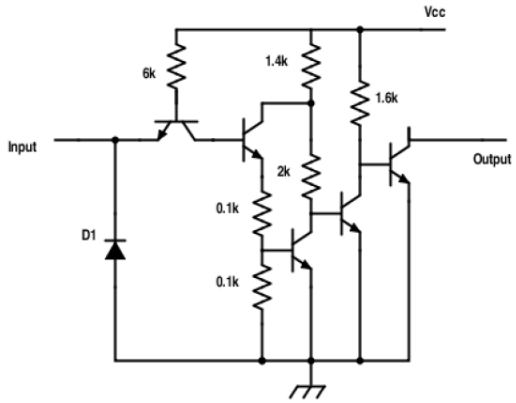

Figure A.10 Schematic diagram of SN7416 TTL hex inverter

A.7 Work Station

The computer used in this work has 12 processors of 3.3GHz, 26 GB RAM. It computer is equipped with software packages that can be used to control, monitor and visualize the waveforms of the input and output signals of the dSPACE.

A.8 Interfacing Board

Voltage and current sensors are mounted on the same board where an inverter drive is placed in order to make the system compact, portable and safe. Moreover, the components in experimental setup have compatibility issues as they cannot take direct signal from each other. dSPACE needs the system voltage and current to scale down within ± 10 volts. Inverter cannot take PWM directly from dSPACE. So, based on that need, one unified circuit board is developed. It can perform two main functions. It measures the system voltage and current and then feed it to digital controller. Secondly it resolves the interfacing issue in-between inverter, dSPACE and the power network.

Figure A.11 shows the schematic of the interfacing board with all input out requirements and capabilities. After completion, the portable interfacing board looks like as shown in Figure A.12.

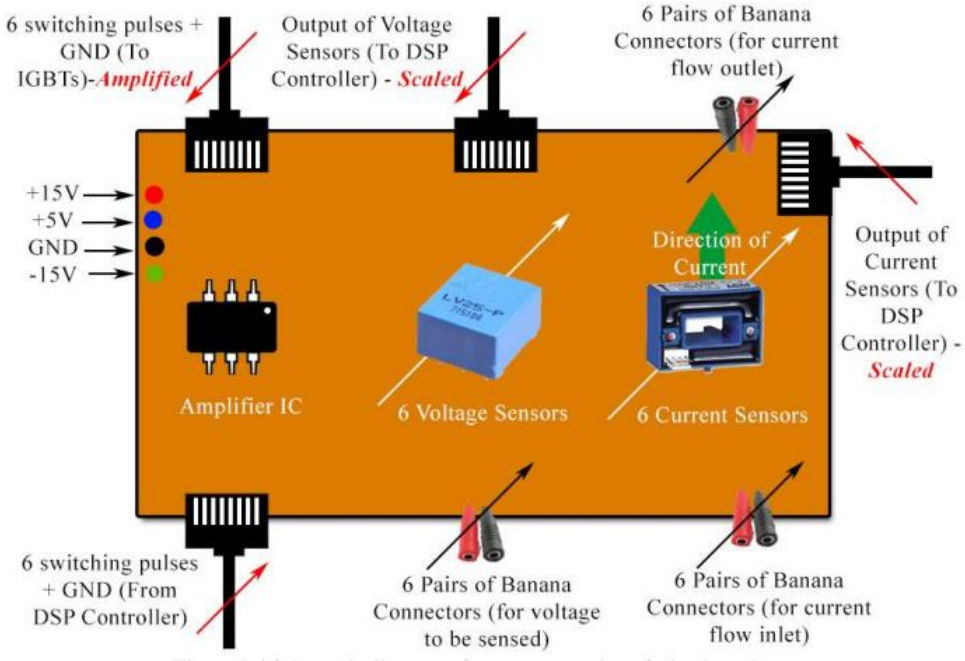

Figure A.11 Schematic of interfacing board

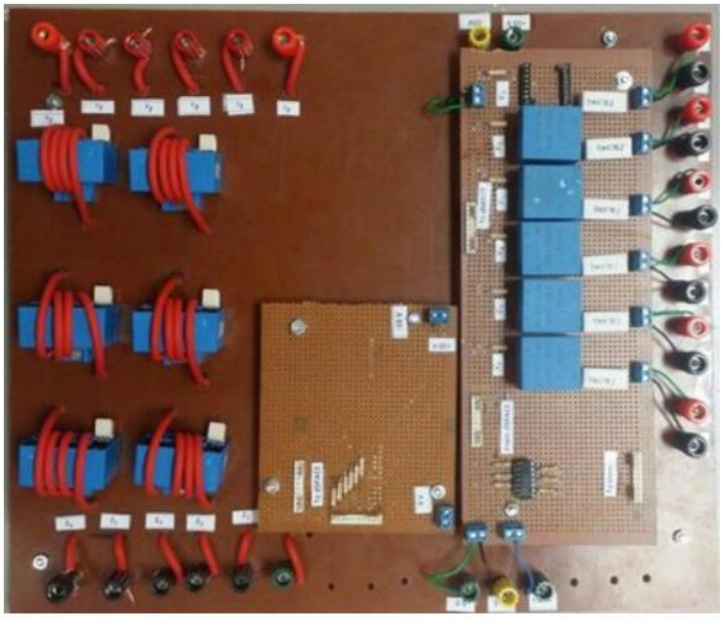

Figure A.12 Interfacing board

For mass production of this circuit board, a PCB design has been proposed. PCB has all the capabilities that are present in the interfacing board discussed above. The copper-layer diagrams of sensors module and inverter driving circuitry are shown in Figure A.13 and Figure A.14, respectively.

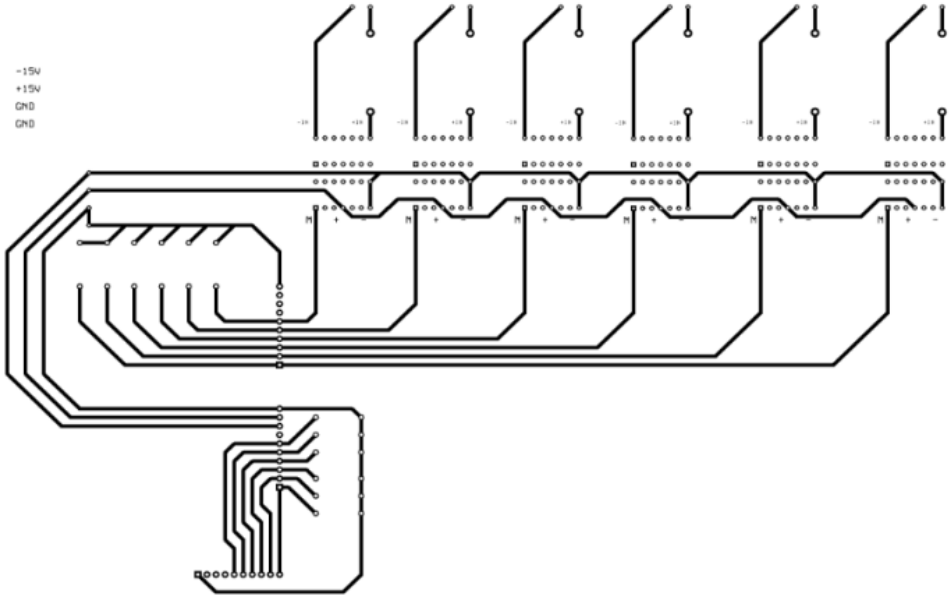

Figure A.13 Copper layer of V/I sensor and power module

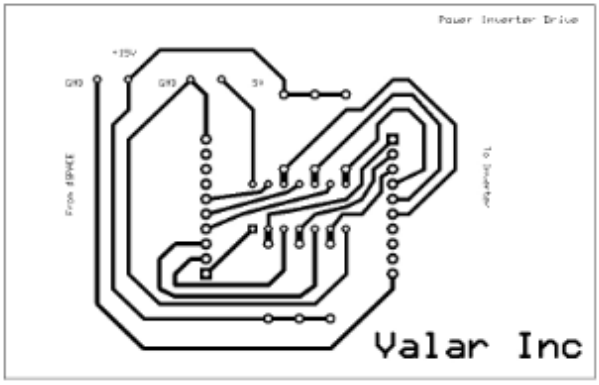

Figure A.14 Copper layer of inverter drive

APPENDIX B

dSPACE DS1103 CONTROLLER BOARD: UTILITY AND APPLICATIONS

The DS1103 controller board is a product of dSPACE GmbH. It is a Programmable process controller (PPC) board which is used for numerous applications in engineering research. A brief overview regarding the applications and functionalities of DS1103 controller board is presented in this appendix.

B.1 dSPACE Controller

dSPACE is an industrial controller mainly used for the application development and prototyping. In this study, DS-1103 is used for the real time controller implementation of ES as shown in Figure B.1. It has two major parts expansion box and connection panel.

The connection panel consists of 50 bit analog and digital I/O channels including 20 analog to digital input channel (ADCH) and 8 digital to analog output channels (DACH). dSPACE can be easily programmed with the Matlab/Simulink with the aid of real time interface (RTI) blocksets. All I/O's can be configured for real time applications using RTI. dSPACE uses controlDesk as a software for the real time monitoring, measurement and control actions. DS-814 interface card is used in the expansion box while DS-817 card in the workstation for real time monitoring and control of the system.

Figure B.1 dSPACE DS-1103 controller

B.2 Prominent Features

- It is a single board system, providing processing in real-time with an ample range of input/output connections.
- High speed and precision of the input/output channels
- Featuring CAN (controller area network) bus which allows communication between controllers and devices without requiring a computer in between
- Providing serial interfaces appropriate for automotive application
- With PLL-based UART (Universal asynchronous receiver transmitter) for high accuracy baud rate

B.3 Major Applications

The DS1103 controller board is an advanced rapid prototyping tool. Some of its major applications are:

- Automation and control systems
- Control of power electronic converters
- Variable speed drives
- Robotics
- Automotive control
- Active vibration control

B.4 Input/output Interfaces

The DS1103 controller board has a variety of input/ output interfaces to meet the needs in a wide range of applications. The details are as following:

- 20 A/D channels with 16 bit resolution
- 8 D/A channels with 16 bit resolution
- 32 bit digital I/O channels
- Digital incremental encoder interface (6 channels)
- Analogue incremental encoder interface (1 channel)
- Serial interface
- CAN interface
- To perform additional I/O task, a slave DSP can be interfaced

B.5 Controller Programming with RTI Simulink Blocks Library

Programming a controller on DS1103 is simplified by RTI (real-time interface) Simulink library. In a very convenient way Simulink models can be programmed on the controller board using the I/O blocks for external connections from this library. It shows the RTI Simulink library. The blocks available in the library enable the user to graphically configure all the I/O interfaces. A view of the RTI master PPC library, which has all the real-time interfacing blocks for the DS1103 controller board is shown in Figure B.2.

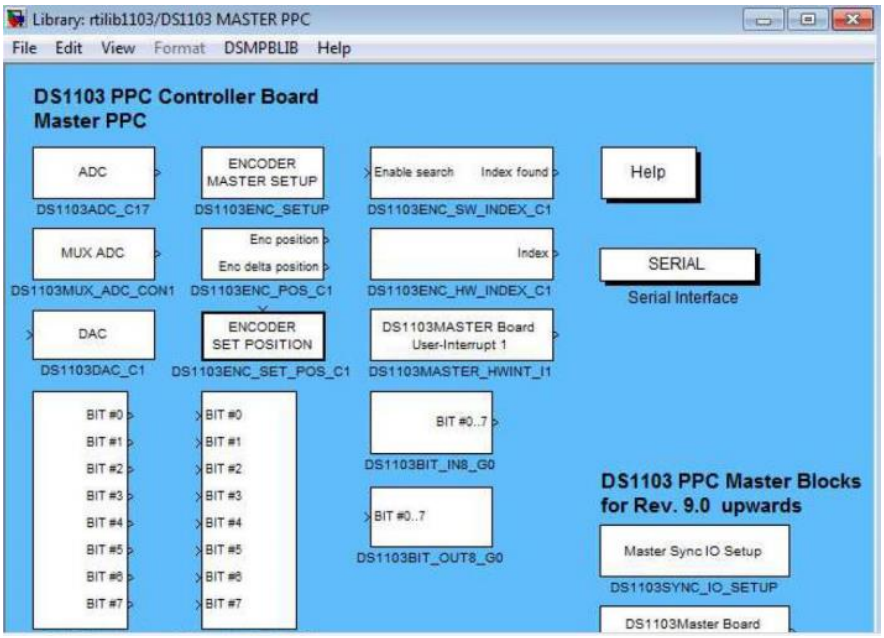

Figure B.2 Input/output blocks of DS1103 PPC controller board

The various I/O blocks are visible in Figure B.2, such as ADC for analog input signals, DAC for analog output signals, DS1103_BIT_IN block for digital input, DS1103_BIT_OUT block for digital output signals. The description of how to use these blocks is also provided. The help documentation can be accessed from the main RTI library. For the work done in this thesis, mainly the analog I/O interfacing was required. Thus the ADC, MUX_ADC and DAC blocks were used.

LIST OF PUBLICATIONS

[J1] M. S. Javaid, M. A. Abido, Usama Bin Irshad, Ali T. Al-Awami, "Design and Implementation of Electric Spring for Constant Power Applications" (Under Review) in *IET Generation, Transmission & Distribution*

[J2] M. S. Javaid, M. A. Abido, Usama Bin Irshad, Ali T. Al-Awami, "Design and Control of Electric Spring for Distribution Network Loaded by Electric Vehicles" (Under Review) in *IET Generation, Transmission & Distribution*

[C1] M. S. Javaid, Usama Bin Irshad, M. Abido, Zorays Khalid, Safiul Alam, Md Juel Rana "Direct Control of Three-Phase Smart Load for Neutral Current Mitigation", Presented in *19th IEEE International Multi-Topic Conference (INMIC), Islamabad*, Pakistan, 2016.

[C2] M. S. Javaid, Usama Bin Irshad and M. A. Abido, "Novel Smart Load Control Based on Fuzzy Logic for Voltage Regulation", Submitted for *9th IEEE-GCC Conference and Exhibition (GCCCE),* 2016

[C3] M. S. Javaid, M. A. Abido, M. Alowaifeer, "Effect of Electric Spring in Improving Smart Grid Voltage Stability and Power Quality", Poster presented in *4th International Conference on Electric Power and Energy Conversions Systems in AUS Sharjah*, Nov 2015

Vitae

Name	:Muhammad Sharjeel Javaid
Nationality	:Pakistani
Date of Birth	:6/4/1991
Email	:sharjeel188@gmail.com
Address	:C-193, Phase 2, Gulshan-e-Hadeed, Bin Qasim, Karachi, Pakistan
Academic Background	:MS Electrical Engineering, King Fahd University of Petroleum and Minerals, Dhahran, Saudi Arabia, January 2017.
	BS Electronic Engineering, GIK Institute of Engineering Sciences and Technology, Swabi, Pakistan, May 2013.